European Journal of Taxonomy 897: 1–56
https://doi.org/10.5852/ejt.2023.897.2293
ISSN 2118-9773
www.europeanjournaloftaxonomy.eu
2023 · Valdez-Mondragón A. & Cabrera-Espinosa L.A.

Monograph

urn:lsid:zoobank.org:pub:A340BD2E-094A-4C84-88B3-5B4ED220F476

Phylogenetic analyses and description of a new species of black widow spider of the genus *Latrodectus* Walckenaer (Araneae, Theridiidae) from Mexico; one or more species?

Alejandro VALDEZ-MONDRAGÓN [1,*] & Luis A. CABRERA-ESPINOSA [2]

[1,2] Colección de Aracnología (CARCIB), Programa Académico de Planeación Ambiental y Conservación (PLAYCO), Centro de Investigaciones Biológicas del Noroeste (CIBNOR), S.C. Km 1 Carretera a San Juan de La Costa «El Comitán», La Paz, Baja California Sur, C.P. 23205, Mexico.

[*] Corresponding author: lat_mactans@yahoo.com.mx
[2] Email: alejandrocabrera91@gmail.com

[1] urn:lsid:zoobank.org:author:05A30CA0-DD93-48CC-BC04-E7042E691FFA
[2] urn:lsid:zoobank.org:author:F6547011-EA5E-482B-B84C-0CD4596E916A

Abstract. A new species of the spider genus *Latrodectus* Walckenaer, 1805 from Mexico is described based on an integrative taxonomic approach. *Latrodectus occidentalis* Valdez-Mondragón sp. nov. is described using the molecular markers cytochrome c oxidase subunit 1 (*CO1*) and internal transcribed spacer 2 (*ITS2*), morphology of male and female specimens, and Species Distribution Models (SDM). Four molecular methods for species delimitation were implemented. The new species is characterized by having a unique dorsal coloration pattern on the abdomen. *Latrodectus occidentalis* sp. nov. is considered a distinct and valid species for four reasons: (1) it can be distinguished by morphological characters (genital and somatic); (2) the average interspecific genetic variation is >2%; (3) 12 haplotypes were recovered within the species, being separated by the next close haplogroup of *L. hesperus* Chamberlin & Ivie, 1935 (30 mutations); and (4) congruence was observed among the four molecular methods. The number of recorded species of *Latrodectus* from Mexico increases to four: *Latrodectus mactans* (Fabricius, 1775), *L. hesperus* Chamberlin & Ivie, 1935, *L. geometricus* C.L. Koch, 1841 (introduced), and *L. occidentalis* sp. nov. The diversity of the genus *Latrodectus* from Mexico is surely underestimated, and more sampling is needed from the different biogeographical provinces and ecoregions to fill in these gaps.

Keywords. Integrative taxonomy, North America, species distribution modeling, DNA barcodes, morphology.

Valdez-Mondragón A. & Cabrera-Espinosa L.A. 2023, Phylogenetic analyses and description of a new species of black widow spider of the genus *Latrodectus* Walckenaer (Araneae, Theridiidae) from Mexico; one or more species? *European Journal of Taxonomy* 897: 1–56. https://doi.org/10.5852/ejt.2023.897.2293

Introduction

The spider family Theridiidae Sundevall, 1833 comprises 124 genera and 2544 species (World Spider Catalog 2023). Commonly known as 'black-widow spiders', the genus *Latrodectus* Walckenaer, 1805 contains the biggest spiders in size of the family Theridiidae and are well known by the medical community and general public due to their venom, which can cause neurological symptomatology in humans. Specifically, the presynaptic neurotoxin toxic α-latrotoxin affects the vertebrate central nervous system by increasing intracellular [Ca2 +] in presynaptic neurons, and stimulating uncontrolled exocytosis of neurotransmitters from nerve terminals (Holz & Habener 1998).

In the last two decades, phylogenetic analyses of the genus *Latrodectus* using morphological characters and the mitochondrial gene *CO1*, suggest that the species are grouped into two main clades: 1) the *geometricus* clade which includes *Latrodectus geometricus* C.L. Koch, 1841, *Latrodectus rhodesiensis* Mackay, 1972 and *Latrodectus umbukwane* Wright, Wright, Lyle & Engelbrecht, 2019; and 2) the *mactans* clade which includes the rest of the species of the genus (Garb *et al.* 2004; Aguilera *et al.* 2009; Rueda *et al.* 2021). Both clades are morphologically supported by the position of the spermathecae in females, being V-shaped in the *mactans* clade and parallel in the *geometricus* clade (Garb *et al.* 2004; Aguilera *et al.* 2009). Garb *et al.* (2004) proposed an African origin for the genus, and that the South African species were the first to colonize the Americas with a posterior diversification in North America.

The genus *Latrodectus* is composed of 34 currently recognized species (World Spider Catalog 2023). *Latrodectus geometricus* has a cosmopolitan distribution that is considered to be the result of human-mediated introductions in several parts of the world, likely a result of anthropochory from commercial trade, in combination with its ability to adapt to disturbed environments (Chamberlin & Ivie 1935; Garb *et al.* 2004; Kaslin 2013). Worldwide, the Americas host the greatest diversity of species of *Latrodectus*, with Argentina having the highest described diversity with nine species (World Spider Catalog 2023).

In Mexico, spiders of the genus *Latrodectus* are known colloquially in Spanish as "viuda negra", "capulina spiders" or "casampulga" in southeastern Mexico, and in the Nahuatl language as "tzintlatlauhqui" or "cintlatlahua", which translates to: the one with the red butt. Currently, three species are reported for Mexico: *L. mactans* (Fabricius, 1775), *L. geometricus*, and *L. hesperus* Chamberlin & Ivie, 1935 (Barreto & Barreto 1994; Cortez-Roldán 2018; Valdez-Mondragón *et al.* 2018; Cabrera-Espinosa 2020; Cabrera-Espinosa & Valdez-Mondragón 2019, 2021; World Spider Catalog 2023). For a long time, *L. mactans* has been supposed to be the species with the largest distribution throughout the country, being reported in all 32 Mexican states and commonly associated with anthropized areas (Cabrera-Espinosa & Valdez-Mondragón 2019, 2021; Cabrera-Espinosa 2020). Even some authors such as Chamberlin & Ivie (1935) based on the variation of the coloration pattern of the abdomen, proposed three subspecies for *L. mactans*: *Latrodectus mactans mactans* Fabricius, 1775, *Latrodectus mactans texanus* Chamberlin & Ivie, 1935 and *Latrodectus mactans hesperus* Chamberlin & Ivie, 1935.

Recently, Cabrera-Espinosa (2020) and Cabrera-Espinosa & Valdez-Mondragón (2021) updated the records of *Latrodectus* from Mexico based on biological collections from various digital information sources, scientific collections, and fieldwork. These studies found *L. mactans* to be the species with the largest distribution in the country. Species determination within *Latrodectus* was done according to traditional taxonomy, mainly using primary sexual characters (male palps and female epigyna) and abdomen coloration patterns. However, these characters are not always reliable at species level due to the wide morphological variation and even character overlapping (Levi 1959; Levi & Randolph 1975; Levy & Amitai 1983; Ubick *et al.* 2005; Cabrera-Espinosa & Valdez-Mondragón 2019; Cabrera-Espinosa 2020).

Currently, the taxonomic identification of species of *Latrodectus* is problematic when based only on sexual features of males and females (Cabrera-Espinosa & Valdez-Mondragón 2019, 2021; Cabrera-Espinosa 2020). The species *L. mactans* and *L. hesperus* show an overlap in the number of turns present on the copulatory duct of the female epigyna (3 to 4 turns in *L. hesperus* and 4 to 5 turns in *L. mactans*), as well as in the number of turns on the male embolus (2 turns for both species) (Cabrera-Espinosa 2020; Cabrera-Espinosa & Valdez-Mondragón 2021).

Molecular markers are now recognized as a useful tool in biodiversity and species delimitation studies, especially in groups of spiders where morphological characters are not informative enough (Valdez-Mondragón *et al*. 2018; Choi *et al.* 2019; Wright *et al.* 2019; Navarro-Rodríguez & Valdez-Mondragón 2020; Valdez-Mondragón 2020). When molecular evidence is complemented with other data sources, such as morphological, ecological, behavioral, biogeographical or reproductive (i.e., integrative taxonomy), more robust taxonomic hypotheses are obtained for the delimitation of lineages or species (Garb *et al*. 2004; DeSalle *et al.* 2005; Aguilera *et al.* 2009; Padial *et al.* 2010; Choi *et al.* 2019; Navarro-Rodríguez 2019; Wright *et al*. 2019; Navarro-Rodríguez & Valdez-Mondragón 2020).

To date, the genus *Latrodectus* has been poorly studied with molecular characters in an integrative taxonomy context. The first work using molecular markers was done by Garb *et al*. (2004), who addressed the phylogeny of the genus with molecular (*CO1*) and morphological characters. This study reported the interspecific genetic divergence of the *CO1* marker between species of the *geometricus* clade to be 2.3%, whereas in the *mactans* clade values greater than 17% were found between species. Aguilera *et al*. (2009) revalidated *Latrodectus thoracicus* Nicolet, 1849 with morphological and molecular evidence (*CO1*), reporting an average intraspecific genetic divergence among the analyzed specimens of 0.8%.

A few years later, Aguilera (pers. com.) in an unpublished study delimitating 13 species of *Latrodectus* using morphological and molecular characters (*CO1* and α-latrotoxin encoding gene) and the bPTP molecular method for species delimitation. The two genes showed similar results of greater than 2% interspecific genetic distances within species of the *mactans* and *geometricus* clades. However, no genetic variation was observed between some specimens of *L. thoracicus*, *L. miriabilis* (Holmberg, 1876) and *L. variegatus* Nicolet, 1849, nor between individuals of *L. corallinus* Abalos, 1980 and *L. diaguita* Carcavallo, 1960 (Aguilera pers. com.). On the contrary, the analyzed specimens of *L. hesperus* show an intraspecific genetic variation greater than 2%. Wright *et al*. (2019) described *Latrodectus umbukwane* from South Africa based on morphological and molecular evidence (*CO1*). This species was allocated to the *geometricus* clade; however, the genetic distance between this species and its sister species *L. geometricus* was 14.7%. Recently, Rueda *et al.* (2021) described two new species of *Latrodectus* from Colombia (*L. garbae* and *L. hurtadoi*) using *CO1* and *16S* molecular markers. Genetic distances between species in this study were generally greater than 2%, with the exception of *L. garbae* having a K2P genetic distance of 1% with respect to *L. diaguita* and *L. corallinus* with the *16S* marker.

None of the previous research for species delimitations have included specimens from Mexico used an integrative taxonomic approach. Furthermore, the genetic variation of Mexican populations of *Latrodectus*, mainly *L. mactans* and *L. hesperus*, is still unknown. The current study aims to assess the species diversity of *Latrodectus* within Mexico using morphological evidence (somatic and sexual structures) and DNA barcoding (*CO1* and *ITS2*), while updating the biogeographic and distribution data.

Material and methods

Biological material

Specimens were hand-collected, collected between 2017 and 2022, 19 field trips were made to 28 states of Mexico; additionally, specimens deposited at the collections cited below were used. Field collections were made at locations previously recorded in works mentioning the genus and preserved in ethanol

(80% for morphology and 96% for molecular studies). Specimens were collected manually. The type specimens and additional examined material are deposited in the following repositories:

CNAN = National Collection of Arachnids, Institute of Biology, Universidad Nacional Autónoma de México (IBUNAM), Mexico City, Mexico (type specimens)
LATLAX = Laboratory of Arachnology, Laboratorio Regional de Biodiversidad y Cultivo de Tejidos Vegetales (LBCTV), IBUNAM, Tlaxcala City, Mexico (additional material)

Descriptions and observations of specimens were performed using a Zeiss Discovery V8 stereo microscope at LATLAX. Digital photographs of specimens were taken with a Zeiss Axiocam 506 color camera attached to a Zeiss AXIO Zoom V16 stereo microscope. Photographs were edited using Photoshop CS6. Male palps and female epigyna were dissected in ethanol (80%). Female epigyna were cleaned in potassium hydroxide (KOH 10%) for 5 to 10 minutes, following the protocol outlined in Valdez-Mondragón *et al.* (2018). The habitus, male palps and female epigyna were submerged in 70% alcohol gel (ethanol) and covered with a thin layer of distilled water to minimize diffraction during photography (Valdez-Mondragón & Francke 2015; Valdez-Mondragón *et al.* 2019). For the photomicrographs, morphological structures (palps, epigyna, prosoma and abdomen) were dissected and cleaned with an ultrasonic cleaner at 20–40 kHz for five minutes; subsequently, they were critical-point dried and examined at low vacuum in a Hitachi S-2460N Scanning Electron Microscope (SEM). Descriptions were carried out following Rueda *et al*. (2021). All morphological measurements are given in millimeters (mm). Scale measurements on photomicrographs are in micrometers (μm). The distribution map was made using Q-QGIS ver. 2.18.

Abbreviations

AER = anterior eye row
ALE = anterior lateral eye
ALS = anterior lateral spinneret
AME = anterior median eyes
BQ = basichelicerae
C = conductor
CA = cymbial apophysis
Cb = conductor base
CD = copulatory duct
Cu = colulus
E = embolus
F = fang
MA = median apophysis
PER = posterior eye row
PLE = posterior lateral eyes
PLS = posterior lateral spinneret
PME = posterior median eyes
PMS = posterior median spinneret
Q = chelicerae
S = spermathecae
T = tegulum
TA = tegular apophysis

Taxon sampling

Molecular analyses are based on 130 individuals of 22 species of *Latrodectus* and two outgroups to root the trees: *Steatoda borealis* (Hentz, 1850) and *Latrodectus katipo* Powell, 1871. This dataset was used

Table 1. PCR primers used for each molecular marker (*CO1* and *ITS2*).

Gene	Primer name	Primer sequence (5′–3′)	Reference
CO1	LCO 1490	GGT CAA CAA ATC ATA AAG ATA TTG G	Folmer *et al.* (1994)
	HCO 2198	TAA ACT TCA GGG TGA CCA AAA AAT CA	
ITS2	5.8S	CAC GGG TCG ATG AAG AAC GC	Ji *et al.* (2003)
	CAS28sB1d	TTC TTT TCC TCC SCT TAY TRA TAT GCT TAA	Planas & Ribera (2015)

for the analyses of the *p* genetic distances (uncorrected) with Neighbor Joining (NJ) using the molecular markers *CO1* and ITS2 respectively (Table 1). The species delimitation analyses with the concatenated matrix (*CO1* + *ITS2*) were focused mainly on species from Mexico, using *L. bishopi* Kaston, 1938 as an outgroup for the topology obtained under Bayesian Inference (BI). Three different partitions were used for BI: 1) *CO1* (580 pb), 2) *ITS2* (402 pb), and 3) *CO1* + *ITS2* (983 pb).

DNA extraction, PCR amplification and sequencing

Two legs from immatures were used for the DNA extraction with the Qiagen DNeasy Tissue Kit (Valencia, CA, USA) following the protocol by Valdez-Mondragón *et al.* (2019). Targeted DNA fragments included approximately 580 bp of the cytochrome c oxidase subunit 1 (*CO1*) mitochondrial gene and 402 bp of the Internal Transcribed Spacer 2 (*ITS2*) nuclear gene (Table 1). Amplifications were carried out in a Veriti Applied-Biosystems 96 Well Thermal Cycler, in a total volume of 25 µl: 3 µl DNA, 8.7 µl H_2O, 12.5 µl Multiplex PCR Kit of QIAGEN and 0.4 µl of each molecular marker (forward and reverse). The PCR program for *CO1* and *ITS2* was: initial step 15 min at 95°C; amplification 35 cycles of 35 s at 94°C (denaturation), 1.5 min at 40°C (annealing), 1.5 min at 72°C (elongation); and final elongation 10 min at 72°C. PCR products were checked to analyze length and purity on 1% agarose gels with a marker of 100 bp and purified directly using the QIAquick PCR Purification kit of QIAGEN according to manufacturer's protocol (Valencia, CA, USA). DNA extraction and amplification were performed at the Molecular Laboratory at the Laboratorio Regional de Biodiversidad y Cultivo de Tejidos Vegetales (LBCTV), Institute of Biology, Universidad Nacional Autónoma de Mexico (UNAM), Tlaxcala City. Sanger sequencing was done at the Laboratory of Molecular Biology and Health, IB-UNAM, Mexico City. Sequencing of both strands (5′–3′ and 3′–5′) of PCR products were performed in a Sequencer Genetic Analyzer RUO Applied Biosystems Hitachi model 3750xL. Sequence data of *CO1* and *ITS2* are deposited in GenBank with accession numbers OP652138–OP652221 and OP686984–OP687043 for *CO1* and *ITS2* respectively (Table 2).

DNA sequence alignment and editing

Sequences were edited using the programs BioEdit ver. 7.0.5.3 (Hall 1999) and Geneious ver. 2021.0.1 (Kearse *et al.* 2012). Sequences were aligned online with the default gap opening penalty of 1.53 in MAFFT (Multiple sequence alignment based on Fast Fourier Transform) ver. 7 (Katoh & Toh 2008) using the following alignment strategy: Auto (FFT-NS-2, FFTNS-i or L-INS-i; depending on data size). These aligned matrices were subsequently used in molecular analyses.

Molecular analyses, species delimitation and haplotype networks

Four different molecular delimitation methods were used under the corrected *p* distances Neighbor-joining (NJ) criteria: 1) ABGD (Automatic Barcode Gap discovery) (Puillandre *et al*. 2012), 2) ASAP (Assemble Species by Automatic Partitioning) (Puillandre *et al.* 2021), 3) GMYC (General Mixed Yule Coalescent) (Pons *et al.* 2006), and 4) bPTP (Bayesian Poisson Tree Process) (Zhang *et al.* 2013; Kapli *et al*. 2017).

Table 2 (continued on next four pages). Specimens sequenced for each species of *Latrodectus* Walckenaer, 1805, DNA voucher numbers, localities, and GenBank accession numbers (*CO1* and *ITS2*). Abbreviations: AZ = Arizona; BC = Baja California; BCS = Baja California Sur; CA = California; FL = Florida; HI = Hawaii; MD = Maryland; MS = Mississippi; NC = North Carolina; NM = New Mexico; SC = South Carolina; SLP = San Luis Potosi.

Species	DNA voucher LATLAX	Locality	GenBank accesion number	
			CO1	*ITS2*
L. antheratus	_	Argentina	AY383047	_
L. bishopi	_	USA: FL	AY383060	_
L. corallinus	_	Argentina	AY383062	_
L. corallinus	_	Argentina	AY383061	_
L. curacaviensis	_	Colombia	KP696811	_
L. curacaviensis	_	Colombia	KP696810	_
L. curacaviensis	_	Colombia	KP696809	_
L. curacaviensis	_	Colombia	KP696808	_
L. curacaviensis	_	Colombia	KP696807	_
L. curacaviensis	_	Colombia	KP696806	_
L. curacaviensis	_	Colombia	KP696805	_
L. curacaviensis	_	Colombia	KP696804	_
L. curacaviensis	_	Colombia	KP696803	_
L. curacaviensis	_	Colombia	KP696802	_
L. diaguita	_	Argentina	AY383063	_
L. diaguita	_	Argentina	AY383064	_
L. geometricus	_	Malaysia	KF227387	_
L. geometricus	_	Malaysia	KF227386	_
L. geometricus	_	Malaysia	KF227390	_
L. geometricus	_	Argentina	AY383066	_
L. geometricus	_	Argentina	AY383065	_
L. geometricus	_	USA: HI	AY383046	_
L. geometricus	_	USA: CA	KC414076	_
L. geometricus	_	USA: FL	AY383068	_
L. geometricus	_	USA: FL	AY383067	_
L. hasseltii	_	New Zealand	EF121037	_
L. hasseltii	_	New Zealand	EF121034	_
L. hasseltii	_	New Zealand	EF121033	_
L. hasseltii	_	New Zealand	EF121031	_
L. hasseltii	_	New Zealand	EF121032	_
L. hasseltii	_	New Zealand	EF121036	_
L. hasseltii	_	New Zealand	EF121035	_
L. hasseltii	_	Australia	KC414079	_
L. hasseltii	_	Australia	KC414078	_
L. hasseltii	_	Australia	KC414077	_
L. hesperus	ARA-0562	Mexico: Coahuila	OP652148	_
L. hesperus	ARA-0670	Mexico: BC	OP652149	OP686995
L. hesperus	ARA-0671	Mexico: BC	OP652150	OP686996
L. hesperus	ARA-0672	Mexico: BC	OP652151	OP686997
L. hesperus	ARA-0673	Mexico: BC	OP652152	OP686998
L. hesperus	ARA-0674	Mexico: BC	OP652153	OP686999

Table 2 (continued). Specimens sequenced for each species of *Latrodectus* Walckenaer, 1805, DNA voucher numbers, localities, and GenBank accession numbers (*CO1* and *ITS2*).

Species	DNA voucher LATLAX	Locality	GenBank accesion number	
			CO1	*ITS2*
L. hesperus	ARA-0677	Mexico: Sinaloa	OP652156	OP687002
L. hesperus	ARA-0679	Mexico: BCS	OP652157	OP687003
L. hesperus	ARA-0680	Mexico: BCS	OP652158	OP687004
L. hesperus	ARA-0681	Mexico: BCS	OP652159	OP687005
L. hesperus	ARA-0682	Mexico: BCS	OP652160	OP687006
L. hesperus	ARA-0683	Mexico: BCS	OP652161	OP687007
L. hesperus	ARA-0684	Mexico: BCS	OP652162	OP687008
L. hesperus	ARA-0685	Mexico: BCS	OP652163	OP687009
L. hesperus	ARA-0686	Mexico: Sonora	OP652164	OP687010
L. hesperus	ARA-0687	Mexico: Sonora	OP652165	OP687011
L. hesperus	ARA-0690	Mexico: Sonora	OP652166	OP687012
L. hesperus	ARA-0692	Mexico: BCS	OP652167	OP687013
L. hesperus	ARA-0693	Mexico: BCS	OP652168	OP687014
L. hesperus	ARA-0815	Mexico: Durango	OP652189	–
L. hesperus	ARA-0817	Mexico: Durango	OP652191	–
L. hesperus	ARA-0936	Mexico: Querétaro	OP652194	–
L. hesperus	ARA-0937	Mexico: Querétaro	OP652195	–
L. hesperus	ARA-0939	Mexico: Querétaro	OP652197	–
L. hesperus	ARA-0946	Mexico: SLP	OP652203	–
L. hesperus	ARA-0948	Mexico: SLP	OP652205	–
L. hesperus	ARA-0949	Mexico: SLP	OP652206	–
L. hesperus	ARA-0950	Mexico: SLP	OP652207	–
L. hesperus	ARA-0951	Mexico: SLP	OP652208	–
L. hesperus	ARA-0952	Mexico: SLP	OP652209	–
L. hesperus	ARA-0953	Mexico: SLP	OP652210	–
L. hesperus	ARA-0961	Mexico: Guanajuato	OP652218	OP687040
L. hesperus	ARA-0963	Mexico: Guanajuato	OP652220	OP687042
L. hesperus	–	USA: CA	KY017971	–
L. hesperus	–	USA: CA	MG299123	–
L. hesperus	–	USA: CA	MG298977	–
L. hesperus	–	USA: CA	MG298971	–
L. hesperus	–	USA: CA	MG299110	–
L. hesperus	–	unknown	MK420122	–
L. hesperus	–	USA: CA	MG299113	–
L. hesperus	–	USA: CA	MG299109	–
L. hesperus	–	USA: CA	MG298978	–
L. hesperus	–	USA: CA	MG299057	–
L. hesperus	–	USA: CA	MG299098	–
L. hesperus	–	USA: CA	MG299093	–
L. hesperus	–	USA: CA	MG298974	–
L. hesperus	–	USA: CA	MG299118	–
L. hesperus	–	USA: CA	MG298970	–
L. hesperus	–	USA: CA	MG299100	–
L. hesperus	–	unknown	DQ127326	–

Table 2 (continued). Specimens sequenced for each species of *Latrodectus* Walckenaer, 1805, DNA voucher numbers, localities, and GenBank accession numbers (*CO1* and *ITS2*).

Species	DNA voucher LATLAX	Locality	GenBank accesion number	
			CO1	***ITS2***
L. hesperus	–	USA: CA	KC414080	–
L. hesperus	–	USA: AZ	KC414081	–
L. hesperus	–	unknown	DQ127324	–
L. hesperus	–	USA: CA	MG299115	–
L. hesperus	–	unknown	DQ127317	–
L. hesperus	–	unknown	DQ127320	–
L. hesperus	–	unknown	DQ127316	–
L. hesperus	–	unknown	DQ127314	–
L. hesperus	–	USA: CA	MG299120	–
L. hesperus	–	USA: NM	AY383071	–
L. hesperus	–	USA: CA	AY383070	–
L. hesperus	–	Canada	HQ977141	–
L. hesperus	–	Canada	MF815806	–
L. hesperus	–	Canada	MF816543	–
L. hesperus	–	unknown	DQ127325	–
L. hesperus	–	unknown	DQ127323	–
L. hesperus	–	Canada	HQ977140	–
L. hesperus	–	Canada	KP656931	–
L. hesperus	–	Canada	KP656707	–
L. hesperus	–	Canada	KP652641	–
L. hesperus	–	Canada	KP649032	–
L. hesperus	–	Canada	KP646487	–
L. hesperus	–	Canada	HQ977093	–
L. hesperus	–	Canada	HQ977092	–
L. hesperus	–	Canada	HQ977091	–
L. hesperus	–	unknown	DQ127315	–
L. katipo	–	New Zealand	EF121028	–
L. katipo	–	New Zealand	EF121027	–
L. katipo	–	New Zealand	EF121023	–
L. katipo	–	New Zealand	EF121022	–
L. katipo	–	New Zealand	EF121009	–
L. katipo	–	New Zealand	EF121019	–
L. katipo	–	New Zealand	EF121018	–
L. katipo	–	New Zealand	EF121017	–
L. katipo	–	New Zealand	EF121013	–
L. katipo	–	New Zealand	EF121012	–
L. katipo	–	New Zealand	–	EF121057
L. mactans	ARA-0816	Mexico: Tamaulipas	OP652190	–
L. mactans	ARA-0942	Mexico: SLP	OP652200	–
L. mactans	ARA-0944	Mexico: SLP	OP652201	–
L. mactans	–	USA: MS	AY383072	–
L. mactans	–	USA: NC	AY383054	–
L. mactans	–	USA: NC	AY231046	–
L. mactans	–	unknown	DQ127321	–

Table 2 (continued). Specimens sequenced for each species of *Latrodectus* Walckenaer, 1805, DNA voucher numbers, localities, and GenBank accession numbers (*CO1* and *ITS2*).

Species	DNA voucher LATLAX	Locality	GenBank accesion number	
			CO1	***ITS2***
L. mactans	–	unknown	DQ127318	–
L. menavodi	–	Madagascar	AY383075	–
L. mirabilis	–	Argentina	AY383076	–
L. mirabilis	–	Argentina	AY383077	–
***L. occidentalis* sp. nov.**	ARA-0550	Mexico: Guerrero	OP652143	OP686989
***L. occidentalis* sp. nov.**	ARA-0559	Mexico: Jalisco	OP652169	OP686994
***L. occidentalis* sp. nov.**	ARA-0694	Mexico: Jalisco	OP652170	OP687015
***L. occidentalis* sp. nov.**	ARA-0696	Mexico: Jalisco	OP652171	OP687016
***L. occidentalis* sp. nov.**	ARA-0697	Mexico: Jalisco	OP652172	OP687017
***L. occidentalis* sp. nov.**	ARA-0698	Mexico: Jalisco	OP652173	OP687018
***L. occidentalis* sp. nov.**	ARA-0699	Mexico: Jalisco	OP652174	OP687019
***L. occidentalis* sp. nov.**	ARA-0701	Mexico: Jalisco	OP652175	OP687020
***L. occidentalis* sp. nov.**	ARA-0702	Mexico: Jalisco	OP652176	OP687021
***L. occidentalis* sp. nov.**	ARA-0703	Mexico: Michoacán	OP652177	OP687022
***L. occidentalis* sp. nov.**	ARA-0704	Mexico: Michoacán	OP652178	OP687023
***L. occidentalis* sp. nov.**	ARA-0705	Mexico: Michoacán	OP652179	OP687024
***L. occidentalis* sp. nov.**	ARA-0706	Mexico: Michoacán	OP652180	OP687025
***L. occidentalis* sp. nov.**	ARA-0707	Mexico: Michoacán	OP652181	OP687026
***L. occidentalis* sp. nov.**	ARA-0708	Mexico: Guerrero	OP652182	OP687027
***L. occidentalis* sp. nov.**	ARA-0709	Mexico: Guerrero	OP652183	OP687028
***L. occidentalis* sp. nov.**	ARA-0711	Mexico: Colima	OP652184	OP687029
***L. occidentalis* sp. nov.**	ARA-0712	Mexico: Colima	OP652185	OP687030
***L. occidentalis* sp. nov.**	ARA-0957	Mexico: Guanajuato	OP652214	OP687036
***L. occidentalis* sp. nov.**	ARA-0958	Mexico: Guanajuato	OP652215	OP687037
***L. occidentalis* sp. nov.**	ARA-0964	Mexico: Guanajuato	OP652221	OP687043
L. pallidus	–	Israel	AY383056	–
L. pallidus	–	Israel	AY383055	–
L. pallidus	–	Israel	KC414083	–
L. pallidus	–	Israel	KC414082	–
L. pallidus	–	Iraq	MG645012	–
L. renivulvatus	–	South Africa	AY383057	–
L. revivensis	–	Israel	AY383078	–
L. rhodesiensis	–	South Africa	AY383079	–
L. rhodesiensis	–	South Africa	AY383058	–
L. thoracicus	–	Chile	GU112105	–
L. thoracicus	–	Chile	GU112104	–
L. thoracicus	–	Chile	GU112103	–
L. thoracicus	–	Chile	GU112102	–
L. thoracicus	–	Chile	GU112098	–
L. thoracicus	–	Chile	GU112101	–
L. thoracicus	–	Chile	GU112099	–
L. thoracicus	–	Chile	GU112100	–
L. thoracicus	–	Iraq	MG645011	–
L. tredecimguttatus	–	Spain	AY383080	–

Table 2 (continued). Specimens sequenced for each species of *Latrodectus* Walckenaer, 1805, DNA voucher numbers, localities, and GenBank accession numbers (*CO1* and *ITS2*).

Species	DNA voucher LATLAX	Locality	GenBank accesion number	
			CO1	***ITS2***
L. tredecimguttatus	–	Israel	AY383081	–
L. tredecimguttatus	–	Iran	KJ787107	–
L. tredecimguttatus	–	unknown	KC414085	–
L. tredecimguttatus	–	unknown	KC414084	–
L. umbukwane	–	South Africa	MN094888	–
L. umbukwane	–	South Africa	MN094889	–
L. variegatus	–	Argentina	AY383084	–
L. variegatus	–	Argentina	AY383083	–
L. variolus	–	Canada	KP651212	–
L. variolus	–	USA: MD	AY383082	–
L. variolus	–	USA: SC	AY383059	–
Latrodectus sp.	–	Dom. Rep.	KC414075	–
Latrodectus sp. 1	ARA-0935	Mexico: Querétaro	OP652193	–
Latrodectus sp. 1	ARA-0940	Mexico: Querétaro	OP652198	–
Latrodectus sp. 1	ARA-0941	Mexico: Querétaro	OP652199	–
Latrodectus sp. 1	ARA-0954	Mexico: Querétaro	OP652211	OP687033
Latrodectus sp. 2	ARA-0495	Mexico: Tlaxcala	OP652138	OP686984
Latrodectus sp. 2	ARA-0496	Mexico: Tlaxcala	OP652139	OP686985
Latrodectus sp. 2	ARA-0497	Mexico: Tlaxcala	OP652140	OP686986
Latrodectus sp. 2	ARA-0499	Mexico: Tlaxcala	OP652141	OP686987
Latrodectus sp. 2	ARA-0544	Mexico: Oaxaca	OP652142	OP686988
Latrodectus sp. 2	ARA-0554	Mexico: Hidalgo	OP652144	OP686990
Latrodectus sp. 2	ARA-0556	Mexico: Hidalgo	OP652145	OP686991
Latrodectus sp. 2	ARA-0557	Mexico: Hidalgo	OP652146	OP686992
Latrodectus sp. 2	ARA-0558	Mexico: Hidalgo	OP652147	OP686992
Latrodectus sp. 2	ARA-0675	Mexico: Sinaloa	OP652154	OP687000
Latrodectus sp. 2	ARA-0676	Mexico: Sinaloa	OP652155	OP687001
Latrodectus sp. 2	ARA-0812	Mexico: Durango	OP652186	OP687031
Latrodectus sp. 2	ARA-0813	Mexico: Durango	OP652187	–
Latrodectus sp. 2	ARA-0814	Mexico: Durango	OP652188	OP687032
Latrodectus sp. 2	ARA-0819	Mexico: Durango	OP652192	–
Latrodectus sp. 2	ARA-0938	Mexico: Querétaro	OP652196	–
Latrodectus sp. 2	ARA-0945	Mexico: SLP	OP652202	–
Latrodectus sp. 2	ARA-0947	Mexico: SLP	OP652204	–
Latrodectus sp. 2	ARA-0955	Mexico: Guanajuato	OP652212	OP687034
Latrodectus sp. 2	ARA-0956	Mexico: Guanajuato	OP652213	OP687035
Latrodectus sp. 2	ARA-0959	Mexico: Guanajuato	OP652216	OP687038
Latrodectus sp. 2	ARA-0960	Mexico: Querétaro	OP652217	OP687039
Latrodectus sp. 2	ARA-0962	Mexico: Guanajuato	OP652219	OP687041
Steatoda borealis	–	Canada	KM826113	–

***p*-distances under Neighbor Joining (NJ)**

A genetic distances tree was reconstructed using MEGA ver. 10.1.7 software (Kumar *et al*. 1994), with the following commands: Number of replicates = 1000, Bootstrap support values = 1000 (significant values ≥50%), Substitution type = nucleotide, Model = *p*-distance, Substitution to include = d: Transitions + Transversions, Rates among sites = Gamma distributed with invariant sites (G+I), Missing data treatment = Pairwise deletion.

Automatic Barcode Gap Discovery (ABGD)

The aim of this method is to find gaps in genetic divergence, considering that the intraspecific genetic variation is smaller than the interspecific divergences. This method first generates an initial data partition into putative species (Initial partitions IP). Then, these initial partitions are recursively partitioned until there is no further partitioning of the data (Recursive partitions RP). ABGD analyses were carried out on the online platform (https://bioinfo.mnhn.fr/abi/public/abgd/) using the following options: K2P distances non-corrected, Pmin = 0.001, Pmax = 0.1, Steps = 10, Relative gap width (X) = 1, Nb bins = 20.

Assemble Species by Automatic Partitioning (ASAP)

This is an ascending hierarchical clustering method in which the sequences are merged into groups that are successively further merged until all sequences form a single group. Partitions are the equivalent to each sequence merge step, then the software analyzes all partitions and scores the most probably groups into a topology or tree (Puillandre *et al*. 2021). ASAP analyses were run on the online platform (https://bioinfo.mnhn.fr/abi/public/asap/) using Kimura (K80) distance matrices under the following parameters: Substitution model = *p*-distances, Probability = 0.01, Best scores = 10, Fixed seed value = –.

General Mixed Yule Coalescent (GMYC)

Using ultrameric trees as input, this approach applies single (Pons *et al*. 2006) or multiple (Monaghan *et al*. 2009) time thresholds to delimit species in a Maximum Likelihood context (Ortiz & Francke 2016). The phylogenetic analyses were carried out in the software BEAUti and BEAST ver. 1.10.4 (Drummond *et al.* 2012) using a coalescent (constant population) tree prior to generating ultrameric trees. An uncorrelated independent log normal clock was applied to each partition with their respective evolution model and substitution rates (*CO1*: GTR+I+G; *ITS2*: K2P; 28S: GTR+I+G). Five independent replicates of 40 million iterations were run for the analyses. Tracer ver. 1.6 (Rambaut *et al.* 2018) was used to evaluate convergence values, with the ESS (Effective Sample Size) > 200. Tree Annotator ver. 2.6.0 (a BEAST package) was used to construct maximum credibility of clades trees, after discarding the first 25% of each of the five independent run as burn-in. The GMYC method was carried out using the online platform (https://species.h-its.org/gmyc/), which uses the original R implementation of the GMYC model (Fujiwasa & Barraclough 2013).

Bayesian Poisson Tree Processes (bPTP)

This molecular delimitation method is similar to GMYC; however, rather than using an ultrametric tree as input, the models of speciation rate are implemented directly using the numbers of substitutions calculated from the branch lengths. The Bayesian (BI) and Maximum Likelihood (ML) variants were carried out on the online version (https://species.h-its.org/ptp/), with the following parameters: Rooted tree, MCMC = 1 000 000, Thinning = 100, Burn-in = 0.1, Seed = 123. Trees from all analyses were edited with the iTOL online version (https://itol.embl.de/) (Letunic & Bork 2021) and Photoshop CS6.

Following Carstens *et al.* (2013), we used the congruence integration criteria to delimit different species, which is based on the correspondence among different molecular methods to generate a high support for species hypotheses. When the information and results of different molecular methods are incongruent, we make conservative assumptions regarding the delimitation of putative species, so we selected as different species when all the methods where congruent delimiting the species.

A haplotypes network for *CO1* was constructed to visualize the mutations among haplotypes of species using the TCS algorithm (Clement *et al*. 2002) in PopArt ver. 1.7 (Leigh & Bryant 2015) and edited using Adobe Photoshop CS6.

Morphological analyses

For the lineal morphometry, 124 adult specimens (36 males and 88 females) of the five putative species of *Latrodectus* from Mexico observed in this study were dissected and measured. The analyzed features included: 1) angle of the spermathecae (Supp. file 1A); 2) number of turns on the embolus; 3) length and 4) width of the genital opening on females (Supp. file 1B); 5) length and 6) width of the female carapace (Supp. file 1C); 7) length and 8) width of the sternum (Supp. file 1D); 9) length and 10) width of the femur of legs I and IV; 11) length and 12) width of the patella+tibia of legs I and IV (Supp. file 1E). For legs and carapace measurements, the coefficient "T" (length/width of the carapace) and "TT" ([patellar length+tibia]/length of the carapace) of legs I and IV were obtained, which have been used for species description (Melic 2000; Aguilera *et al*. 2009). The coefficient of each measured structure was also obtained (length/width). All measurements are in millimeters (mm) and only taken from adult specimens of both sexes. The RStudio ver. 1.4.1106 program was used to perform normality (Shapiro-Wilk) and equality of variances (Levene) tests to explore the distribution of the data and implement the corresponding analysis. Due to the nature of the data (non-normal), a non-parametric Kruskal-Wallis test was implemented to analyze the measurements of the different structures among the putative species.

Species Distribution Models (SDM)

Species Distribution Models (SDM) were carried out for *L. mactans*, *L. hesperus* and *L. occidentalis* Valdez-Mondragón sp. nov. Species records were obtained from the CNAN and LATLAX databases, Institute of Biology, UNAM; the Global Biodiversity Information Facility (GBIF) (www.gbif.org); and from 19 field trips to 28 states along Mexico between 2017 and 2022 as was previously mentioned. To avoid spatial autocorrelation, spatial filtering of the records within a radius of 10 km^2 was performed for *L. mactans* and *L. hesperus* using the "Wallace" ver. 1.1.3 package in RStudio (Kass *et al*. 2022). Since few records (15) exist of *L. occidentalis*, spatial filtering for this species was set to 5 km^2 to reduce the loss of occurrence records. The temporality of the records with climatic variables is another important factor in the creation of the SDM, and so records were separated into two databases: (1) including all records whose dates correspond to the time interval of the climatic variables (Cortez-Roldán 2022), and (2) including the remainder of the records. To increase the number of usable records (>10) in the SDM, records outside the time interval of the climatic variables were recovered (altitude, average annual temperature, annual precipitation and isothermality) corresponding spatially and ecologically with the records of the first database in RStudio ver. 2022.02.1. For georeferencing and corroborating localities, two programs were used: GeoLocate online version (http://www.geo-locate.org/web/WebGeoref.aspx/) and Google Earth ver. 7.1.5.1557. Geographic coordinates were transformed from NAD83 to WGS84 online on INEGI, and geographical coordinates are given in degrees. The SDM data were generated using the "Kuenm" ver. 1.1.7 package in RStudio (Cobos *et al*. 2019). For the SDM of *L. occidentalis*, 15 bioclimatic variables from Mexico proposed by Cuervo-Robayo *et al*. (2013) were used, with an interval of years spanning from 1910–2009. These layers were downloaded from the web page: http://idrisi.uaemex.mx/distribucion/superficies-climaticas-para-mexico. For the SDM of *L. mactans* and *L. hesperus*, 15 climate layers from WorldClim ver. 2.1 were downloaded, spanning the interval from 1970–2000, as well as an elevation layer, available on https://www.worldclim.org/data/worldclim21.html (Fick & Hijmans 2017). From the two sets of bioclimatic variables downloaded with a resolution of 30s (~1 km^2), the variables Bio8, Bio9, Bio18, and Bio19 were excluded, since they show spatial anomalies (Escobar *et al*. 2014; Marques *et al.* 2020) (Table 3). The selection of sets of variables for each species were determined based on Analysis of Inflation Factors (AIF) <10 (Set 1), Contribution Percentage >5% (Set 2), and Jacknife of AUC (Area Under the Curve) >0.56 (Set 3), with the first run in RStudio

Table 3. Bioclimatic variables used in the Species Distribution Models (SDM). [a] = sets of variables selected for the SDM of *Latrodectus mactans* (Fabricius, 1775); [b] = sets of variables selected for the SDM of *L. occidentalis* Valdez-Mondragón sp. nov. [c] = sets of variables selected for the SDM of *L. hesperus* Chamberlin & Ivie, 1935.

Acronym	Description
Bio1	Annual mean temperature
Bio2 [a, b, c]	Mean diurnal range
Bio3 [a, c]	Isothermality
Bio4 [b]	Temperature seasonality
Bio5 [a, b, c]	Max temperature of the warmest month
Bio6 [b]	Min temperature of the coldest month
Bio7 [b]	Temperature Annual Range
Bio10 [b]	Mean Temperature of the warmest quarter
Bio11	Mean Temperature of the coldest quarter
Bio12 [b, c]	Annual precipitation
Bio13 [a, b]	Precipitation of the wettest month
Bio14 [c]	Precipitation of the driest month
Bio15 [a, c]	Precipitation seasonality
Bio16 [b]	Precipitation of the wettest quarter
Bio17	Precipitation of the driest quarter

ver. 2022.02.1 and the latter two using Maxent ver. 3.4.1 (Philips *et al*. 2006; Cobos *et al*. 2019b). The delimitation of the calibration area (M) for each species was obtained from the presence records with respect to the Ecoregions of Mexico and the United States downloaded from the website: Terrestrial Ecoregions of the World (worldwildlife.org) (Olson *et al*. 2001). The calibration area and the cut of the climatic variables were carried out in RStudio. For the creation of the candidate models, two runs were made with different values of the regularization multiplier as suggested by Cobos *et al.* (2019b) using the "Kuenm" ver. 1.1.7 package for RStudio. In order to the first analysis, all possible combinations of linear (l), quadratic (q), product (p), threshold (t), and hinge (h) features were tested with different regularization multipliers (1, 2, 3, 4, 5, 6, 7, 8, 9, and 10). The second analysis was performed with the same combinations, but with finer regularization multipliers (intervals of 0.1) within the threshold of the values selected in the first run. The extrapolation analyses were carried out with the "Kuenm_mmop" function available in the package used to elaborate the SDMs (Cobos *et al.* 2019a).

Results

Molecular analyses of *p* genetic distances under Neighbor Joining (NJ)

The analyzed matrix of *CO1* includes 213 terminals of 25 putative species of the genus *Latrodectus* (Fig. 1). Specimens used in this study, including GenBank accession numbers and localities of the sequences used, are listed in Table 1. In this phenetic analysis under *p* genetic distances, two large groups are recovered: the *geometricus* "clade" (Fig. 1, red box) and the *mactans* "clade" (Fig. 1, blue box), with significant bootstrap statistical support values of 60% and 80%, respectively. Based on the barcoding criterion of 2%, 25 groups corresponding to 25 putative species were recovered. Most terminals from other regions of the world form groups with bootstrap values ≥ 90%, with interspecific *p* genetic distances > 2%, recovering several species already described (e.g., *L. geometricus*, *L. rhodesiensis*, *L. umbukwane*,

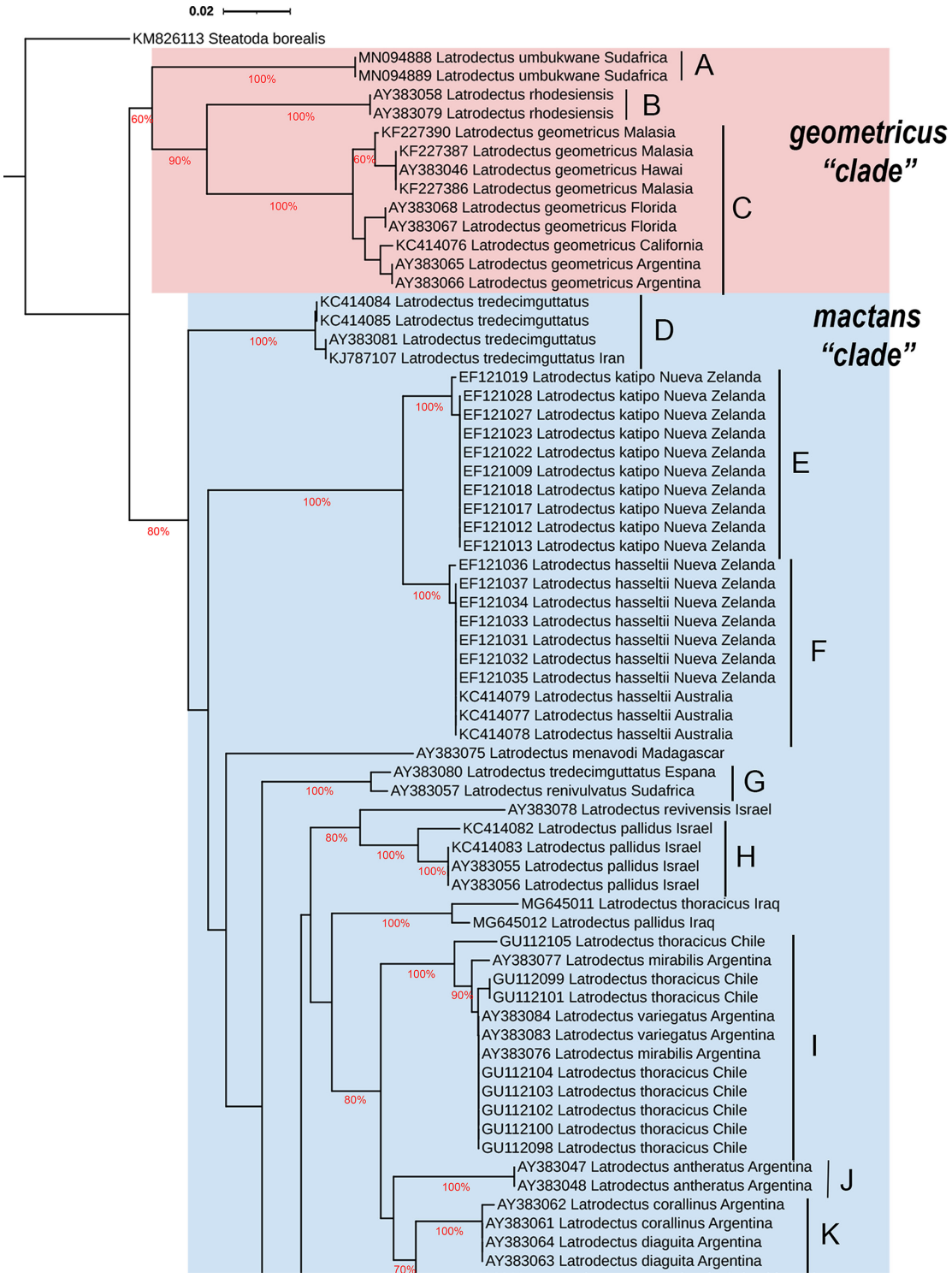

Fig. 1 (continued on next two pages). Neighbour–Joining (NJ) tree constructed with *p* distances of *CO1* barcode sequences from different specimens and species of *Latrodectus* Walckenaer, 1805. Colors in the branches indicate species (grey box), yellow branches indicate the new species (*L. occidentalis* Valdez-Mondragón sp. nov.). Abdomen dorsal and ventral patterns (numbers 1 and 2, respectively) and spermathecae and epigyna (numbers 3 and 4, respectively) of females are shown only for Mexican species. Numbers on branches represent bootstrap support values (>50% significant). Letters beside the groups are described and discussed in the text.

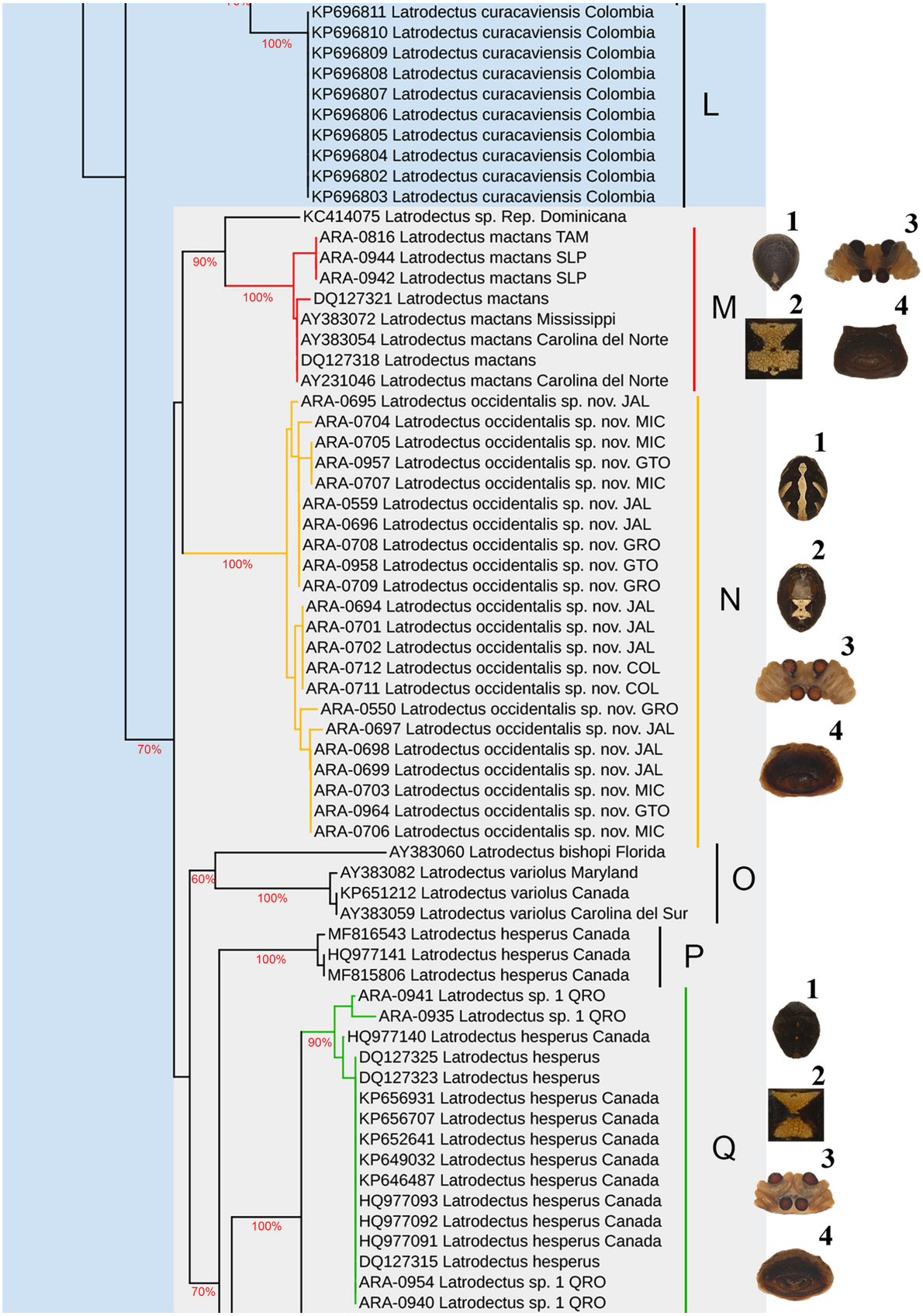

Fig. 1 (continued).

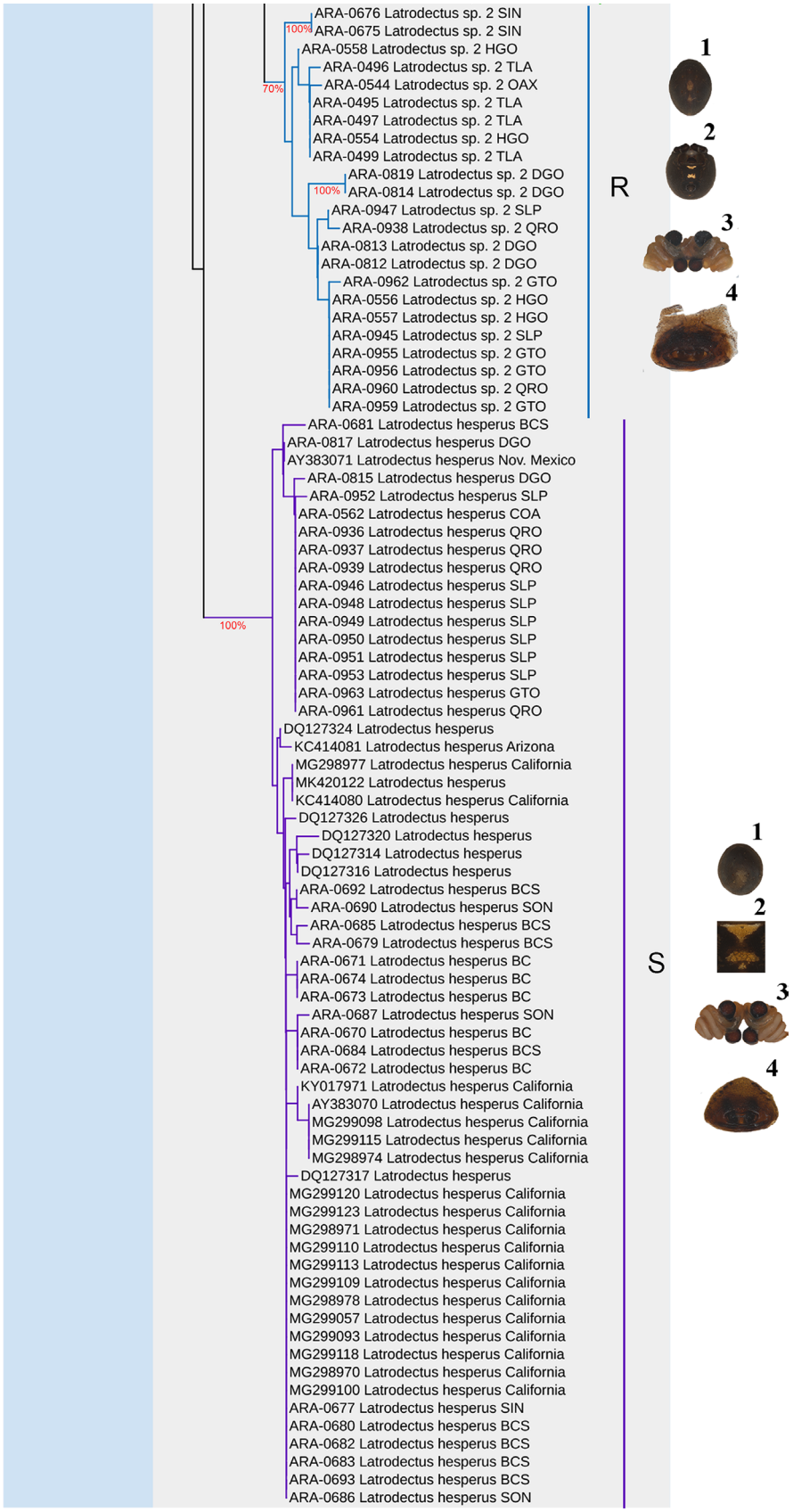

Fig. 1 (continued).

L. katipo, *L. hasseltii*, *L. curacaviensis*, *L. antheratus*, *L. mactans*), including *L. occidentalis* sp. nov. (Fig. 1; Appendix 1).

Within the *mactans* "clade", *L. tredecimguttatus* is divided into two groups, group D with a high bootstrap value (100%) and an intraspecific genetic distance of 0.2% (Fig. 1), and group G composed of two terminals containing *L. tredecimguttatus* and *L. renivulvatus*, and an intraspecific genetic distance of 0.1%. The genetic distance between groups D and G within *L. tredecimguttatus* is 7%, being samples from Iran and Spain (Appendix 1). Similar to *L. tredecimguttatus*, not all terminals of *L. pallidus* were found grouped together. Three of the four terminals from Israel are grouped with high bootstrap value (100%) and an intraspecific genetic distance of 1% (group H), while one terminal from Iraq groups with another *L. thoracicus* also from Iraq with an interspecific genetic distance of 2.5% between them (Fig. 1). The intraspecific genetic distance between *L. pallidus* from Iraq and group H from Israel is 9% (Fig. 1, Appendix 1). The terminals of *L. thoracicus* from Chile are grouped with terminals of *L. mirabilis* and *L. variegatus* from Argentina (group I) with high bootstrap support (100%), showing intra- and interspecific distances of 0.5% and 5%, respectively (Fig. 1). Group K is composed of *L. corallinus* and *L. diaguita* from Argentina, with high 100% bootstrap support and an intraspecific genetic distance of 0.1% and interspecific distance > 5% (Fig. 1, Appendix 1).

Regarding the terminals from North America in the *CO1* tree (Fig. 1, gray box), *L. mactans* from the United States groups with terminals from Mexico, the states of Tamaulipas and San Luis Potosi (Fig. 1, group M). These terminals showed an intraspecific genetic distance of 0.4% and high bootstrap support of 100% (group M, red branch Fig. 1). Terminals of *L. occidentalis* sp. nov. (group N, yellow lines Fig. 1) have an intraspecific variation of 0.5% with a high bootstrap value of 100% and an interspecific genetic distance > 6% (Fig. 1; Appendix 1). *Latrodectus hesperus* had the highest number of terminals used in the analysis (Fig. 1), yet the species was found to be composed of three different groups (P, Q, S), with average genetic distances between groups > 6%. Terminals of *L. hesperus* from Canada form two distinct groups, the first with three terminals (group P) and an intraspecific genetic distance of 0.2% and high bootstrap support (100%, Fig. 1). Group Q (green branch) includes sequences from Canada and four sequences from Querétaro, Mexico, with an average intraspecific genetic distance of 0.3% and an interspecific distance of 6.7% with respect to group P (Fig. 1). Group Q of *L. hesperus* groups with group R (blue branch) with a high a bootstrap value of 100%. Group R includes several populations from an undetermined species (*Latrodectus* sp. 2) from the central region of Mexico, including the states of: Durango, Guanajuato, Hidalgo, Oaxaca, Querétaro, San Luis Potosí, Sinaloa, and Tlaxcala. Group R shows an intraspecific genetic variation of 1%, and 2.9% genetic distance from group Q (Fig. 1). Comprising group S (purple branch) are terminals of *L. hesperus* from the United States and terminals from Mexico (Baja California, Baja California Sur, Coahuila, Durango, Guanajuato, Querétaro, San Luis Potosi, Sinaloa and Sonora), with an average intraspecific genetic distance of 0.8%, and interspecific variation > 6% with respect to groups P, Q, and R (Fig. 1, Appendix 1).

The analyzed matrix of *ITS2* includes 58 terminals of specimens only from Mexico (Fig. 2). Since no GenBank sequences have been published for North American species at the *ITS2* marker, all sequences in these analyses were generated for this study. Three species are recovered: *L. occidentalis* sp. nov. (group A, yellow box), *L. hesperus* (group E, blue box), and *Latrodectus* sp. 1 + *Latrodectus* sp. 2 (groups C and D) (Fig. 2). Overall, the *ITS2 p* distance analysis with NJ shows less resolution than the *CO1* analysis and does not recover the same topology and groups of putative species for the Mexico samples (Figs 1–2). However, *L. occidentalis* (Fig. 2) was recovered with a high bootstrap support in both analyses (75% in *ITS2* and 100% in *CO1*). Terminals in this clade come from the Mexican states of Guerrero, Jalisco, Michoacán, Colima, and Guanajuato (Fig. 2). Group B is composed of eight terminals of *Latrodectus* sp. 2 from the states of Durango and Guanajuato (Fig. 2). Groups C and D are composed of terminals of the species *Latrodectus* sp. 2 as well as on individual of *L. hesperus*. In addition, group

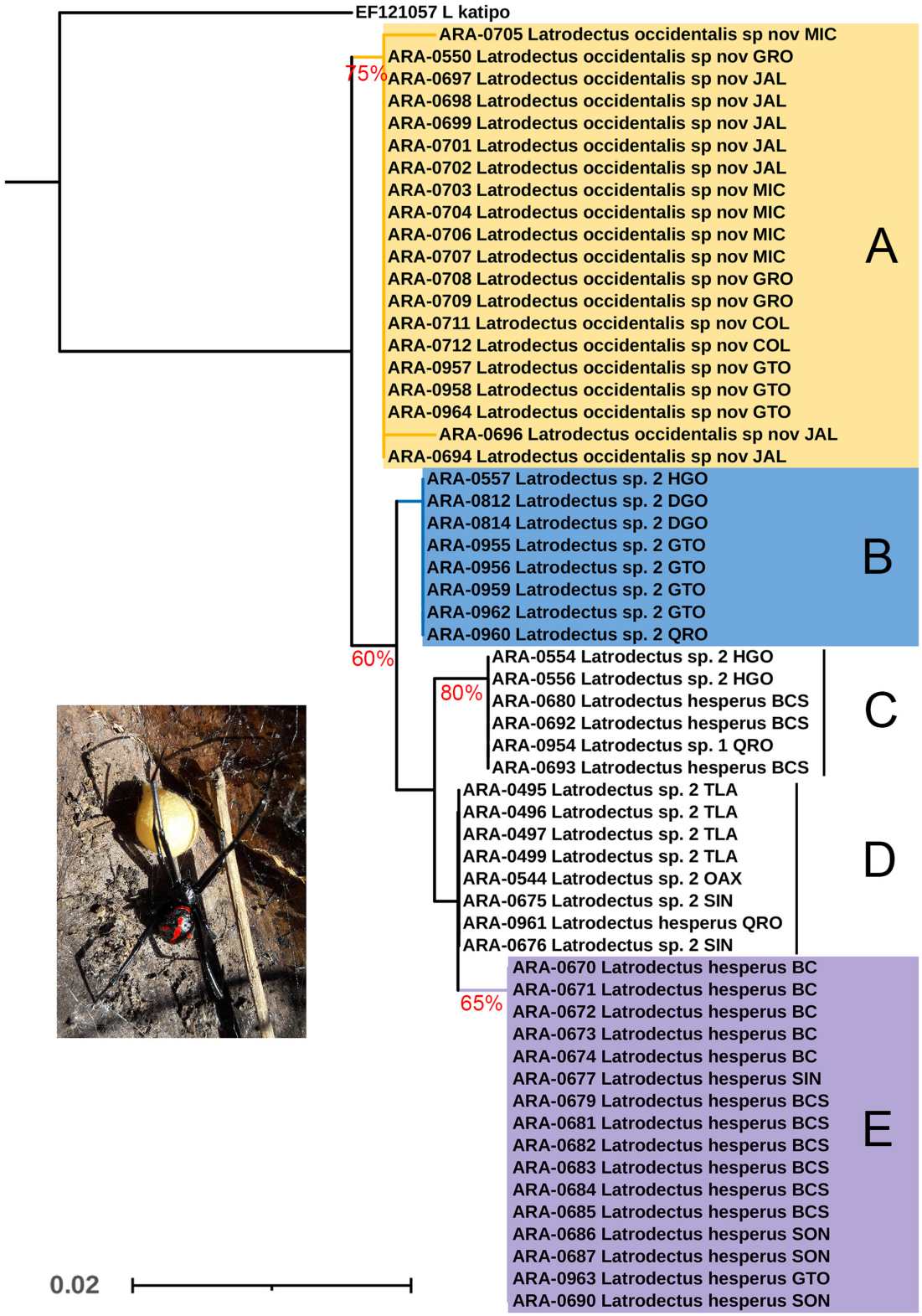

Fig. 2. Neighbour-Joining (NJ) tree constructed with *p* distances tree of *with ITS2* barcode sequences from different specimens and species of *Latrodectus* Walckenaer, 1805 from Mexico only. Branch and box colors indicate putative species. Percentages on branches represent bootstrap support values (>60% significant). Letters beside groups are described and discussed in the text.

C contains one terminal of *Latrodectus* sp. 1 (ARA-0954) from Querétaro, with a bootstrap value of 80% (Fig. 2). Group E, with a bootstrap value of 65%, is composed entirely of terminals pertaining to *L. hesperus* from Baja California, Baja California Sur, Sinaloa, Sonora, and Guanajuato (Fig. 2).

Species delimitation analyses under *COI+ITS2*

In addition to the single locus species delimitation analyses, concatenated analyses (*COI+ITS2*) were run using only populations/species from Mexico (Fig. 3). Using a Bayesian Inference (BI) tree, the four different molecular methods for species delimitation, including the *p* genetic distances (NJ), were congruent among most methods (Fig. 3). The analyses recovered five putative species with high Posterior Probabilities (PP) support values of 100% under BI: *L. mactans*, *L. occidentalis* sp. nov., *Latrodectus* sp. 1, *Latrodectus* sp. 2, and *L. hesperus* (Fig. 3).

The barcoding methods ASAP and ABGD (IP and RP) were congruent in recovering four species: *L. mactans*, *L. occidentalis* sp. nov., [*Latrodectus* sp. 1 + *Latrodectus* sp. 2], and *L. hesperus* (Fig. 3). The GMYC and PTP analyses were incongruent in the number of species recovered, with GMYC recovering seven species, and PTP recovering 11 and 13 species with the ML and BI analyses, respectively (Fig. 3). *Latrodectus mactans* is recovered as a single species in all methods except PTP (IB), where the terminals from the Unites States and Mexico are separated into two different species. Only *L. occidentalis* sp. nov. was recovered as a distinct species in all four molecular methods, including the *p* genetic distances under NJ (Fig. 3).

As the mitochondrial marker *CO1* is of maternal inheritance and lacking recombination, a haplotype network was generated for populations/species from Mexico: *L. mactans*, *L. occidentalis* sp. nov., *Latrodectus* sp. 1, *Latrodectus* sp. 2 and *L. hesperus* (Fig. 4). From the sampled populations of these putative species: 2, 12, 3, 13, and 23 haplotypes were recovered, respectively (Supp. file 2). An average of 21 mutations among the putative species is observed (Fig. 4). *Latrodectus* sp. 1 and sp. 2 are separated by only 8 mutations, whereas *L. occidentalis* sp. nov. and *L. hesperus* are separated by 30 mutations (Fig. 4).

Morphological analyses and sexual dimorphism

For the linear morphometry, 20 measurements were obtained from males (Table 4) and 24 from females (Table 5) of the next structures: 1) carapace, 2) sternum, 3) legs I and IV, and 4) female epigyna. Due to the reduced number of males and females of *Latrodectus* sp. 1 and males of *L. mactans*, neither species was included in the analyses. Of the five species, *Latrodectus* sp. 1 is the species with the largest males, with a carapace of up 3 mm, whereas the smallest males belong to *L. hesperus* (Table 4). *Latrodectus* sp. 2 is the species with the largest females, with an average carapace length of 4.18 mm, and *L. hesperus* once again is the species with the smallest specimens, with females having a carapace length of 3.43 mm (Table 5). Females of *L. occidentalis* sp. nov. have the longest leg I compared to the other putative species (Table 5).

Sexual dimorphism is marked in all five species, with the females of *L. mactans*, *L. occidentalis* sp. nov., and *Latrodectus* sp. 1 being between 1.2 and 1.8 times as large as their male counterparts. Females of *Latrodectus* sp. 2 and *L. hesperus* have carapaces more than twice (2.07 and 2.24 respectively) the size of their male counterparts (Tables 4–5). However, males of all five species have proportionally longer legs I than females, with the tibia-patella twice as long as the carapace (TT1) in the males of *L. mactans*, *Latrodectus* sp. 1, *Latrodectus* sp. 2, and *L. hesperus*, and more than three times as long in males of *L. occidentalis* (Table 4). Compared to males, the proportions of tibia-patella I and carapaces in females is no longer than 2.0 in all five putative species (Table 5).

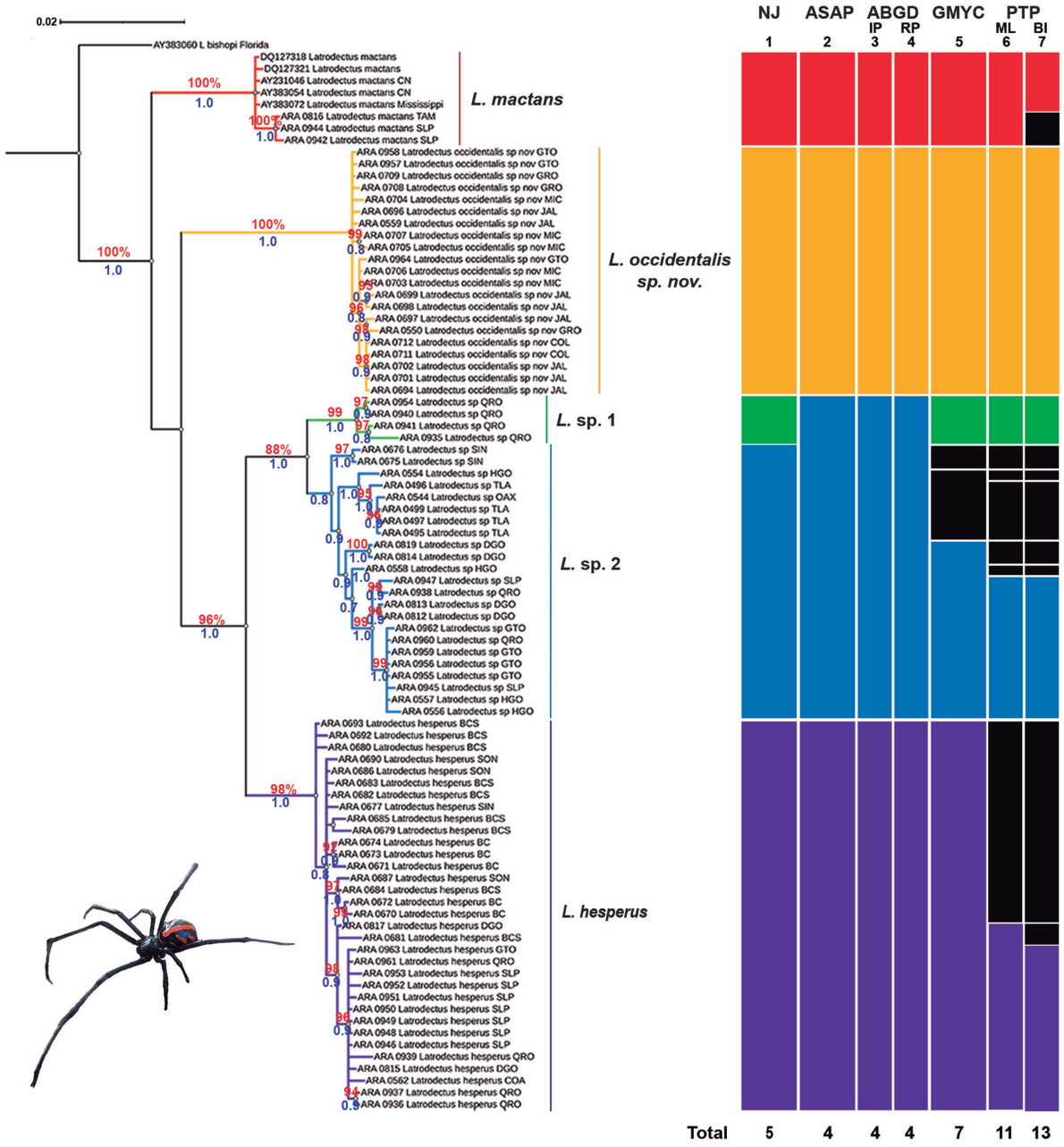

Fig. 3. Bayesian Inference tree (BI) constructed with the concatenated matrix (*CO1* + *ITS2*) of barcode sequences of *Latrodectus* Walckenaer, 1805 from Mexico. Branch colors indicate putative species and correspond to vertical bars, which represent different species delimitation methods used for their validation. Numbers below bars represent the number of species recovered in each species delimitation method (not considering the outgroup: *L. bishopi*): 1: Neighbor-Joining (NJ); 2: ASAP; 3: ABGD with initial partitions (IP); 4: ABGD with recursive partitions (RP); 5: GMYC; 6: bPTP with ML; 7: bPTP with IB; Numbers above branches are bootstrap support values under NJ (>50% significant), number below branches are posterior probabilities (PP) support values under BI (>95% significant).

Regarding the females of the four putative species analyzed, *L. mactans* and *L. occidentalis* sp. nov. show the greatest statistical differences, with significant differences in 15 of the 24 measurements analyzed (Table 6). Females of *L. mactans* had statistical differences with *Latrodectus* sp. 2 in the femur IV coefficient and length of the genital opening of the epigyna (Figs 5–6), and with *L. hesperus* in the tibia-patella I and IV coefficients, femur IV length, and the TT4 coefficient (Figs 5–6). Between females of *L. occidentalis* and *Latrodectus* sp. 2, statistical differences were found in all measurements except in the genital structures (Figs 5, 6). Differences between females of *L. occidentalis* and *L. hesperus* were seen in the tibia-patella I coefficient, the three femur I measurements, the femur IV coefficient, the TT1 coefficient, and the length and width of the genital opening of the epigyna (Figs 5–6). Females of *L. hesperus* and *Latrodectus* sp. 2 showed differences in the coefficients of the sternum, tibia-patella I and IV, femur I and IV, TT1 and TT4, and the femur I and IV lengths (Figs 5–6).

Fifteen measurements presented significant differences ($p < 0.05$) in both males and females for all species (Table 6). Males of *L. occidentalis* sp. nov. had significant differences to those of *Latrodectus* sp. 2 and *L. hesperus* in the tibia-patella length of the legs, the femur lengths of legs II and IV, and the coefficient of the tibia-patella I (Figs 7–8). Males of *L. occidentalis* sp. nov. showed differences in the carapace width when compared to those of *L. hesperus*, and the TT4 coefficient with *Latrodectus* sp. 2 (Figs 7–8). Males of *Latrodectus* sp. 2 had significant differences with males of *L. occidentalis* and *L. hesperus* in the femur I and IV coefficients, the tibia-patella IV, and the sternum and TT1

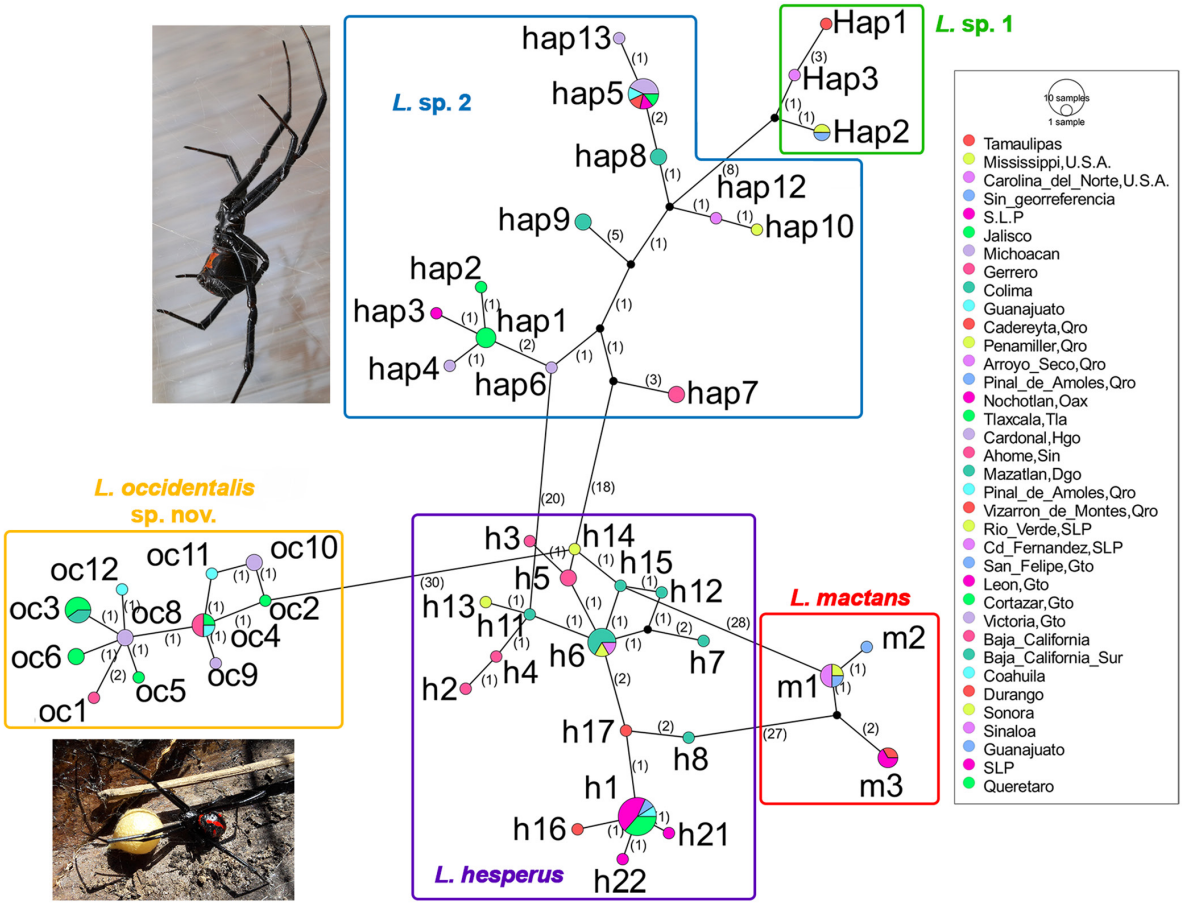

Fig. 4. Haplotype network from CO1 data obtained with TCS using PopArt. Circles represents haplotypes found within each populations/species (squares) of *Latrodectus* Walckenaer, 1805 in Mexico. Numbers on branches and between parenthesis indicate the number of mutations between haplotypes.

Table 4. Average linear measurements (mm) analyzed of male specimens from the putative species of *Latrodectus* Walckenaer, 1805 in Mexico recorded in this study. Values in parentheses represent minimum and maximum. "T" = length/width of carapace. "TT" = Tibia-Patella length of legs I or IV.

	Males				
	L. mactans	***L. occidentalis*** sp. nov.	***Latrodectus*** sp. 1	***Latrodectus.*** sp. 2	***L. hesperus***
Carapace length	2.28	2.11 (1.82–2.53)	2.5–3.03	2.01 (1.46–2.5)	1.8 (1.34–2.62)
Carapace width	1.85	1.78 (1.5–2.075)	2.2–2.656	1.68 (1.28–1.94)	1.43 (1.1–2.02)
T coefficient	1.232	1.19 (1.08–1.25)	1.136–1.141	1.19 (1.06–1.3)	1.25 (1.19–1.29)
Sternum length	1.12	1.11 (1–1.2)	1.4–1.68	1.1 (0.96–1.18)	0.93 (0.78–1.16)
Sternum width	1.12	1 (0.8–1.24)	1.28–1.507	1 (0.6–1.28)	0.89 (0.7–1.16)
Coefficient sternum	1	1.23 (1.16–1.35)	1.093–1.114	1 (0.75–1.09)	1.13 (1.11–1.16)
Tibia-Patella I length	5.625	5.77 (5.31–6.8)	6.125–7.68	4.54 (3.56–5.68)	4.64 (3.32–7.04)
Tibia-Patella I width	0.36	0.34 (0.3–0.4)	0.437–0.55	0.3 (0.22–0.36)	0.29 (0.22–0.42)
Tibia-Patella I coefficient	15.625	16.73 (15.8–18.01)	13.963–14	13.86 (11–16.18)	15.5 (15.09–15.83)
Femur I length	5	5.34 (4.8–6.16)	5.437–6.96	3.99 (3.12–5.12)	4.24 (3.12–6.4)
Femur I width	0.42	0.38 (0.36–0.46)	0.562–0.675	0.4 (0.28–0.5)	0.34 (0.24–0.54)
Femur I coefficient	11.904	13.88 (13.21–15.45)	9.666–10.311	9.91 (8.36–11.42)	11.99 (11.19–12.85)
TT1 coefficient	2.467	2.76 (2.56–2.95)	2.45–2.533	2.26 (2.02–2.52)	2.58 (2.37–2.68)
Tibia–Patella IV length	4.35	4.20 (3.75–5)	4.8–6.187	3.59 (2.65–4.56)	3.46 (2.27–5.31)
Tibia–Patella IV width	0.24	0.365 (0.3–0.44)	0.487–0.562	0.33 (0.22–0.44)	0.23 (0.22–0.26)
Tibia–Patella IV coefficient	18.125	11.53 (10.93–12.5)	9.846–11	10.22 (9.7–10.65)	11.21 (10.34–12.07)
Femur IV length	4.55	4.49 (4.05–5.37)	4.95–6.16	3.8 (3.52–4.05)	3.68 (2.45–5.68)
Femur IV width	0.38	0.34 (0.24–0.44)	0.475–0.575	0.36 (0.24–0.44)	0.27 (0.22–0.42)
Femur IV coefficient	11.973	13.35 (11.31–17.29)	10.421–10.713	9.96 (8.85–11.45)	12.64 (9.42–16.66)
TT4 coefficient	1.907	2 (1.9–2.16)	1.92–2.041	1.78 (1.63–1.95)	1.89 (1.67–2.02)

Table 5. Average linear measurements (mm) analyzed of female specimens from the putative species of *Latrodectus* Walckenaer, 1805 in Mexico recorded in this study. Values in parentheses represent minimums and maximums. "T" = Length/Width of the Cephalothorax. "TT" = Tibia-Patella length of legs I or IV.

	Females				
	L. mactans	***L. occidentalis*** sp. nov.	***Latrodectus*** sp. 1	***Latrodectus*** sp. 2	***L. hesperus***
Carapace length	4.11 (3.8–4.45)	4.03 (3.68–4.5)	3.56–3.96	4.18 (3.81–4.87)	4.04 (3.43–4.56)
Carapace width	3.53 (3.16–3.76)	3.6 (3.2–3.95)	3.062–3.36	3.76 (3.2–4.55)	3.56 (2.96–4.2)
T coefficient	1.13 (1.1–1.67)	1.11 (0.98–1.22)	1.162–1.178	1.09 (0.98–1.22)	1.13 (1.01–1.22)
Sternum length	2.15 (2.07–2.31)	2.22 (2.02–2.4)	1.84–2	2.21 (1.9–2.5)	2.18 (1.77–2.5)
Sternum width	1.94 (1.82–2.02)	1.87 (1.7–2.12)	1.62–1.82	1.96 (1.7–2.32)	1.88 (1.6–2.3)
Sternum coefficient	1.13 (1.06–1.21)	1.18 (1.1–1.3)	1.136–1.099	1.11 (1.03–1.19)	1.15 (1.07–1.29)
Tibia-Patella I length	7.08 (6.56–7.8)	7.96 (6.4–9.1)	6.96–6.88	7.06 (6.06–8.4)	7.56 (6.48–8.7)
Tibia-Patella I width	0.72 (0.68–0.76)	0.68 (0.64–0.75)	0.675–0.725	0.68 (0.6–0.76)	0.69 (0.6–0.8)
Tibia-Patella I coefficient	10.01 (9.37–10.54)	11.67 (10.16–12.71)	10.311–9.49	9.82 (9.04–10.23)	10.88 (9.77–12)
Femur I length	6.49 (5.68–7.04)	7.74 (6.24–9.1)	6.4–6.48	6.22 (5.81–6.88)	7.09 (6.08–8.1)
Femur I width	0.85 (0.78–0.9)	0.81 (0.76–0.86)	0.8–0.838	0.9 (0.76–1.06)	0.87 (0.74–1.02)
Femur I coefficient	7.7 (7.52–8)	9.79 (8.85–11.06)	7.642–8.1	6.87 (6.36–7.64)	8.06 (7.51–8.86)
TT1 coefficient	1.69 (1.65–1.73)	2 (1.56–2.36)	1.737–1.955	1.71 (1.51–2)	1.85 (1.63–1.97)
Tibia–Patella IV length	6.12 (6–6.32)	6.63 (6.06–7.2)	5.75–5.875	6.14 (5.31–7.04)	6.41 (5.12–7.52)
Tibia–Patella IV width	0.82 (0.74–0.9)	0.81 (0.64–0.96)	0.75–0.875	0.82 (0.74–0.96)	0.82 (0.64–0.98)
Tibia–Patella IV coefficient	7.41 (7.02–7.77)	8.16 (7.44–9.35)	7.581–7.667	7.49 (6.78–8.63)	7.9 (7.5–8.38)
Femur IV length	6.06 (5.75–6.32)	6.83 (5.44–7.9)	5.875–5.938	6.14 (5.43–7.44)	6.59 (5.6–7.6)
Femur IV with	0.82 (0.74–0.88)	0.81 (0.64–0.96)	0.762–0.812	0.87 (0.74–1.04)	0.85 (0.7–1)
Femur IV coefficient	7.51 (7.09–7.93)	8.45 (7.52–9.37)	7.231–7.787	6.79 (6.38–7.34)	7.66 (6.76–8.47)
TT4 coefficient	1.47 (1.42–1.59)	1.66 (1.47–1.95)	1.484–1.615	1.49 (1.3–1.68)	1.61 (1.49–1.7)
Angle of the spermathecae	25.67 (18.88–34.83)	32.99 (18.86–44.19)	44.036–46.79	31.93 (26.61–38.20)	30.2 (20.4–38.08)
Genital opening length	0.207 (0.2–0.21)	0.25 (0.2–0.31)	0.232–0.233	0.25 (0.21–0.28)	0.22 (0.19–0.28)
Genital opening width	0.63 (0.53–0.70)	0.73 (0.64–0.85)	0.614–0.615	0.67 (0.65–0.69)	0.64 (0.59–0.71)
Genital opening coefficient	0.33 (0.28–0.4)	0.35 (0.26–0.43)	0.377–0.379	0.37 (0.31–0.41)	0.33 (0.3–0.36)

coefficients (Fig. 7). Males of *L. hesperus* showed significant differences in sternum length and tibia-patella IV width in comparison with the other two species (*L. occidentalis* sp. nov. and *Latrodectus* sp. 2) (Figs 7–8).

Species Distribution Models (SDM)

The SDM of *L. mactans* predicts the presence of the species across large parts of the states of Tamaulipas, Coahuila, Nuevo Leon, and San Luis Potosi, as well as the northern parts of Hidalgo, Puebla, and Veracruz (Fig. 9). This region corresponds to the Tamaulipeca and Sierra Madre Oriental biogeographic provinces below 1000 m (Morrone 2004, 2005, 2017) (Figs 9, 12). The SDM of *L. occidentalis* sp. nov.

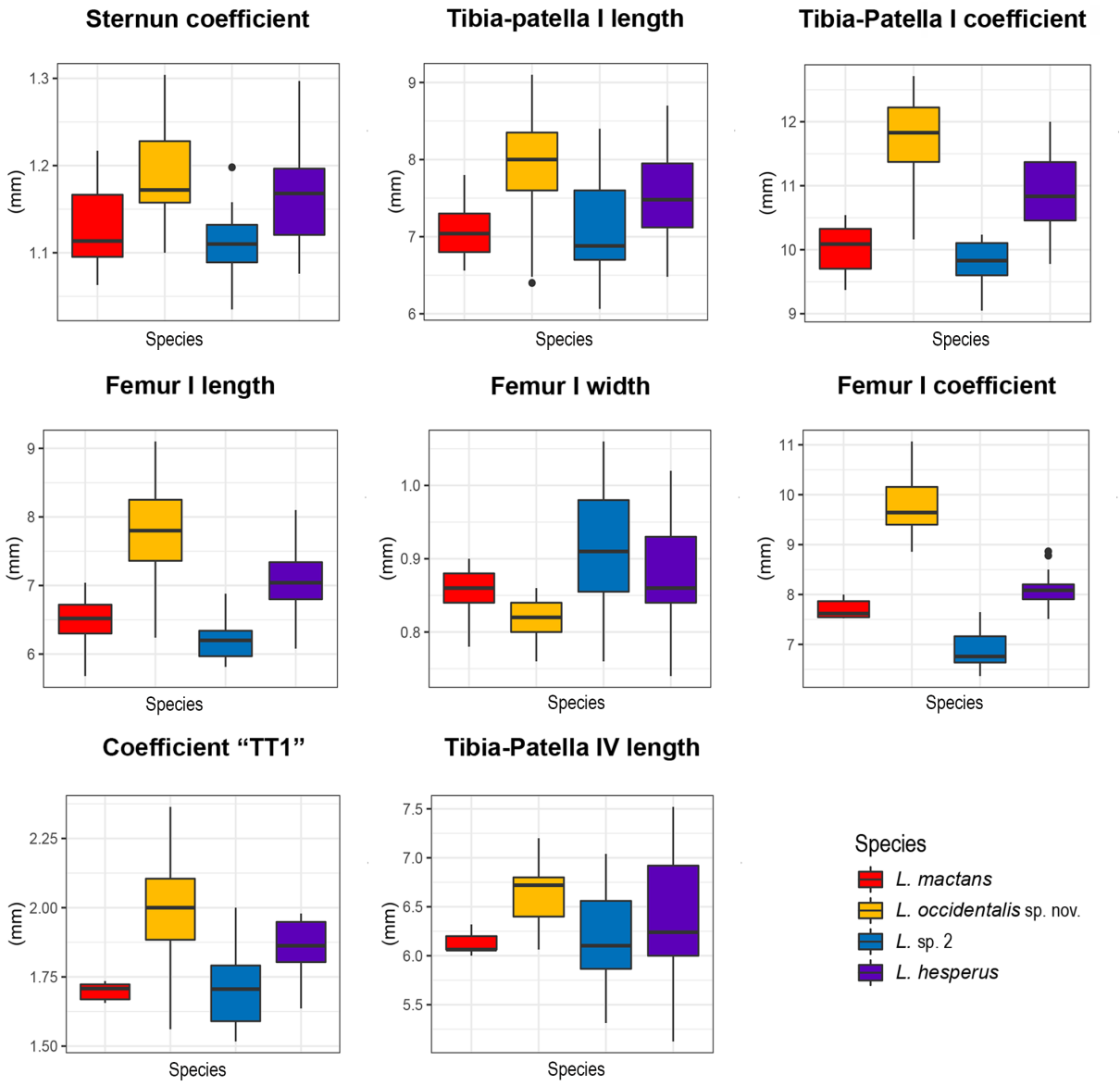

Fig. 5. Comparison of variances (ANOVA) and medians (Kruskal-Wallis) of different structures analyzed under linear morphometry that showed significant differences ($p > 0.05$) in females of three putative species of *Latrodectus* Walckenaer, 1805 from Mexico.

shows a potential distribution throughout several states from the western region of Mexico (Fig. 10). This region corresponds to the Pacific coast and the Sierra Madre del Sur, encompassing the biogeographic provinces of the Pacific lowlands, the southern region of the Mexican Altiplano, part of the Trans-Mexican Volcanic Belt, and the Balsas Depression, at altitudes below 2000 m (Figs 10, 12). Finally, the SDM analyses predicted *L. hesperus* to have a widespread distribution from northwest to central Mexico, with records in nine states, all between 0–2000 m (Figs 11–12).

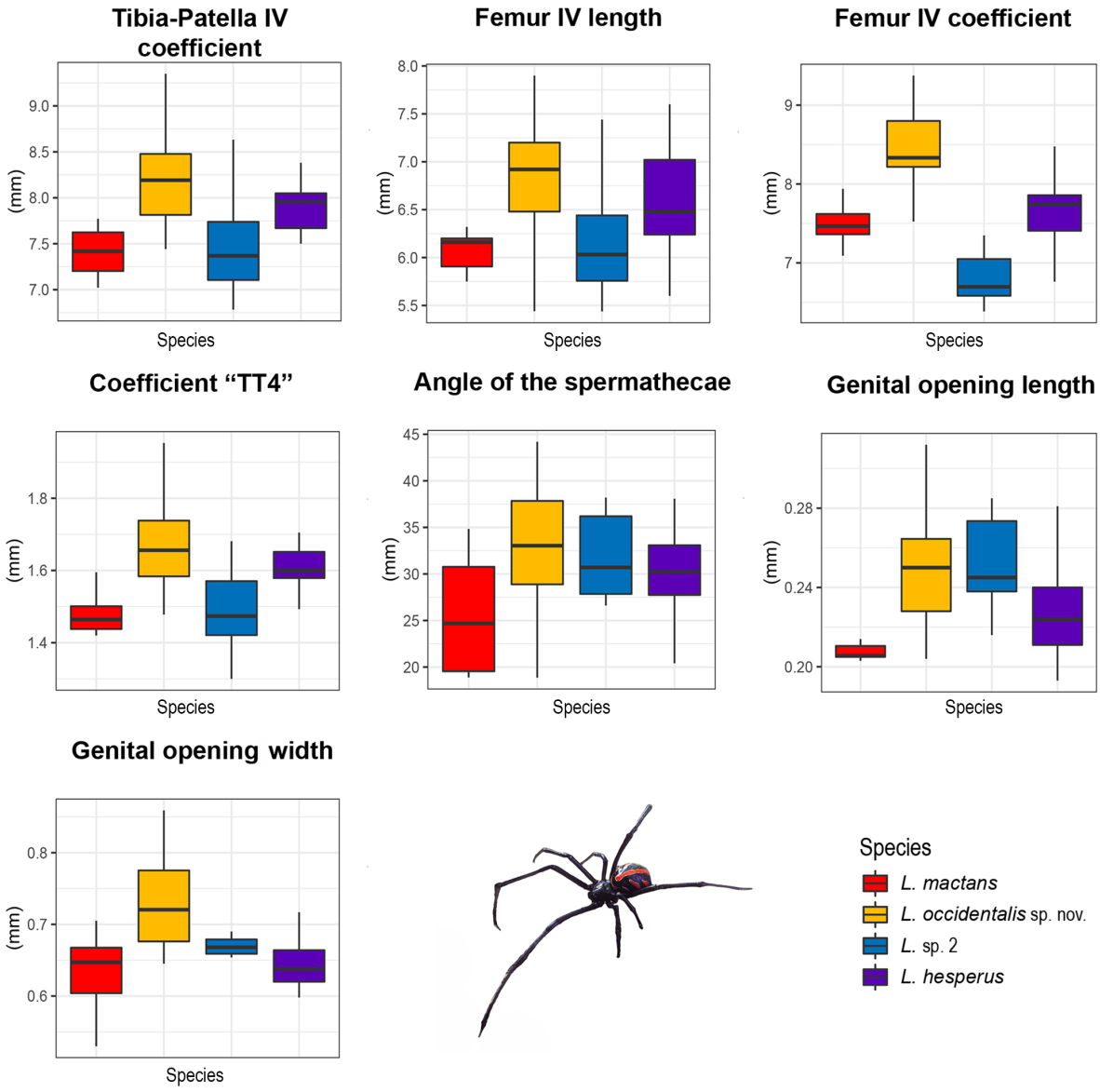

Fig. 6. Comparison of variances (ANOVA) and medians (Kruskal-Wallis) of different structures analyzed under linear morphometry that showed significant differences ($p > 0.05$) in females of three putative species of *Latrodectus* Walckenaer, 1805 from Mexico.

Table 6. Significance values of the ANOVA or Kruskal-Wallis analyses of the data set analyzed under linear morphometry. Significant differences are presented in bold. α = 0.05; T = Carapace (length/width); TT = Tibia-Patella length of leg I or IV.

Measured structure	Males		Females	
	F/X^2	*p*	F/X^2	*p*
Carapace length	1.923	1.65E-01	1.196	3.17E-01
Carapace width	5.06	**1.30E-02**	3.9818	2.63E-01
T coefficient	3.363	5.91E-02	4.9412	1.76E-01
Sternum length	9.641	**9.85E-04**	2.2008	5.32E-01
Sternum width	1.123	3.40E-01	1.701	1.74E-01
Sternum coefficient	20.16	**4.19E-05**	8.832	**4.37E-05**
Tibia-Patella I length	12.459	**1.97E-03**	9.392	**2.31E-05**
Tibia-Patella I width	2.443	1.07E-01	4.7016	1.95E-01
Tibia-Patella I coefficient	19.309	**6.41E-05**	51.442	**3.94E-11**
Femur I length	9.85	**5.77E-04**	30.16	**8.61E-13**
Femur I width	3.414	1.81E-01	21.034	**1.04E-04**
Femur I coefficient	69.62	**3.62E-11**	62.234	**1.96E-13**
TT1 coefficient	34.69	**4.50E-08**	36.114	**7.09E-08**
Tibia-patella IV length	7.0681	**2.92E-02**	15.426	**1.49E-03**
Tibia-patella IV width	11.69	**2.20E-04**	0.1127	9.90E-01
Tibia-Patella IV coefficient	22.51	**3.12E-06**	24.915	**1.61E-05**
Femur IV length	12.548	**1.89E-03**	7.549	**1.72E-04**
Femur IV width	7.7032	**2.13E-02**	4.698	1.95E-01
Femur IV coefficient	18.915	**7.81E-05**	61.7	**2.00E-16**
Coefficient TT4	11.73	**2.00E-04**	31.232	**7.56E-07**
Angle of the spermathecae			3.066	**3.70E-02**
Genital opening length			7.12	**5.01E-04**
Genital opening width			10.38	**2.46E-05**
Genital opening coefficient			5.8162	1.21E-01

Taxonomy

Order Araneae Clerck, 1757
Family Theridiidae Sundevall,1833

Genus ***Latrodectus*** Walckenaer, 1805

Type species

Aranea brevipes Martini & Goeze, 1778: 286 (description: suppressed for lack of usage).
Aranea 13-guttata Rossi, 1790: 136, pl. 9 fig. 10 (description: female), currently *Latrodectus tredecimguttatus* (Rossi, 1790). See World Spider Catalog (2023) for complete taxonomic records.

Latrodectus occidentalis Valdez-Mondragón sp. nov.
urn:lsid:zoobank.org:act:3A193510-15D4-4E30-AAC3-DC224288C792
Figs 13–81

Differential diagnosis

Females of *Latrodectus occidentalis* sp. nov. can be identified from those of other species of *Latrodectus* from Mexico by the combination of several features. Dorsal coloration: distinct red stripes and dots on dorsal surface of the abdomen: 1) one V-shaped stripe on anterior part (Fig. 25, red arrow), 2) long and sigmoid stripe dorsally along the abdomen (Fig. 25, blue arrow), and 4) two pairs of stripes towards lateral part of abdomen (Fig. 25, green arrows). Ventral coloration: abdomen with hourglass pattern always

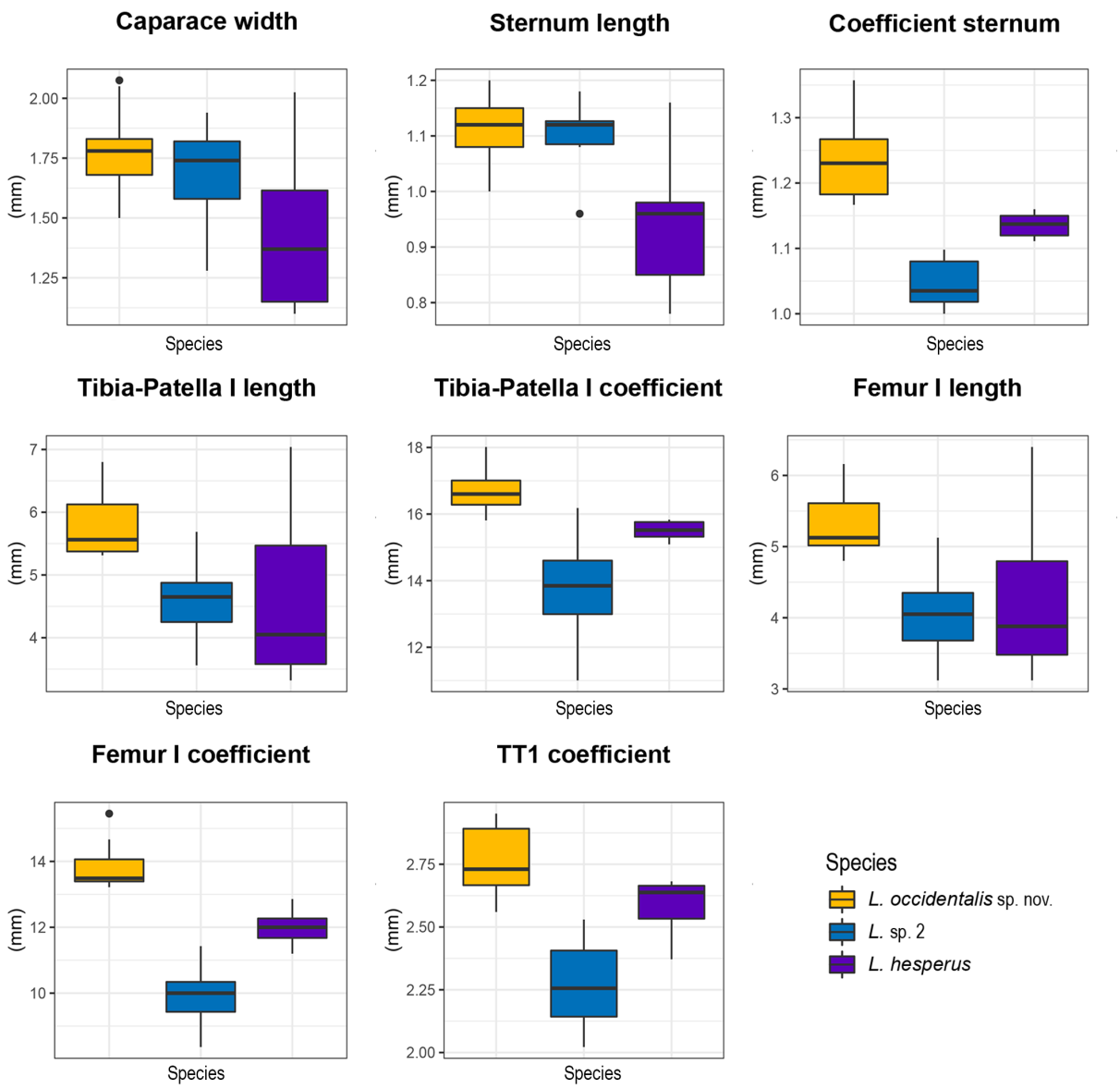

Fig. 7. Comparison of variances (ANOVA) and medians (Kruskal-Wallis) of different structures analyzed under linear morphometry that show significant differences ($p > 0.05$) in males of three putative species of *Latrodectus* Walckenaer, 1805 from Mexico.

complete, wide, and never separated as in *L. hesperus* and *L. mactans* (Fig. 26). Body measurements (Figs 5–6): sternum coefficient (length/width) longer than other species analyzed herein, tibia-patella I longer than other species, tibia-patella coefficient longer than other analyzed species, femur I longer than other species, femur I and IV coefficient longer than other species, TT1 and TT4 coefficients slightly longer than other species. Angle between the spermathecae position in dorsal view longer than other species. Genital opening of epigynum wider than other species (Figs 29, 31–42 (ventral views)). Copulatory ducts forming four or five loops around spermathecae (Figs 30, 33–43 (ventral views), 72). Males: similar to females, but abdomen oval (Figs 17, 27–28). Coloration: ventrally, abdomen with hourglass pattern always complete, thinner than females (Fig. 28). Body measurements (Figs 7–8): sternum coefficient (length/width) longer than other species analyzed herein, tibia-patella 1 length and

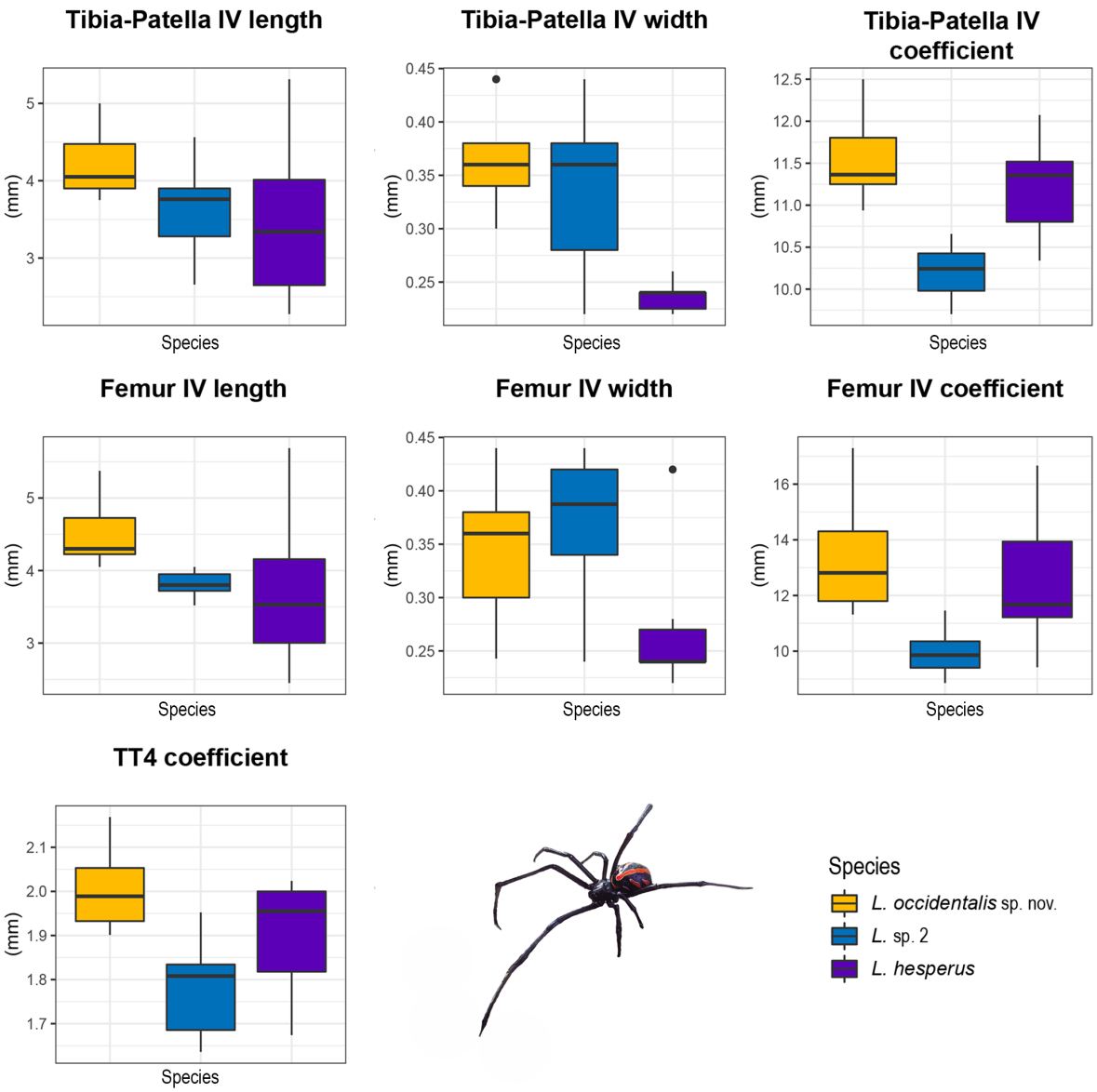

Fig. 8. Comparison of variances (ANOVA) and medians (Kruskal-Wallis) of different structures analyzed under linear morphometry that show significant differences ($p > 0.05$) in males of three putative species of *Latrodectus* Walckenaer, 1805 from Mexico.

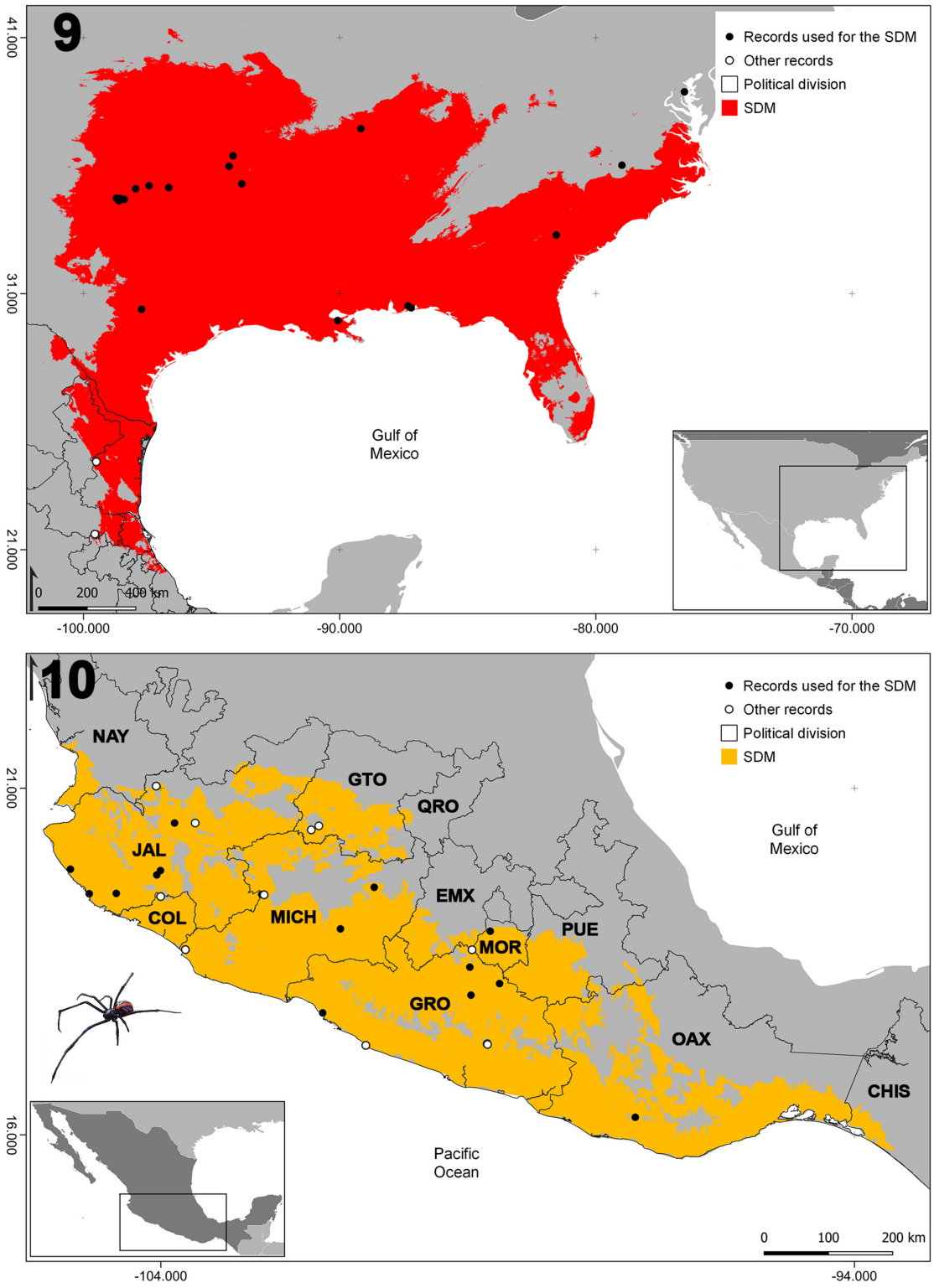

Figs 9–10. 9. Records and Species Distribution Model (SDM) (red) of *L. mactans* (Fabricius, 1775) in Mexico and the USA. **10.** Records and SDM (yellow) of *L. occidentalis* Valdez-Mondragón sp. nov. in Mexico. Abbreviations: CHIS = Chiapas; COL = Colima; EMX = Edo. Mex; GRO = Guerrero; GTO = Guanajuato; JAL = Jalisco; MICH= Michoacán; MOR = Morelos; NAY = Nayarit; OAX = Oaxaca; PUE = Puebla; QRO = Querétaro.

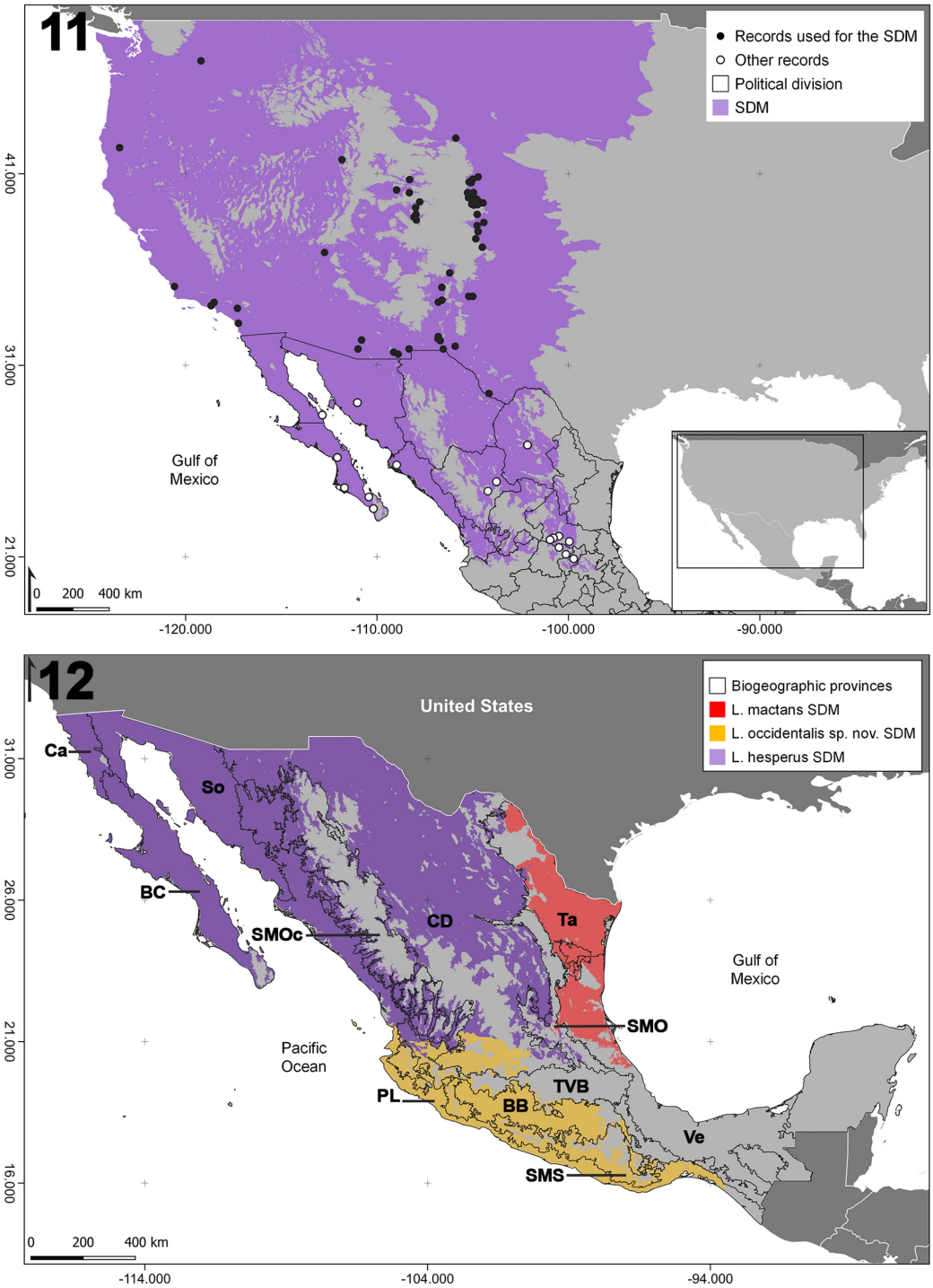

Figs 11–12. 11. Records and Species Distribution Model (SDM) of *L. hesperus* Chamberlin & Ivie, 1935 for Mexico and the USA. **12.** SDM of *L. mactans* (Fabricius, 1775) (red), *L. occidentalis* Valdez-Mondragón sp. nov. (yellow), and *L. hesperus* (purple) confined only to Mexico, showing a lack of overlap in their distributions, using the biogeographical provinces proposed by Morrone (2004, 2005, 2017). Abbreviations: BB = Balsas Basin; BC = Baja Californian; Ca = Californian; CD = Chihuahuan Desert; PL = Pacific Lowlands; SMO = Sierra Madre Oriental; SMOc = Sierra Madre Occidental: SMS = Sierra Madre del Sur; So = Sonoran; Ta = Tamaulipas; TVB = Transmexican Volcanic Belt; Ve = Veracruzan.

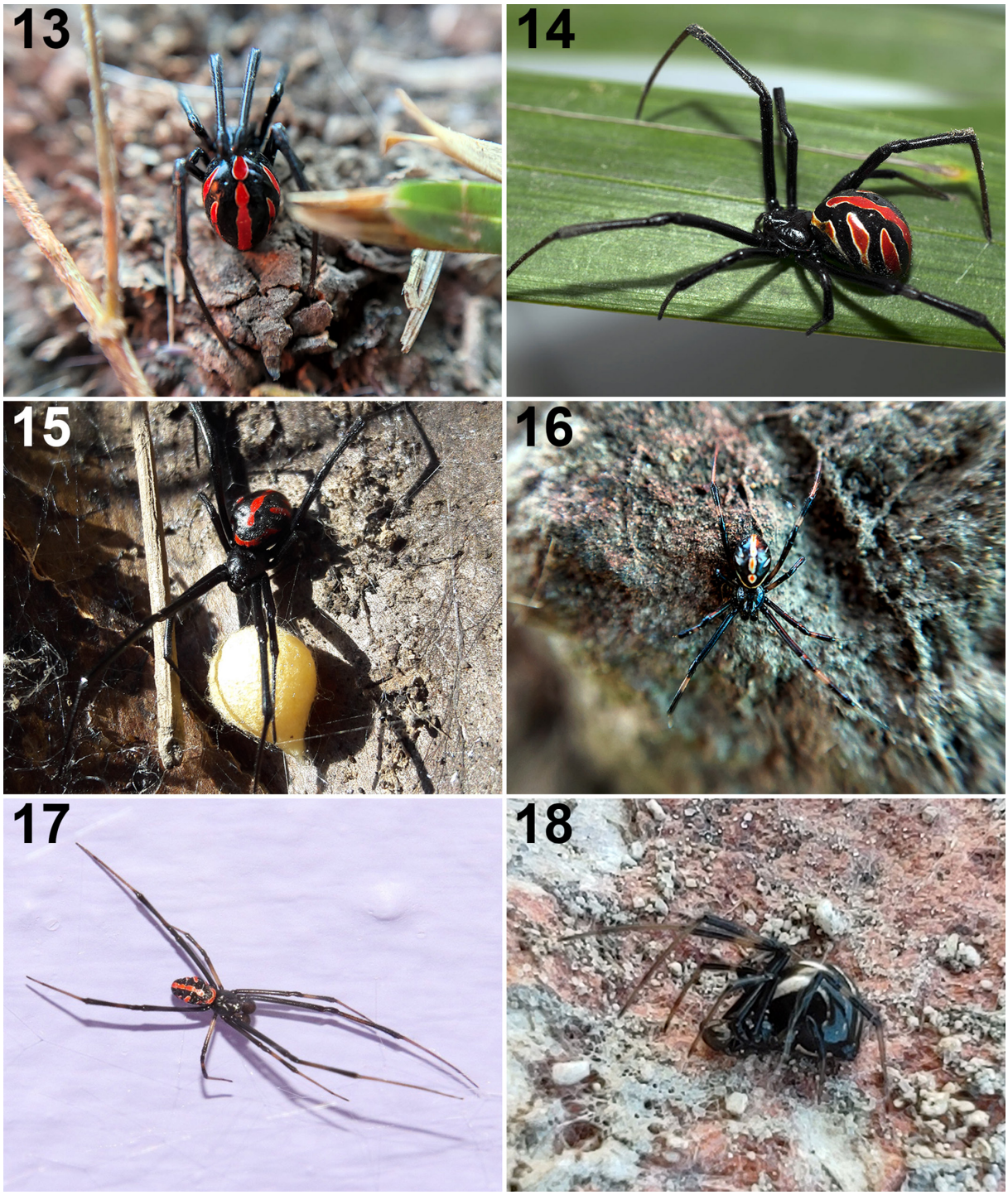

Figs 13–18. Live females (13–15) and males (16–18) of *Latrodectus occidentalis* Valdez-Mondragón sp. nov. **13, 16**. Salvatierra, Guanajuato, Mexico. **14**. Camichines, Cocula, Jalisco, Mexico (type locality). **15**. Hostotipaquillo, Jalisco, Mexico. **17**. 1 km North of San Nicolás de Ibarra, Jalisco, Mexico. **18**. "Las Letras", Pénjamo, Guanajuato, Mexico. Photographs 13, 16, 18 by Cabrera-Espinosa (2021). Photograph 14 by Navarro-Rogríguez I. (2021). Photograph 15 by Valdez-Mondragon A. Photograph 17 by Mamole in https://www.naturalista.mx/observations/126985294

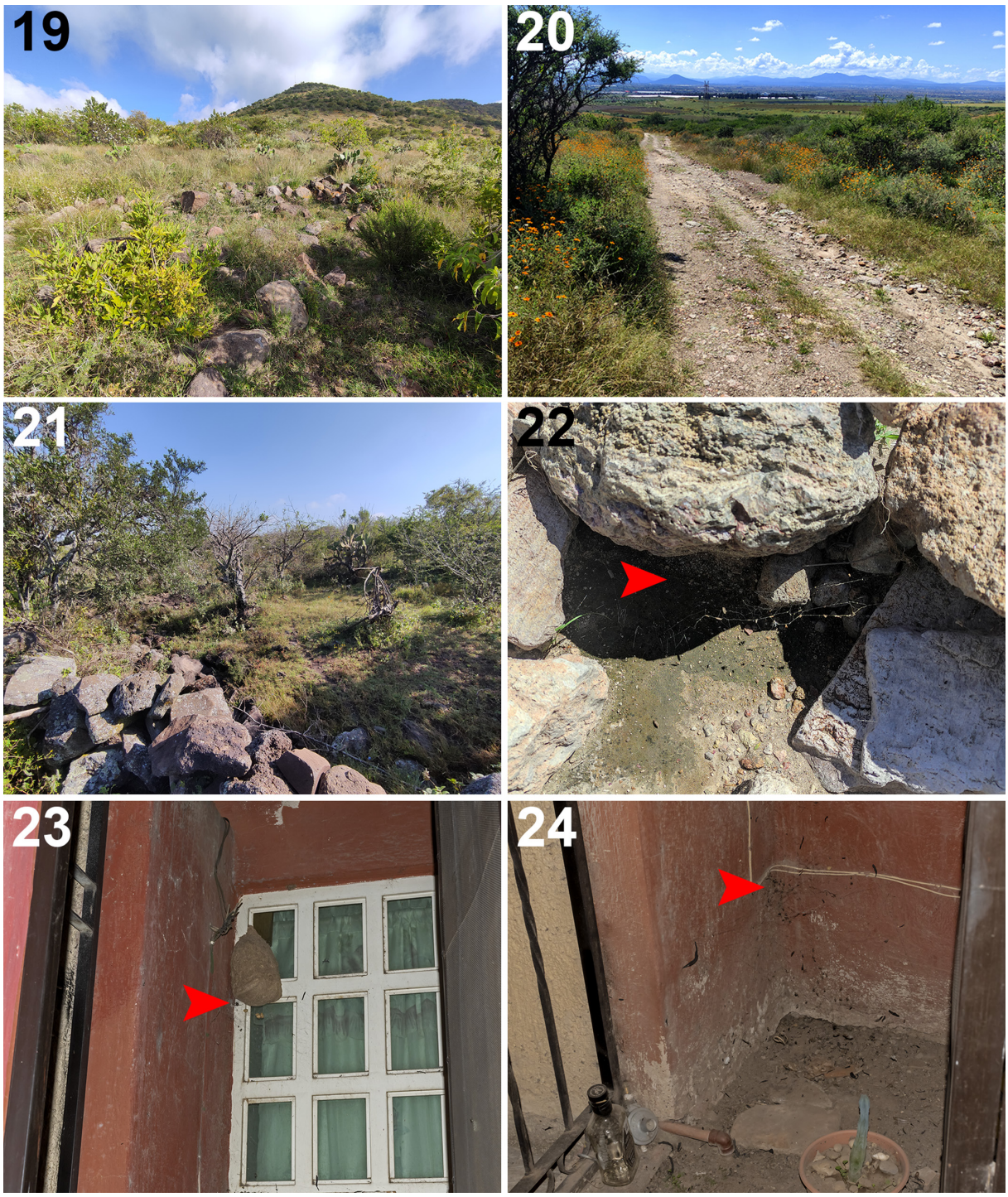

Figs 19–24. Habitats and microhabitats of *Latrodectus occidentalis* Valdez-Mondragón sp. nov. Red arrow indicates the microhabitat where the specimens were collected. **19, 22**. "Las Letras", Pénjamo, Guanajuato, Mexico. **20**. Zona arqueológica "Plazuelas", Pénjamo, Guanajuato, Mexico. **21**. Salvatierra, Guanajuato, Mexico. **23–24**. Cocula, Jalisco, Mexico (type locality) (red arrow in figure 23 shows the female found below a wasp nest). Photographs 19–22 by Cabrera-Espinosa (2021); 23–24 by Jared Lacayo (2021).

tibia-patella coefficient longer than other species, tibia-patella 1 coefficient longer than other species, tibia-patella 1 coefficient longer than other species, length and coefficient of femur I longer than other species, TT1 coefficient longer than other species, tibia-patella IV longer than other species, femur IV longer than on other species. Embolus with 3 coils, located distally on cymbium (Figs 44–48, red arrows), last coil extending medially, curving downwards along retrolateral part of palp, continuing ventrally, ending in a long thin tip (Figs 44–60). In *L. mactans* and *L. hesperus* (native species from North America), the embolus has 2 coils (Cabrera-Espinosa & Valdez-Mondragón 2021: figs 30–37).

Etymology

This species is a name in apposition and refers to the distribution of the species in the Spanish language: '*Occidente de México*' ('western Mexico'), '*occidentalis*', that includes the states of Guerrero, Michoacán, Colima, and Jalisco (type locality).

Material examined

Holotype

MEXICO – **Jalisco** • ♀; Municipality of Cocula, Camichines; 20.4991° N, 103.8020° W; 1268 m a.s.l; 1 Jun. 2020; C.I. Navarro-Rodríguez leg.; night collecting; CNAN-T01589.

Paratypes

MEXICO – **Jalisco** • 1 ♂; same collection data as for holotype; CNAN-T01590 • 3 ♀♀, 2 ♂♂; same collection data as for holotype; CNAN-T01591, CNAN-T01593.

Other material

MEXICO − **Colima** • 1 ♀; Municipality of Coquimatlán, watering place Los Amiales; 19.1676° N, 103.834° W; 296 m a.s.l.; 16 Nov. 2020; A. Valdez, I. Navarro, A. Juárez, S. Nolasco leg.; LATLAX Ara-1074 • 5 ♀♀, 1 ♂, 2 immatures; Municipality of Minatitlán, 2.5 km NW of San Antonio crossroads; 19.438° N, 104.0019° W; 195 m a.s.l.; 16 Nov. 2020; A. Valdez,I. Navarro, A. Juarez, S. Nolasco leg.; diurnal collecting; LATLAX Ara-1073, Ara-1051, Ara-1061, Ara-1066. – **Guerrero** • 1 ♀; Municipality of Chilpancingo de los Bravo; 17.3119° N, 99.2979° W; 1205 m a.s.l.; 1 Jul. 2018; P. Solís, S. Rodríguez leg.; LATLAX Ara-0771 • 2 ♀♀; Municipality of Pilcaya, Botanical garden, Grutas de Cacahuamilma; 18.6703° N, 99.5134° W; 1145 m a.s.l.; 15 Oct. 2018; A. Valdez, P. Solís, I. Navarro, A. Juárez, L. Cabrera leg.; diurnal collecting; LATLAX Ara-0767, Ara-0772 • 1 ♀; Municipality of Quechultenango, Tourist Center Grutas de Juxtlahuaca; 17.4392° N, 99.1593° W; 923 m a.s.l.; 14 Oct. 2018; A. Valdez, P. Solís, I. Navarro, A. Juárez, L. Cabrera leg.; LATLAX Ara-1057 • 1 ♀; Municipality of Taxco de Alarcón, 10 km SW of Taxco, on the way to Cerro de Huixteco park; 18.5908° N, 99.6033° W; 2330 m a.s.l.; 21 Sep. 2018; D. Montiel leg.; LATLAX Ara-1065 • 1 ♀; Municipality of Taxco de Alarcón, Miguel Hidalgo Street, #23; 18.4197° N, 99.545° W; 930 m a.s.l.; 19 Sep. 2017; A. Valdez, I. Navarro, P. Solís, J. Valerdi leg.; LATLAX Ara-1075 • 2 ♀♀, 1 ♂, 1 immature; Municipality of Técpan de Galeana, path to microwave repeater El Tamarindo, 1.5 km SW of viewpoint Bahía de Papanoa; 17.2918° N, 101.045° W; 79 m a.s.l.; 22 Nov. 2020; A. Valdez, I. Navarro, A. Juárez, S. Nolasco leg.; diurnal collecting; LATLAX Ara-1056, Ara-1063, Ara-1064. – **Jalisco** • 1 ♀; same collection data as for holotype; 21 Sep. 2018; I. Navarro leg.; diurnal collecting; LATLAX Ara-0765 • 1 ♀; same collection data as for holotype; 5 Jan. 2019; I. Navarro leg.; LATLAX Ara-0776 • 1 ♀, 3 immatures; same collection data as for holotype; 21 Jun. 2019; A. Valdez, I. Navarro, L. Cabrera, J. Flores leg.; LATLAX Ara-1083, Ara-1084 • 6 ♀♀, 3 ♂♂, 6 immatures; municipality of Hostotipaquillo, 3 km SW of Hostotipaquillo; 21.0314° N, 104.0668° W; 1336 m a.s.l.; 8 Nov. 2020; A. Valdez, I. Navarro, A. Juárez, S. Nolasco leg.; LATLAX Ara-1043 to Ara-1050, Ara-1058, Ara-1059 • 3 ♀♀; Municipality of Jilotlán de los Dolores, 4 km S of Agua Bendita; 19.4634° N, 102.5112° W; 1406 m a.s.l.; 5 Nov. 2020; A. Valdez, I. Navarro, A. Juárez, S. Nolasco leg.; LATLAX Ara-1060, Ara-1071, Ara-1072 • 3 ♂♂; Municipality of Jilotlán de los Dolores, Agua Bendita; 19.4689° N, 102.546° W; 1163 m a.s.l.; 5 Nov. 2020; A. Valdez, I. Navarro, A. Juárez, S. Nolasco

leg.; diurnal collecting; LATLAX Ara-1053 to Ara-1055 • 1 ♀; Municipality of Tomatlán, 9 km NO of Campo Acosta; 19.8327° N, 105.304° W; 109 m a.s.l.; 14 Nov. 2020; A. Valdez, I. Navarro, A. Juárez, S. Nolasco leg.; diurnal collecting; LATLAX Ara-1077 • 1 ♀, 1 immature; Municipality of Tonaya, 1 km W of Amacuautitlán; 19.8133° N, 104.0059° W; 905 m a.s.l.; 7 Nov. 2020; A. Valdez, I. Navarro, A. Juárez, S. Nolasco leg.; diurnal collecting; LATLAX Ara-1078 • 1 ♀; Municipality of Zapopan, Lince

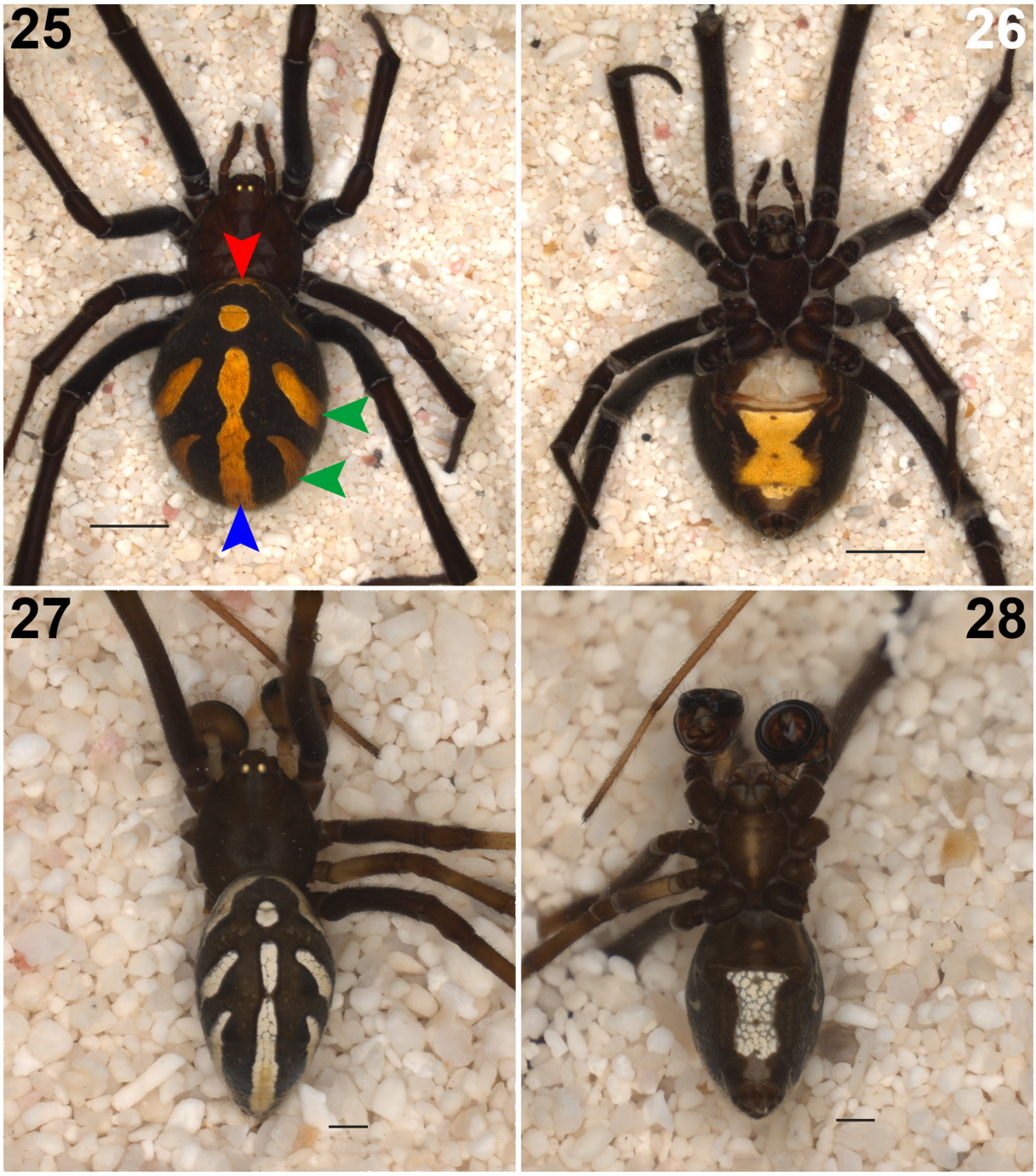

Figs 25–28. *Latrodectus occidentalis* Valdez-Mondragón sp. nov. **25–26**. Holotype, ♀ (CNAN-T01589), dorsal and ventral habitus, respectively. **27–28**. Paratype, ♂ (CNAN-T01590), dorsal and ventral habitus, respectively. Red arrow indicates coloration patterns. Scale bars = 0.5 mm.

Cave, La Primavera common; 20.712° N, 103.57° W; 1605 m a.s.l.; 8 Nov. 2020; A. Valdez, I. Navarro, A. Juárez, S. Nolasco leg.; diurnal collecting; LATLAX Ara-1068. – **Michoacán** • 8 ♀♀, 10 immatures; Municipality of Coahuayana de Hidalgo, La Piedra hill; 18.6721° N, 103.6464° W; 65 m a.s.l.; 19 Nov. 2020; A. Valdez, I. Navarro, A. Juárez, S. Nolasco leg.; diurnal collecting; LATLAX Ara-1062, Ara-1067, Ara-1079, Ara-1080 • 1 immature; Municipality of Cotija de la Paz, Luis G. Urbina street; 19.8087° N, 102.6884° W; 1630 m.a.s.l; 6 Nov. 2020; A. Valdez, I. Navarro, A. Juárez, S. Nolasco leg.; diurnal collecting; LATLAX Ara-1052 • 1 ♀, 1 immature; Municipality of Tzitzio, 2 km O of Tzitzio; 19.572° N, 100.9235° W; 1466 m a.s.l.; 3 Nov. 2020; A. Valdez, I. Navarro, A. Juárez, S. Nolasco leg.; diurnal collecting; LATLAX Ara-1070.

Description

Female (holotype CNAN-T01589)

Measurements. Total length 10.70. Carapace 4.30 long, 3.75 wide (ratio l/w: 1.14). Clypeus 0.75 long. Diameter AME 0.25, ALE 0.20, PME 0.22, PLE 0.23. Distance AME–ALE 0.14, ALE–PLE 0.22, PME–PLE 0.33, PME–PME 0.19. Leg I: total 28.80 (femur 8.10+patella 2.30+tibia 7.20+metatarsus 8.70+tarsus 2.50); leg II: 18.32 (5.50+1.80+4.00+5.30+1.72); leg III: 13.23 (4.20+1.48+2.50+3.68+1.37), leg IV: 24.18 (7.20+2.08+5.60+7.30+2.00). Leg formula: 1-4-2-3.

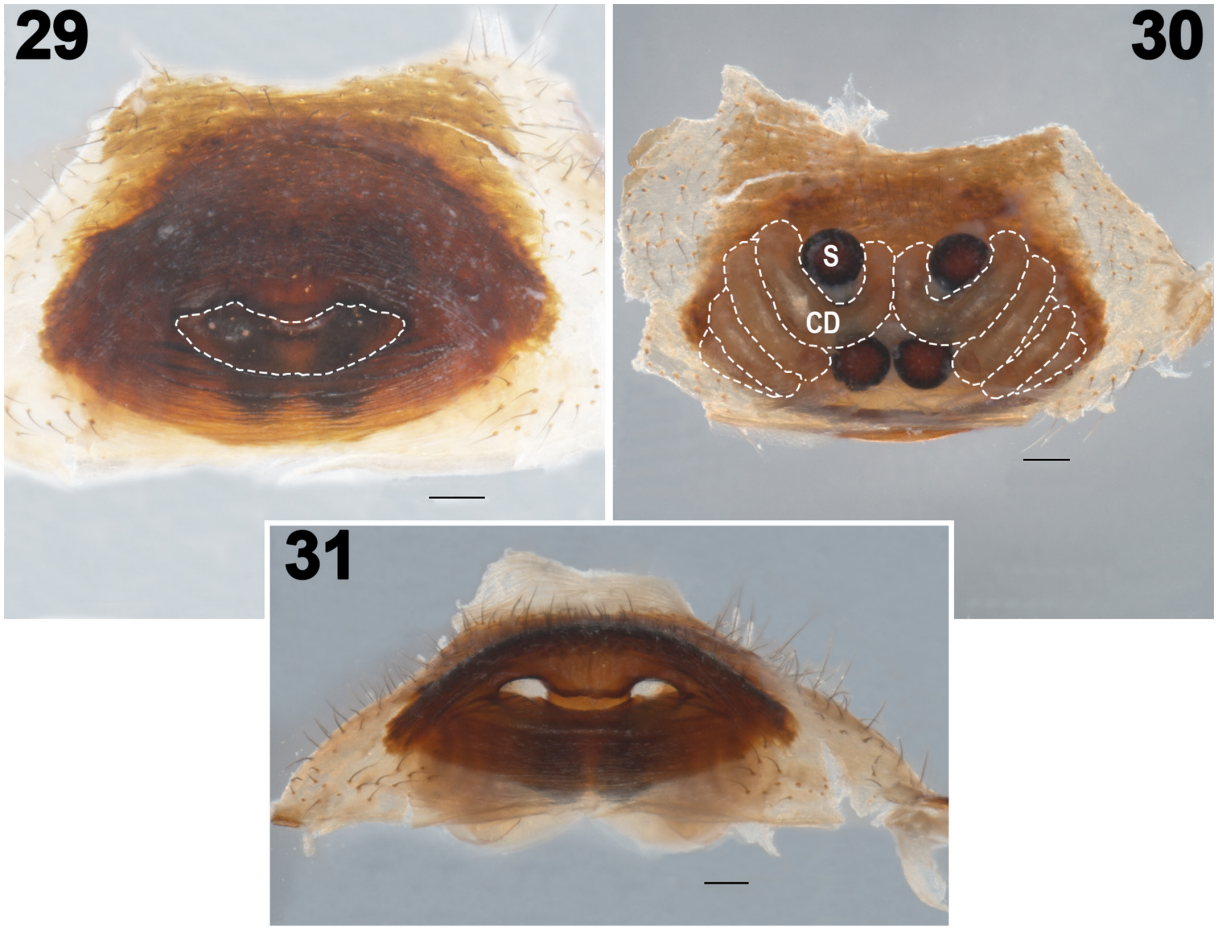

Figs 29–31. *Latrodectus occidentalis* Valdez-Mondragón sp. nov., holotype, ♀ (CNAN-T01589). Epigynum, ventral, dorsal, and posterior views, respectively. Dotted lines indicate genital opening (29) and copulatory ducts (30). Abbreviations: CD = copulatory duct; S= spermathecae. Scale bars = 0.2 mm.

Coloration. Live adult specimen dark brown, with distinctive red stripes dorsally on abdomen (Figs 13–15, 25) and ventrally with a red hourglass pattern, complete, located between epigynum and spinnerets (red coloration pattern is lost under ethanol) (Fig. 26). Chelicerae dark brown, white apically. Sternum, labium, and endites dark brown. Legs dark brown, metatarsi and tarsi paler coloration than other segments (Figs 13–15, 25–26). Tarsi darker distally.

Prosoma. Carapace with small translucid setae scattered across, dark setae on clypeus and posterior part of ocular region. Fovea transverse, M-shaped. In lateral view, clypeus oblique, protruding close to chelicerae. Eyes widely separated, different sizes (Fig. 70). In dorsal view of carapace, AER and PER recurved. AME slightly elevating, protruding from carapace. ALE and PLE protruding from carapace (Fig. 70). Sternum setose, subtriangular, shield shaped (Fig. 26). Labium setose, pale distally, trapezoidal,

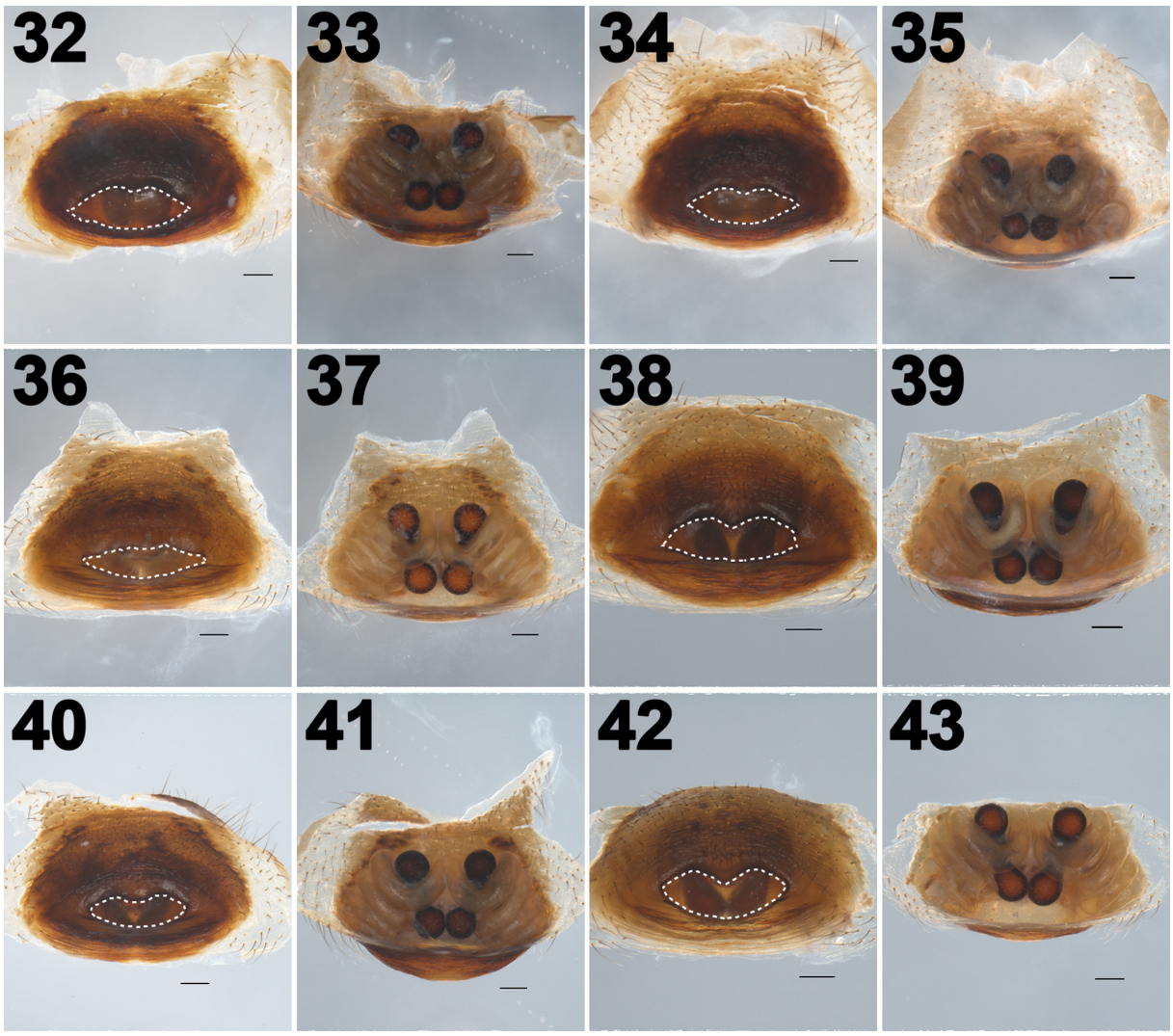

Figs 32–43. *Latrodectus occidentalis* Valdez-Mondragón sp. nov. Variation of the seminal receptacles of females, dorsal view. **32–33**. Cocula, Jalisco, Mexico (type locality). **34–35**. Jilotitlán de los Dolores, Jalisco, Mexico. **36–37**. Minatitlán, Colima, Mexico. **38–39**. Coahuayana de Hidalgo, Michoacán, Mexico. **40–41**. Quechultenango, Guerrero, Mexico. **42–43**. Hostotipaquillo, Jalisco, Mexico. Dotted lines indicate genital opening. Scale bars = 0.5 mm.

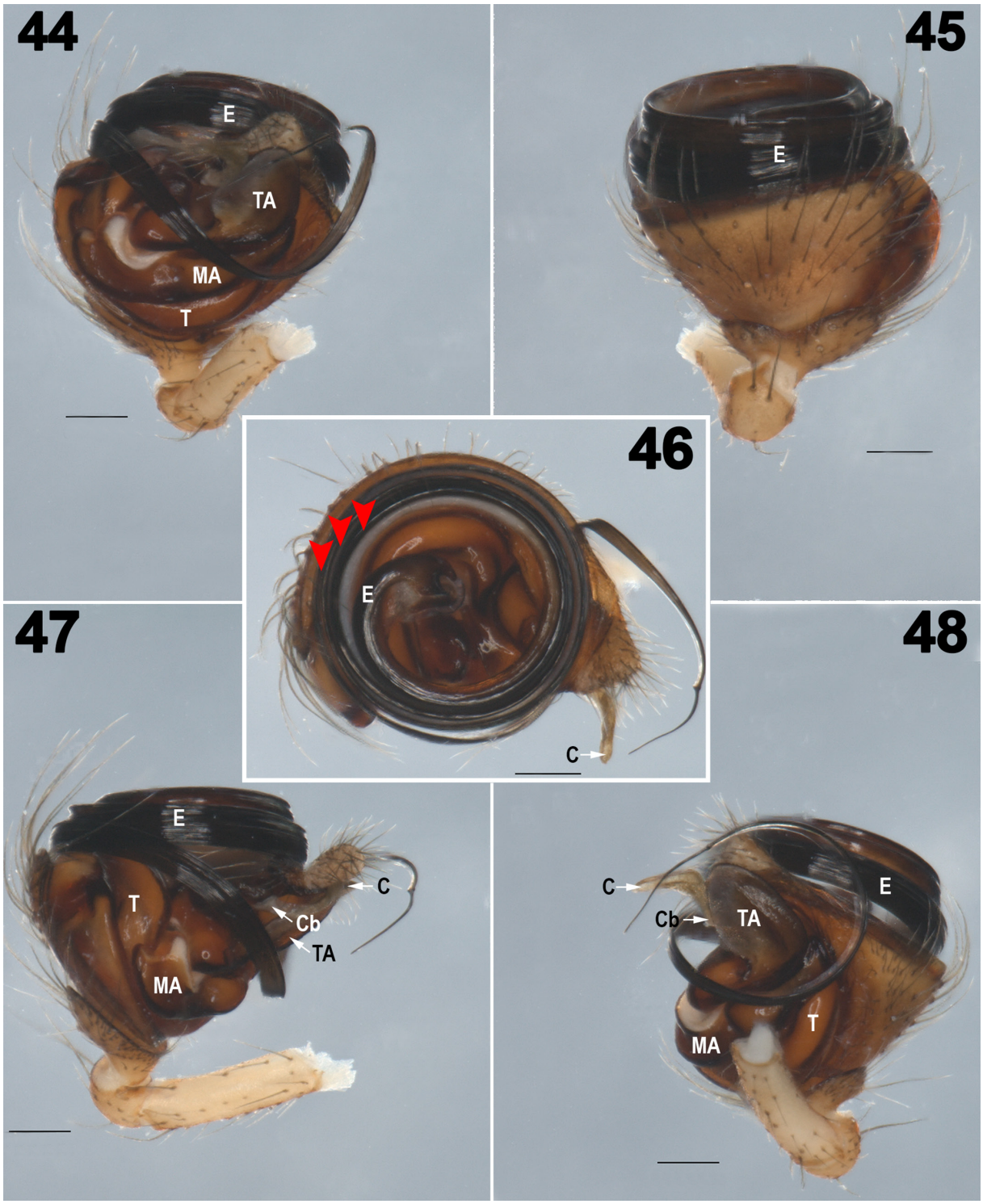

Figs 44–48. *Latrodectus occidentalis* Valdez-Mondragón sp. nov., paratype, ♂ (CNAN-T01590), right palp. **44**. Anterior view. **45**. Dorsal view. **46**. Ventral view, **47**. Retrolateral view. **48**). Prolateral view. Red arrows indicate the number of turns of the embolus. Abbreviations: C = conductor; Cb = conductor base; E = embolus; MA = median aphophysis; T = tegulum; TA = tegular aphophysis. Scale bars = 0.2 mm.

longer setae apically. Endites setose, pale distally, sub square, longer setae apically. Chelicerae with long setae distally, close to the fangs (Fig. 71). Palps with long setae, more setose in tarsus, with single toothed claw.

Legs. Uniformly moderately setose throughout, tapering in metatarsi and tarsi (Figs 73–75). Femora I wider basally, femora I and IV slightly curved in lateral view. Tibiae I slightly curved distally. Three tarsal claws present, lateral claws with one row of teeth, which become larger distally. Tarsi IV with distinct comb macrosetae.

Abdomen. Globular, moderately setose, with all setae of uniform length (Figs 13, 15, 25–26).

Epigynum. In ventral view oval, sclerotized and elevated, with oval and continuous opening, which is M-shaped in anterior part, opening 3.4× wider than long (Fig. 29). In posterior view, copulatory openings visible, separated by a median septum (Fig. 31). In dorsal view, four spermathecae, dumbbell-shaped, two anterior slightly bigger than others; copulatory ducts thinned-walled, transparent, weakly sclerotized, coiled around duct between spermathecae (Fig. 30).

Male (paratype CNAN-T01590)

Measurements. Total length 4.80. Carapace 2.00 long, 1.68 wide (ratio l/w: 1.19). Clypeus 0.40 long. Diameter AME 0.16, ALE 0.13, PME 0.14, PLE 0.13. Distance AME–ALE 0.06, ALE–PLE 0.06, PME–PLE 0.15, PME–PME 0.10. Leg I: total 17.70 (5.00+1.06+4.50+5.30+1.84); leg II: 10.28 (3.00+0.84+2.34+2.88+1.22); leg III: 7.25 (2.25+0.68+1.48+2.00+0.84), leg IV: 13.53 (4.05+0.90+3.16+4.00+1.42). Leg formula: 1-4-2-3.

Coloration. Live adult specimens black, paler than female, with distinctive red stripes dorsally on abdomen, white line around stripes (Figs 16–18, 27). Abdomen ventrally with a red hourglass pattern, complete, thinner than females (red coloration pattern is lost under ethanol) (Fig. 28). Chelicerae brown, paler than female, white apically. Palp femora and patellae, pale yellow; cymbium dark brown (Figs 44–48). Sternum, labium, and endites paler brown than female, sternum with a pale brown line medially (Fig. 28). Leg femora dark brown, except femora III, which is pale orange (Figs 16, 18, 27–28). Tibiae pale orange, becoming dark brown towards joints. Metatarsi and tarsi pale orange (Figs 16–18, 27–28).

Prosoma. Carapace with fewer small translucid setae scattered across than in female, less dark setae on clypeus and posterior part of ocular region than in female. Fovea transverse, M-shaped. In lateral view, clypeus oblique, protruding close to chelicerae (Fig. 76). Eyes widely separated, different sizes (Fig. 76). In dorsal view of carapace, AER and PER recurved (Fig. 76). AME slightly elevated, protruding from carapace. ALE and PLE protruding from carapace (Fig. 76). Chelicerae with long setae distally, close to fangs (Fig. 77). Sternum setose, subtriangular, shield shaped (Fig. 28). Labium setose, pale distally, trapezoidal, longer setae apically. Endites setose, pale distally, sub square, longer setae apically (Fig. 71).

Legs. Uniformly moderately setose throughout, tapering in metatarsi and tarsi. Femora I slightly wider basally, femora I and IV less curved in lateral view than female. Tibiae I and IV slightly curved distally. Three tarsal claws present, lateral claws with one row of teeth, which become larger distally. Tarsi IV with distinct comb macrosetae.

Abdomen. Oval, longer than wide, and high, moderately setose, with setae all uniform length. ALS longer than PMS and PLS, oval colulus (Figs 17, 27–28, 81).

Palp. In retrolateral view, cymbial apophysis (ca) oval, setose: with tegular apophysis (ta), hook-shaped, transparent, weakly sclerotized (Figs 44–48, 78–80). In ventral-basal view, median apophysis bent, almost 90° degrees, ending in blunt point, with a notch in the middle (Fig. 46).

Variation

Females have black carapace and abdomen coloration, black or dark brown legs, never light shades (Figs 25–26). Globular abdomen always black with distinctive red lines in dorsal region (Figs 61–69, red coloration is lost under ethanol), lines may be outlined by a thin white line in juveniles. The frontal region of the dorsal sigmoidal line may or may not be separated at an isolated point between the rest of the line and the V-shape. The two pairs of lines laterally may be attenuated or reduced, but always present (Figs 13–15, 25, 61–69). Males always present a black body coloration (Fig. 17), legs black or dark brown with light brown on the mid tibia, metatarsus, and tarsus (Figs 17–18). Abdomen oval with distinctive red lines on the dorsal region, which may be outlined by a thin white line (Figs 17–18, 27). As in females, the frontal region of the transverse dorsal line may or may not be separated at an isolated point between the rest of the line and the V-shape (Fig. 27). Males can vary greatly in body size

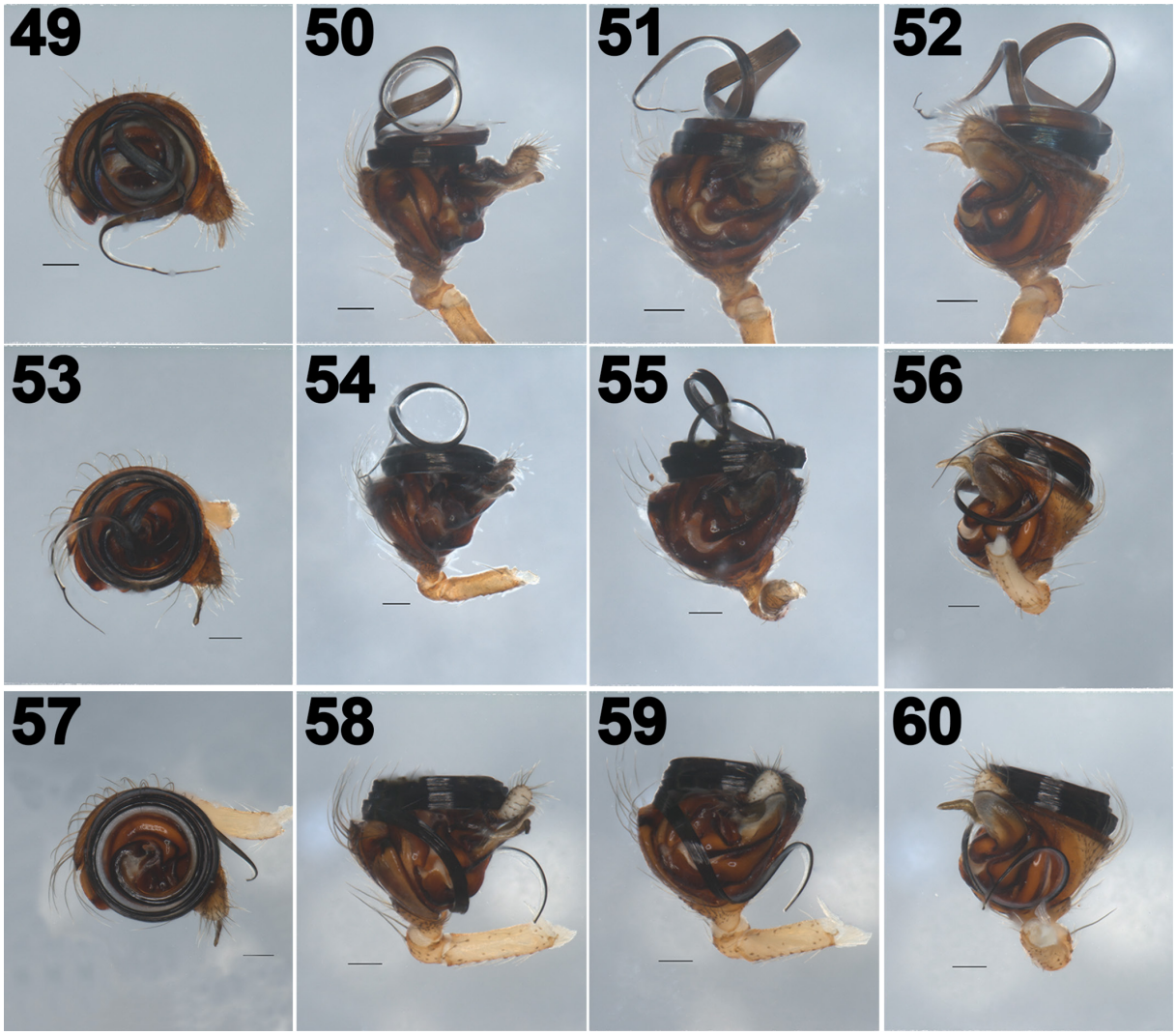

Figs 49–60. *Latrodectus occidentalis* Valdez-Mondragón sp. nov. Variation of the male left palps, prolateral views. **49–52**. Quechultenango, Guerrero, Mexico. **53–56**. Minatitlán, Colima, Mexico. **57–60**. Cocula, Jalisco, Mexico (type locality). Ventral view (49, 53, 57); retrolateral-frontal view (50, 54, 59); retrolateral view (51, 55, 59); posterior view (52, 56, 60). **49–56**. Postcopulatory palps. Scale bars = 0.2 mm.

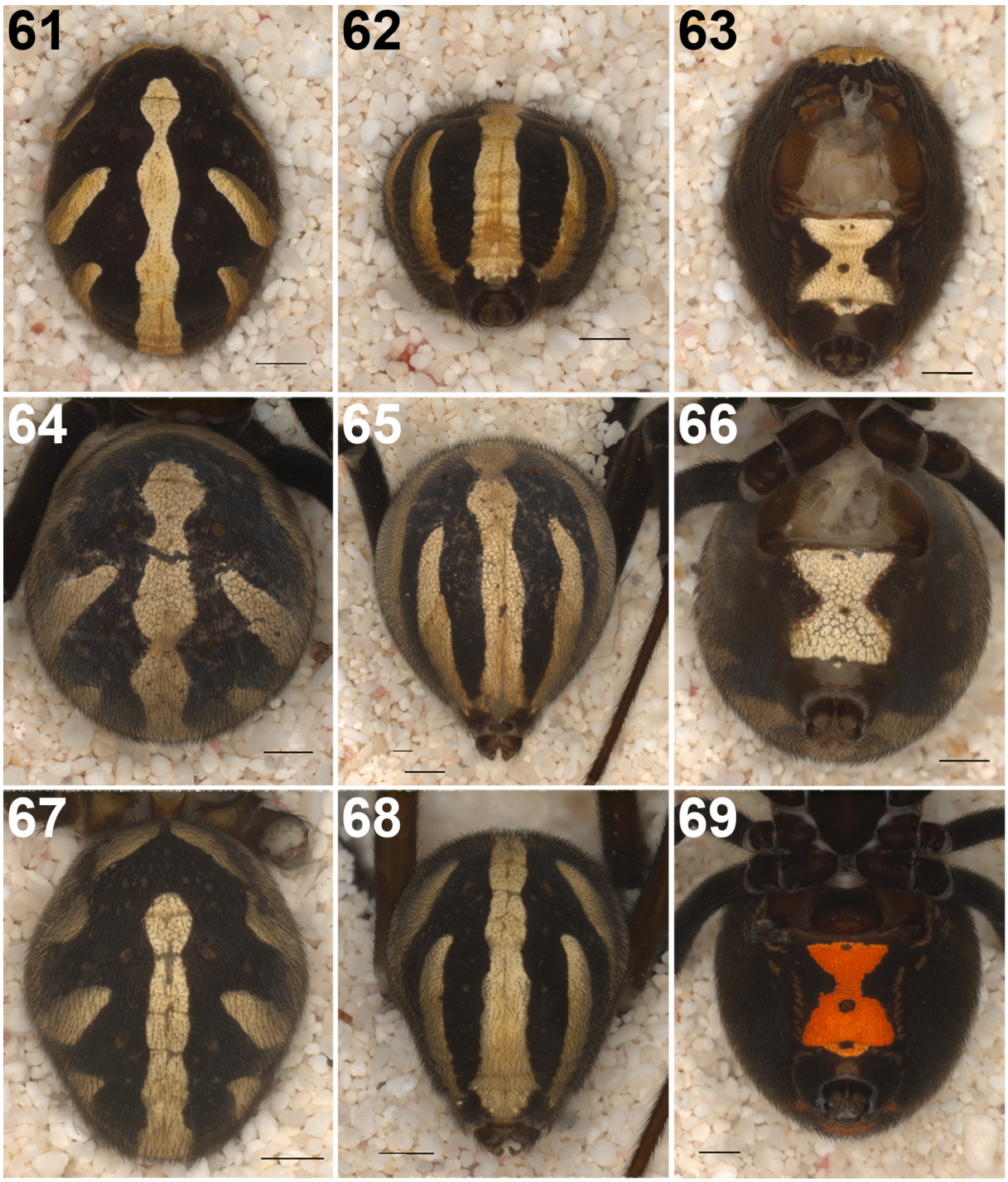

Figs 61–69. *Latrodectus occidentalis* Valdez-Mondragón sp. nov. Variation of the dorsal and ventral pattern coloration of the abdomen of the females of *Latrodectus occidentalis* sp. nov. Dorsal, posterior, and ventral views respectively. **61–63**. Chilpancingo, Guerrero, Mexico. **64–66**. Minatitlán, Colima, Mexico. **67–69**. Cocula, Jalisco, Mexico (type locality). Red coloration pattern gets lost under ethanol. Scale bars = 1 mm.

(Table 4), however sexual dimorphism is always marked, with females being more than twice the size of males, but males with proportionately longer legs (Tables 4–5). The genital opening of females varies in shape, but is always wider than long (Figs 29, 32–42 (ventral views)), the spermathecae are arranged in a

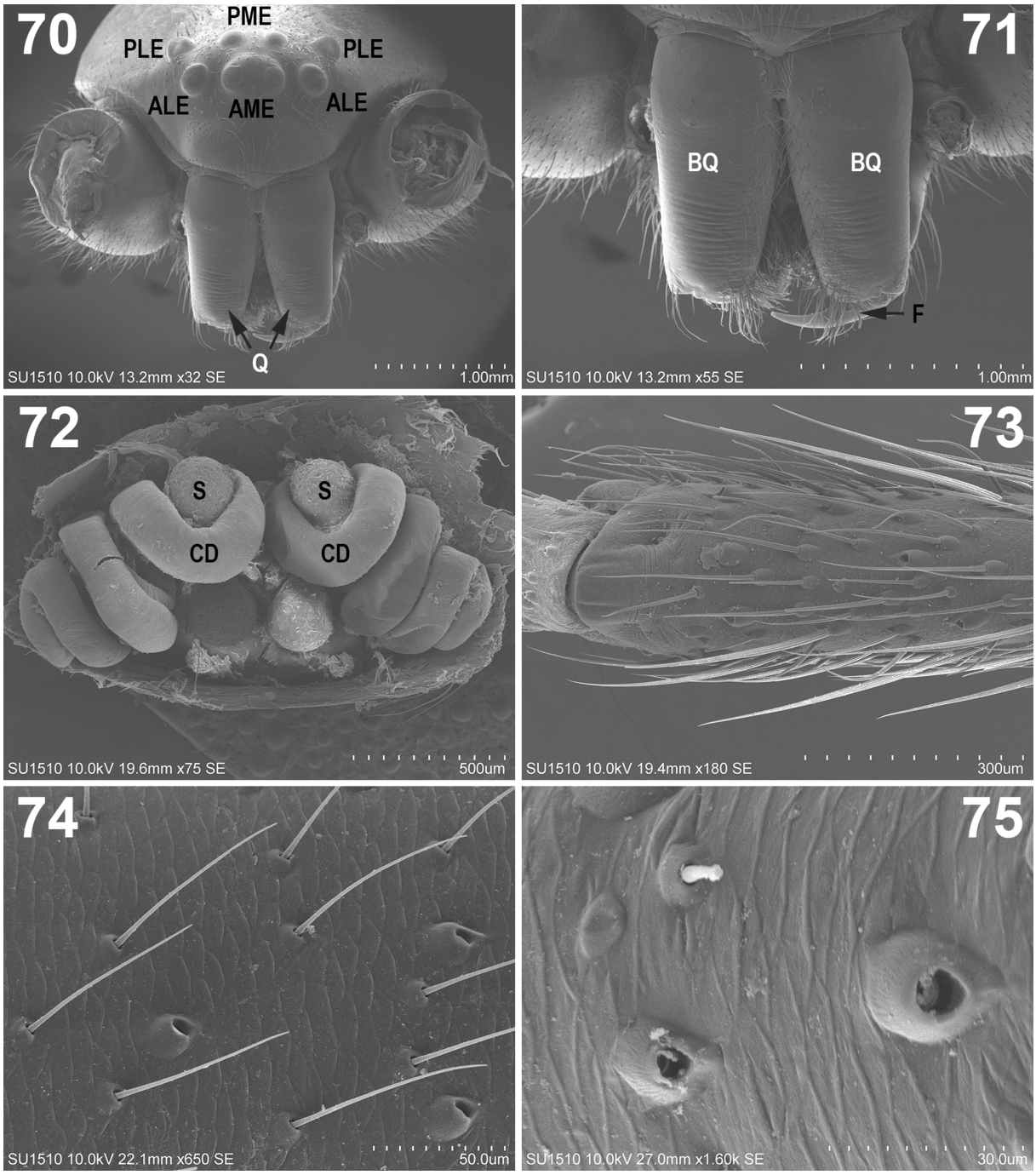

Figs 70–75. Scanning electron microscopy of *L. occidentalis* Valdez-Mondragón sp. nov. (female). **70**. Frontal view of prosoma. **71**. Detail of the chelicerae. **72**. Dorsal view of epigynum. **73–75**. Details of the setae and sockets on the legs. Abbreviations: ALE = anterior lateral eye; AME = anterior median eye; BQ = basichelicera; CD= copulatory duct; F = fang; PLE= posterior lateral eye; PME= posterior median eye; Q= chelicerae; S = spermathecae.

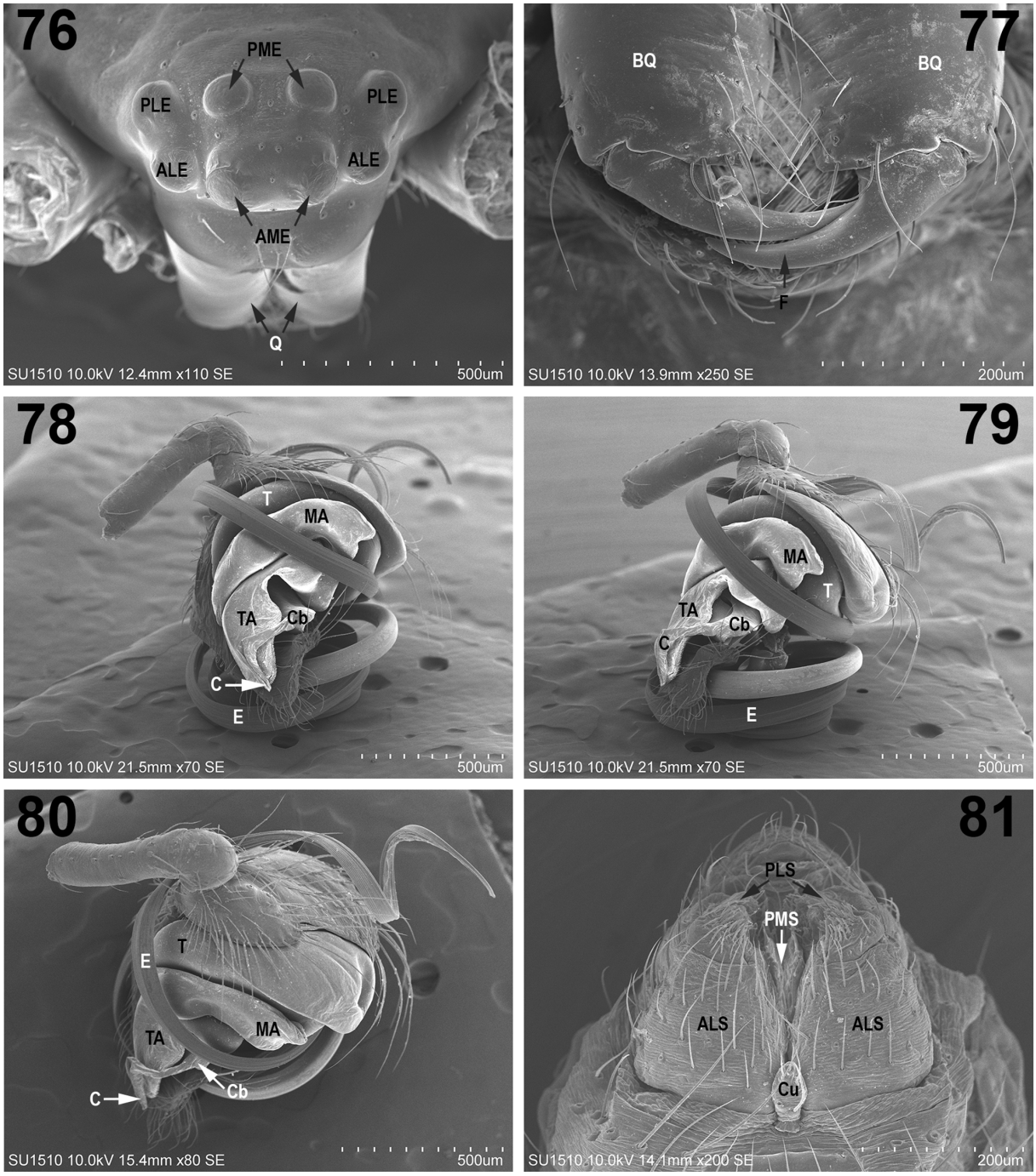

Figs 76–81. Scanning electron microscopy of *L. occidentalis* Valdez-Mondragón sp. nov. (male). **76.** Frontal view of carapace. **77.** Detail of distal part of the chelicera. **78–80.** Right palp: prolateral, retrolateral, and dorsal views, respectively. **81**. Ventral-apical view of the spinnerets. Abbreviations: ALE = anterior lateral eye; ALS = anterior lateral spinneret; AME = anterior median eye; BQ = basichelicera; C = conductor; Cb = conductor base; Cu = colulus; E = Embolus; F = fang; MA = median aphophysis; PLE= posterior lateral eye; PLS= posterior lateral spinneret; PME= posterior median eye; PMS = posterior median spinneret; Q = chelicera; T = tegulum; TA = tegular aphophysis.

V-shape surrounded by the copulatory ducts which may have four or five turns around them (Figs 33–43 (dorsal views)). The angle of the spermathecae may vary, but they are never parallel as in *L. geometricus* (Table 5). Palps of males show little variation, sclerites with little variation, embolus always with three complete turns (Fig. 46); however, there is variation in the apical part (Figs 49–60).

Males (N = 12): Tibia-Patella I: 5.31–6.8 (x = 5.77); T coefficient: 1.08–1.25 (x = 1.19). Females (N = 30): Tibia-Patella I: 6.4–9.1 (x = 7.96); T coefficient: 0.98–1.22 (x = 1.11). See Table 4 and 5 for intra and interspecific morphological variation.

Natural history

The specimens were collected in their cobwebs in natural and anthropized localities (Figs 19–24). The species is distributed mainly in tropical deciduous forests in the western states of Mexico: Jalisco, Guerrero, Michoacán, Colima, Guanajuato, Morelos, and Oaxaca (Fig. 21). The specimens from the type locality were collected inside the same house, under chairs, on window frames, under stowed dishes, and furniture (Figs 23–24, red arrows). Specimens collected in nature were found under and between big boulders on the ground (Figs 19, 22, red arrow), under mounds of rocks, inside cavities on walls along road-cuts, at the bases of alive cacti such as "nopales" (*Opuntia* spp.) and columnar cacti, and even under rotten cacti (Figs 19–21). Some females were collected with egg sacs, which are usually big, oval and yellow in coloration (Fig. 15), differing from other Mexican species (e.g. *Latrodectus* sp. 1 and sp. 2) that have smaller egg sacs whitish or pale-yellow in coloration.

Distribution

MEXICO: Jalisco, Colima, Michoacán, Guerrero, Oaxaca, Morelos, Guanajuato (Fig. 10).

Discussion

The use of separate lines of evidence in systematic studies, including morphological, molecular, ecological, and biogeographical data, provides more robust hypotheses when identifying and describing species that cannot be delimited by traditional morphology (DeSalle *et al.* 2005; Zhang *et al.* 2013; Valdez-Mondragón *et al*. 2019; Navarro-Rodríguez & Valdez-Mondragón 2020; Hazzi & Hormiga 2021). In recent years, molecular methods for species delimitation have provided a new way to resolve problems with species complexes or underestimated diversity. This has been especially useful in morphologically conservative groups by providing infra-specific genealogical information from DNA markers, which allows for objective implementation of modern species concepts (e.g., biological, phylogenetic, genotypic cluster, cladistics, etc.). Analyzing the data with a wide variety of species delimitation methods and delimiting lineages that are consistent across results follows the integrative taxonomy approach of species delimitation (DeSalle *et al.* 2005; Carstens *et al.* 2013; Luo *et al*. 2018; Valdez-Mondragón 2020).

Mitochondrial markers have been shown to be robust in the delimitation, revalidation, and description of several species within the genus *Latrodectus*, and often recover the main species groups or clades "*mactans*" and "*geometricus*" (Garb *et al.* 2004; Aguilera *et al*. 2009; Wright *et al*. 2019; Rueda *et al*. 2021). In this study, both of these clades were recovered in the phenetic and phylogenetic analyses; however, some discrepancies within the groups were found, as also recorded by Garb *et al.* (2004). For the terminals analyzed from Mexico, two of the five putative species belong to species already described (*L. mactans* and *L. hesperus*). However, some terminals from the state of Querétaro are grouped with terminals of *L. hesperus* from Canada, which reflects a possible introduction by anthropochory from Canada to Mexico or, more likely, from Mexico to Canada, although more research is needed to be conclusive. This would not be the first case of species of *Latrodectus* being introduced by anthropochory, as *L. geometricus* has been recorded in several countries around the world and is considered cosmopolitan

and invasive (Garb *et al*. 2004; Cabrera-Espinosa & Valdez-Mondragón 2021; Rueda *et al*. 2021). Recently, using the *CO1* barcoding marker, Choi *et al.* (2019) recorded *L. hesperus* from South Korea, representing another human-mediated introduction of the species. Although Chamberlin & Ivie (1935) mentioned that *L. hesperus* is distributed as far south as Mexico, there were no records of this species in Mexico from that time. Recent faunistic inventories, however, have since reported the presence of *L. hesperus* in the Mexican states of Baja California Sur, Chihuahua, Coahuila and Hidalgo, in addition to additional records of *L. mactans* and *L. geometricus* from several other states (Castañeda-Gómez *et al.* 2012; Jiménez *et al.* 2015; Salceda-Sánchez *et al.* 2017; Desales-Lara *et al.* 2018; Cabrera-Espinosa 2020; Cabrera-Espinosa & Valdez-Mondragón 2021).

Species delimitation is the process by which individuals from different populations are assigned to one or more already described or new species, while also the intraspecific variation is assessed (Rannala & Yang 2020). Aguilera *et al.* (2009) noted that molecular species delimitation methods are good tools for recognizing supposedly cryptic species or potential species complexes, as well as identifying species that had been synonymized through the use of solely morphological characters (e.g., *Latrodectus thoracicus*). However, a discrepancy between different species delimitation methods is often found, mainly due to the different statistical capacities of each model to recognize species or lineages (Carstens *et al*. 2013; Navarro-Rodríguez 2019; Valdez-Mondragón 2020; Nolasco & Valdez-Mondragón 2022). Therefore, the use of a concatenated matrix such as *CO1* + *ITS2* in this study, has shown to provide robust evidence for species delimitation analyses, mainly in tree-based analyses. These tend to separate over-sampled lineages (Pérez-Delgado *et al.* 2021), such as *Latrodectus* sp. 2 and *L. hesperus* in this work. To avoid possible overestimates of putative species of *Latrodectus* from Mexico, conservative estimates of the total number of species were calculated when discrepancies were observed between different molecular delimitation methods (Cartens *et al*. 2013).

Based on the criteria of genetic distances (*p*) and species delimitation methods, we consider that the putative species *Latrodectus* sp. 2 might correspond to *L. mactans mexicanus*, a subspecies not recognized by Levi (1959). However, further study is required to determine if specimens from the central region of Mexico constitute a separate species or possibly another species complex. As found in this work, previous taxonomic studies of *Latrodectus* using molecular markers have recovered interspecific genetic distances greater than 2%, except for some species pairs such as *L. thoracicus–L. variegatus*, and *L. corallinus–L. diaguita* (Garb *et al.* 2004; Aguilera *et al*. 2009; Rueda *et al*. 2021). The polyphyletic allocation of specimens of *L. hesperus* from USA–Mexico (group S, Fig. 1) and from Canada–Querétaro (Mexico) (group Q, Fig. 1) has been previously reported by Barrett & Hebert (2005) and Rueda *et al.* (2021), with a corrected genetic distance (K2P) greater than 7%, suggesting the possibility that the Canadian specimens correspond to a new and undescribed species.

Phylogenies are a useful approach to estimating relationships between groups of organisms; however, establishing genealogical relationships at the population level through the use of molecular characters (genes) is very complicated with traditional phylogenetic methods (e.g., Neighbor-Joining, Parsimony, or Maximum Likelihood) (Clement *et al*. 2002). Haplotype networks, in particular the TCS method (Fig. 4), offer an alternative way to estimate and visualize relationships between sampled organisms and can help to elucidate phylogeographic histories (Clement *et al*. 2002). Genetic analyses of populations combined with phylogenetic and morphological analyses have been used to recognize cryptic species (Pérez-Delgado *et al*. 2021). The mitochondrial marker *CO1* has been shown to be an effective locus for the genetic analysis of arachnid populations, including spiders (Valdez-Mondragón *et al.* 2019; Navarro-Rodríguez & Valdez-Mondragón 2020; Pérez-Delgado *et al*. 2021; Rueda *et al*. 2021; Nolasco & Valdez-Mondragón 2022). The present genetic analyses of populations of putative species of *Latrodectus* from Mexico provide inferences about their genealogical relationships. The presence of the same haplotype in two or more geographically distant populations suggests that these originated from the same ancestral

population or the existence of gene flow between them. This was observed for haplotypes m1 in *L. mactans*, oc4 in *L. occidentalis* sp. nov., hap5 in *Latrodectus* sp. 2, and h6 and h21 in *L. hesperus* (Fig. 4). Between *CO1* haplotype groups of the putative species recognized in this work, we found a maximum of 16 mutations, whereas Rueda *et al.* (2021) report a maximum of seven mutations between haplotype groups using the Median Joining Networks method. Despite this discrepancy, the haplotype networks from both results recover and corroborate the different estimated putative species (Planas & Ribera 2015; Valdez-Mondragón *et al.* 2019; Navarro-Rodríguez & Valdez-Mondragón 2020; Rueda *et al.* 2021).

The use of sexual characters to recognize species is widely used in spiders and other arthropods since sexual structures both evolve faster than other (i.e., somatic) structures and generally present little intraspecific variation in order to maintain compatibility between the sexes (Huber *et al.* 2005). It has been documented in spiders that such sexual characters are not always reliable for distinguishing between species (Huber *et al*. 2005; Aguilera *et al.* 2009). This has led to a complicated taxonomic history of the genus *Latrodectus* that has to date been based essentially on the use of morphological characters, mainly primary sexual structures (Chamberlin & Ivie 1935; Gonzales 1954; Levi 1959; Kaston 1970; Lotz 1994; Aguilera *et al*. 2009); such as male palps and female epigyna, which, as was demonstrated herein, present interspecific and intraspecific variation. The use of linear measurements as complementary characters in the description of species in most cases is not informative due to large variations in size of adult specimens, oftentimes within the same population (Aguilera, pers. com.). Traditionally, specimen measurements have focused on the carapace, tibia, or tibia-patella of leg I (Chamberlin & Ivie 1935; Lotz 1994). Although the use of solely linear somatic measurements is not appropriate for species delimitation as was demonstrated in this work, they provide useful evidence to help understand both interspecific and intraspecific variation, in addition to being useful for the descriptive purposes in species accounts.

Recent taxonomic works on *Latrodectus* have used the "T" (length/width of carapace) and "TT" (length tibia-patella of leg I or IV) coefficients to reflect body proportions and determine intra and interspecific variation (Melic 2000; Aguilera *et al.* 2009; Rueda *et al*. 2021). In our study, the T coefficient was not found to be useful for explaining the variation of the putative species from Mexico; however, as seen in Rueda *et al.* (2021), the TT coefficient for legs I and IV was useful for recognizing morphological differences between species in both females and males. Except for the genital opening coefficient in females, the rest of the coefficients analyzed herein (i.e., sternum, tibia-patella I and IV, femur I and IV), showed significant differences in both males and females and thus are useful for the identification of specimens and as complementary taxonomic characters. As in previous works (Rueda *et al.* 2021), no qualitative characters were found in the sexual structures of the putative species analyzed in this study; however, the length, width, and angle in which the female spermathecae are arranged with respect to each other showed differences as quantitative characters.

The dorsal pattern of the abdomen, mainly on females, has been recognized as an important and complementary taxonomic character in the diagnosis of some species of *Latrodectus* (e.g., *L. geometricus*, *L. rhodesiensis*, *L. pallidus*, *L. lilinae*, *L. tredecimguttatus*, *L. curacaviensis*, *L. garbae*) (Melic 2000; Rueda *et al.* 2021) since it allows the species recognition without observing the genitalia. The first taxonomic revision of *Latrodectus* was published by Pickard-Cambridge (1902) using color patterns, setae, or spines on the abdomen to distinguish all species known at that time. Chamberlin & Ivie (1935) carried out a study on the "black widow spiders" from northern Mexico, recognizing three subspecies of *L. mactans*: *Latrodectus mactans mactans* Fabricius, 1775, *Latrodectus mactans texanus* Chamberlin & Ivie, 1935 and *Latrodectus mactans hesperus* Chamberlin & Ivie, 1935. Levi (1959) grouped these subspecies as one single species (*L. mactans*) based on structural similarities of the palps in adult males. In this same work, only three species were recorded for the Americas: *L. geometricus*, with a tropical distribution; *L. mactans*, limited to tropical regions; and *L. curacaviensis*, an American endemic

distributed from Canada to Argentina. Levi (1958) also suggested the possibility that *Latrodectus hasselti* Thorell, 1870, *Latrodectus indistinctus* O. Pickard-Cambridge, 1904 and *Latrodectus tredecimguttatus* (Rossi, 1790) were synonyms of *L. mactans* since he found no obvious morphological differences. Eight years later, Levi (1966) admitted that two or more species might present morphological similarities in the male palps, rendering this character unreliable at the species level. Recently, Cabrera-Espinosa (2020) and Cabrera-Espinosa & Valdez-Mondragón (2021) updated the adult female abdomen dorsal pattern colorations of *Latrodectus* from Mexico, reporting eight different dorsal patterns of the eleven types of *L. mactans* previously reported by Levi (1959). The geographic regionalization of some dorsal coloration patterns of the abdomen of Mexican *L. mactans* suggests that a complex of unidentified species may be present.

As for the putative species analyzed in this study, only *L. occidentalis* sp. nov. is easily identifiable and diagnosable by the dorsal pattern of the abdomen of adult females. While primary sexual structures have traditionally been used for decades in spider taxonomy, body color patterns on the carapace and abdomen have been useful to diagnose groups that lack differentiation in sexual structures (e.g., *Psilochorus* Simon, 1893, *Pholcus* Walckenaer, 1805 (Pholcidae), and *Maratus* Karsch, 1878 (Salticidae)) (Huber *et al.* 2005; Waldock 2013, 2014; Huber & Dimitrov 2014).

Although Species Distribution Models (SDMs) are not a species delimitation method, they allow for the estimations of species' geographic ranges based on environmental conditions associated with each record (Kaslin 2013). SDMs have been an additional criterion in recent years for taxonomic decisions, providing important information that models the distributions of lineages or species (Valdez-Mondragón *et al.* 2019). The SDMs of the three species found their distributions to be well defined by altitude. This variable is likely driven by associated temperature and precipitation, as previous works have found the importance of these variables as limiting factors in the distribution of other species of *Latrodectus* (Vink *et al.* 2011; Kaslin 2013). The genus *Latrodectus*, unlike other groups of spiders in Mexico, displays a broad distribution across different climates, vegetation types, and altitudes, ranging from sea level in tropical deciduous forests to cold temperate forests above 2300 m (Cabrera-Espinosa & Valdez-Mondragón 2019, 2021; Cabrera-Espinosa 2020). Similar to Taucare-Ríos *et al*. (2016), our results found that temperature is the most important factor in the distribution of species of *Latrodectus* from Mexico, with this variable (maximum temperature of the warmest month and mean diurnal range) being present in the three SDM data sets.

Contrary to what is reported by Levi (1959) and Cabrera-Espinosa & Valdez-Mondragón (2019, 2021), we report that *L. mactans* does not have a wide distribution in Mexico. Rather, the distribution is limited by the Sierra Madre Oriental in the west and possibly by the Trans-Mexican Volcanic Belt in the south, with records of *L. mactans* found in the Great Plains ecoregion on the coast of the Gulf of Mexico (Figs 9, 12). This suggests that *L. mactans* is only distributed in the Tamaulipeca, Veracruzana, and lower parts of the Sierra Madre Oriental biogeographical provinces. Of the three species, *L. occidentalis* sp. nov. is the only one with a distribution in the Neotropical region of Mexico, mainly associated with the lowland forests of the Pacific coast (Figs 10, 12). The highlands (>2000 m) of the Trans-Mexican Volcanic Belt and the Sierra Madre del Sur present a barrier for the distribution of this species to reach the central region of Mexico. The distribution of *L. hesperus* is reported by Chamberlin & Ivie (1935) to extend from southern Canada to Mexico, down the western coast of the USA. This distribution is recovered in our SDM analysis, while also extending to the central region of Mexico on both sides of the Sierra Madre Occidental. However, molecular analyses in this study and previous works (e.g., Barrett & Hebert 2005; Rueda *et al*. 2021) find the populations of *L. hesperus* from Canada to likely represent an undescribed species. Unfortunately, the material from these populations deposited in GenBank lacks locality information, so it was not possible to verify that these records lie within the area estimated by our SDM.

In conclusion, the diversity of the genus *Latrodectus* is underestimated in Mexico, and more sampling is needed throughout the country, mainly from distinct biogeographical provinces. As previously reported, we also find that traditional morphology alone does not provide robust characters for species-level identification for Mexican and North American lineages. However, the combination of sexual features such as male palps and female epigyna plus the use of somatic characters such as the dorsal pattern of the abdomen in females, as well as some somatic linear measurements, proved to be informative characters for the identification of some species in the genus. Altogether, our integrative taxonomic approach using morphological and molecular data (*CO1* and *ITS2*) adds to the knowledge of this group and increases the species sampling from North America.

Acknowledgments

The first author thanks the program "Cátedras CONAHCYT", Consejo Nacional de Humanidades, Ciencias y Tecnologías (CONAHCYT), Mexico, for scientific support of the project No. 59: "Laboratorio Regional de Biodiversidad y Cultivo de Tejidos Vegetales (LBCTV) del Institute of Biology, Universidad Nacional Autónoma de México (IBUNAM)-Tlaxcala". The first author also thanks SEP-CONAHCYT for financial support of the project of Basic Science (Ciencia Básica) 2016, No. 282834. The second author thanks to CONAHCYT for the financial support. We thank Dr Oscar F. Francke and Dr Edmundo González Santillán of the Colección Nacional de Arácnidos (CNAN), Instituto de Biología, UNAM, for providing loans of specimens of *Latrodectus*. We are grateful to MSc. Laura M. Márquez Valdelamar for molecular sequencing of the samples, MSc. María Berenit Mendoza Garfias for the SEM photographs, Brett O. Butler for the English language review of the manuscript, and the reviewers for their comments and suggestions that improved the manuscript. We thank the American Arachnological Society (AAS) for the Vincent Roth Grant provided for fieldwork of this project. We also thank the students of the Laboratory of Arachnology (LATLAX), IBUNAM-Tlaxcala, for the help in the field work and processing of materials in the laboratory. All specimens were collected under Scientific Collector Permit FAUT-0309 from the Secretaría de Medio Ambiente y Recursos Naturales (SEMARNAT) provided to Dr Alejandro Valdez Mondragón.

References

Aguilera M.A., D'Elía G. & Casanueva M. E. 2009. Revalidation of *Latrodectus thoracicus* Nicolet, 1849 (Araneae: Theridiidae): biological and phylogenetic antecedents. *Guyana* 73 (2): 161–171.

Barrett R.D. & Hebert P.D. 2005. Identifying spiders through DNA barcodes. *Canadian Journal of Zoology* 83: 481–491. https://doi.org/10.1139/z05-024

Barreto P. & Barreto M. 1994. Arañas. Importancia médica y llave para familias. *Colombia Médica* 25: 3–12.

Cobos M.E., Peterson A.T., Osorio-Olvera L. & Jiménez-García D. 2019. An exhaustive analysis of heuristic methods for variable selection in ecological niche modeling and species distribution modeling. *Ecological Informatics* 53:100983. https://doi.org/10.1016/j.ecoinf.2019.100983

Cabrera-Espinosa L.A. 2020. *Arañas de Importancia Médica: Registros Actualizados de las Especies de Arañas "Viudas Negras" del Género Latrodectus Walckenaer, 1805 (Araneae: Theridiidae) de México*. Bachelor thesis, Benemérita Universidad Autónoma de Puebla, México.

Cabrera-Espinosa L.A. & Valdez-Mondragón A. 2019. El género de arañas "viudas negras" *Latrodectus* (Araneae: Theridiidae) en México, ¿qué se conoce ahora sobre su distribución? *Boletín de la AMXSA* 3 (2): 15–21.

Cabrera-Espinosa L.A. & Valdez-Mondragón A. 2021. Distribución y modelaje de nicho ecológico, comentarios biogeográficos y taxonómicos del género de arañas *Latrodectus* Walckenaer (Araneae, Theridiidae) de México. *Revista Mexicana de Biodiversidad* 92: e923665. https://doi.org/10.22201/ib.20078706e.2021.92.3665

Carstens B.C., Pelletier T.A., Reid N.M. & Satler J.D. 2013. How to fail at species delimitation. *Molecular Ecology* 22: 4369–4383. https://doi.org/10.1111/mec.12413

Castañeda-Gómez J., Pinkus-Rendón M., Arisqueta-Chablé C., Barrera-Pérez M., Ortiz-Martínez D. & Manrique-Saide P. 2012. Nuevos registros del género *Latrodectus* en Yucatán, México. *Revista Biomédica* 23: 105–111.

Chamberlin R.V. & Ivie W. 1935. The black widow spider and its varieties in the United States. *Bulletin of the University of Utah* 25 (8): 1–29.

Choi M.B., Lee S.Y., Yoo J.S., Jun J. & Kwon O. 2019. First record of the western black widow spider *Latrodectus hesperus* Chamberlin & Ivie, 1935 (Araneae: Theridiidae) in South Korea. *Entomological Research* 49 (3): 141–146. https://doi.org/10.1111/1748-5967.12350

Clement M., Snell Q., Walker P., Posada D. & Crandall K. 2002. TCS: estimating gene genealogies. *Proceedings 16th International Parallel and Distributed Processing Symposium*, Ft. Lauderdale, FL, USA. https://doi.org/10.1109/IPDPS.2002.1016585

Cobos E.M., Townsend P. & Osorio-Olvera L. 2019a. kuenm: an R package for detailed development of ecological niche models using Maxent. *PeerJ* 7: e6281. https://doi.org/10.7717/peerj.6281

Cobos E.M., Townsend P., Osorio-Olvera L. & Jiménez-García L. 2019b. An exhaustive analysis of heuristic methods for variable selection in ecological niche modeling and species distribution modeling. *Ecological Informatics* 53: e100983. https://doi.org/10.1016/j.ecoinf.2019.100983

Cortez-Roldán M. 2018. *Arañas de Importancia Médica: Distribución y Modelaje de Nicho Ecológico de las Especies de Arañas Violinista del Género Loxosceles Heineken y Love, 1832 (Araneae, Sicariidae) de México*. Bachelor thesis, Universidad Autónoma de Tlaxcala, México.

Cortez-Roldán. M. 2022. *Distribución Potencial y Escenarios de Cambio Climático en Cuatro Especies del Género Loxosceles (Araneae: Sicariidae) del Centro–Occidente de México*. Master tesis, Universidad Autónoma de Tlaxcala, México.

Cuervo-Robayo A.P., Téllez-Valdés O., Gómez-Albores M.A., Venegas-Barrera C.S., Manjarrez J. & Martínez-Meyer E. 2013. An update of high-resolution monthly climate surfaces for Mexico. *International Journal of Climatology* 34 (7): 2427–2437. https://doi.org/10.1002/joc.3848

Desales-Lara M.A., Jiménez M.L. & Corcuera P. 2018. Nuevos registros de arañas (Arachnida: Araneae) para México y listado actualizado de la araneofauna del estado de Coahuila. *Acta Zoológica Mexicana* 34 (1): 50–63. https://doi.org/10.21829/azm.2018.3411183

DeSalle R., Egan M.G. & Siddall M. 2005. The unholy trinity: taxonomy, species delimitation and DNA Barcoding. *Philosophical Transactions of the Royal Society B* 360: 1905–1916. https://doi.org/10.1098/rstb.2005.1722

Drummond A.J., Suchard M.A., Xie D. & Rambaut A. 2012. Bayesian phylogenetics with BEAUti and the BEAST 1.7. *Molecular Biology and Evolution* 29 (8): 1969–1973. https://doi.org/10.1093/molbev/mss075

Escobar L.E., Medina-Vogel G. & Peterson A.T. 2014. Potential for spread of the white-nose fungus (*Pseudogymnoascus destructans*) in the Americas: use of Maxent and NicheA to assure strict model transference. *Geospatial Health* 9 (1): 221–229. https://doi.org/10.4081/gh.2014.19

Fick S.E. & Hijmans R.J. 2017. WorldClim 2: new 1km spatial resolution climate surfaces for global land areas. *International Journal of Climatology* 37 (12): 4302–4315. https://doi.org/10.1002/joc.5086

Folmer O., Black M., Hoeh W., Lutz R. & Vrijenhoek R. 1994. DNA primers for amplification of mitochondrial cytochrome C oxidase subunit I from diverse metazoan invertebrates. *Molecular Marine Biology Biotechnology* 3: 294–299.

Fujisawa T. & Barraclough T.G. 2013. Delimiting species using single-locus data and the Generalized Mixed Yule Coalescent approach: a revised method and evaluation on simulated data sets. *Systematic Biology* 62 (5): 707–724. https://doi.org/10.1093/sysbio/syt033

Garb J.E., Gonzáles A. & Gillespie R.G. 2004. The black widow spider *Latrodectus* (Araneae; Theridiidae): phylogeny, biogeography, and invasion history. *Molecular Phylogenetics and Evolution* 31: 1127–1142. https://doi.org/10.1016/j.ympev.2003.10.012

González T.L. 1954. *Latrodectus mactans mexicanus* subsp. nov. *Anales del Instituto Biológico de la Universidad Nacional Autónoma de México* 24: 455–457.

Hall T.A. 1999. BioEdit: a user-friendly biological sequence alignment editor and analysis program for Windows 95/98NT. *Nucleic Acid Symposium Series* 41: 95–98.

Hazzi N.A. & Hormiga G. 2021. Morphological and molecular evidence support the taxonomic separation of the medically important Neotropical spiders *Phoneutria depilata* (Strand, 1909) and *P. boliviensis* (FO Pickard-Cambridge, 1897) (Araneae, Ctenidae). *ZooKeys* 1022: 13–50. https://doi.org/10.3897/zookeys.1022.60571

Holz G.G. & Habener J.F. 1998. Black widow spider alpha-latrotoxin: a presynaptic neurotoxin that shares structural homology with the glucagon-like peptide-1 family of insulin secretagogic hormones. *Comparative Biochemistry and Physiology. Part B, Biochemistry & Molecular biology* 121 (2): 177–184. https://doi.org/10.1016/S0305-0491(98)10088-3

Huber B.A. & Dimitrov D. 2014. Slow genital and genetic but rapid non-genital and ecological differentiation in a pair of spider species (Araneae, Pholcidae). *Zoologischer Anzeiger* 253 (5): 394–403. https://doi.org/10.1016/j.jcz.2014.04.001

Huber B.A., Rheims C.A. & Brescovit A.D. 2005. Speciation without changes in genital shape: a case study on Brazilian pholcid spiders (Araneae: Pholcidae). *Zoologischer Anzeiger* 243 (4): 273–279. https://doi.org/10.1016/j.jcz.2004.12.001

Ji Y.J., Zhang D.X. & He L.J. 2003. Evolutionary conservation and versatility of a new set of primers for amplifying the ribosomal internal transcribed spacer regions in insects and other invertebrates. *Molecular Ecology Notes* 3: 581–585. https://doi.org/10.1046/j.1471-8286.2003.00519.x

Jiménez M.L., Nieto-Castañeda I.G., Correa-Ramírez M.M. & Palacios-Cardiel C. 2015. Las arañas de los oasis de la región meridional de la península de Baja California, México. *Revista Mexicana de Biodiversidad* 86: 319–331. https://doi.org/10.1016/j.rmb.2015.04.028

Kapli P., Lutteropp S., Zhang J., Pavlidis P., Stamatakis A. & Flouri T. 2017. Multi-rate Poisson tree processes for single-locus species delimitation under maximum likelihood and Markov chain Monte Carlo. *Bioinformatics* 33 (11): 1630–1638. https://doi.org/10.1093/bioinformatics/btx025

Kaslin J.R. 2013. *Distribución Actual y Potencial de las Poblaciones del Género Latrodectus (Araneae: Theridiidae) en Ecuador*. Bachelor thesis, Pontifica Universidad Católica del Ecuador, Ecuador.

Kass J.M., Pinilla-Buitrago G.E., Vilela B., Aeillo-Lammens M.E., Muscarella R., Merow C. & Anderson R.P. 2022. *Wallace: A modular platform for reproducible ecological modeling*. Version 1.1.3. Available from http://wallaceecomod.github.io/wallace/ [accessed 5 Sep. 2023].

Kaston B.J. 1970. Comparative biology of American black widow spiders. *Transactions of the San Diego Society of Natural History* 16: 33–82.

Katoh K. & Toh H. 2008. Recent developments in the MAFFT multiple sequence alignment program. *Briefings in Bioinformatics* 4: 286–298. https://doi.org/10.1186/1471-2105-9-212

Kearse M., Moir R., Wilson A., Stones-Havas S., Cheung M., Sturrock S., Buxton S., Cooper A., Markowitz S., Duran C., Thierer T., Ashton B., Meintjes P. & Drummond A. 2012. Geneious Basic: an integrated and extendable desktop software platform for the organization and analysis of sequence data. *Bioinformatics* 28: 1647–1649. https://doi.org/10.1093/bioinformatics/bts199

Kumar S., Tamura K. & Nei M. 1994. MEGA: Molecular Evolution Genetics Analysis software for microcomputers. *Computer Applications in the Biosciences* 10: 189–191. https://doi.org/10.1093/bioinformatics/10.2.189

Leigh J.W. & Bryant D. 2015. POPART: full-feature software for haplotype network construction. *Methods in Ecology and Evolution* 6: 1110–1116. https://doi.org/10.1111/2041-210X.12410

Letunic I. & Bork P. 2021. Interactive Tree Of Life (iTOL) v5: an online tool for phylogenetic tree display and annotation. *Nucleic Acids Research* 49 (W1): W293–W296. https://doi.org/10.1093/nar/gkab301

Levi H.W. 1958. Number of species of black-widow spiders (Theridiidae: *Latrodectus*). *Science* 127: 1055. https://doi.org/10.1126/science.127.3305.1055.a

Levi H.W. 1959. The spider genus *Latrodectus* (Araneae, Theridiidae). *Transactions of the American Microscopical Society* 78: 7–43. https://doi.org/10.2307/3223799

Levi H.W. 1966. The three species of *Latrodectus* (Araneae), found in Israel. *Journal of Zoology* 150: 427–432. https://doi.org/10.1111/j.1469-7998.1966.tb03016.x

Levi H.W. & Randolph D.E. 1975. A key and checklist of American spiders of the family Theridiidae north of Mexico (Araneae). *Journal of Arachnology* 3: 31–51. Available from http://www.jstor.org/stable/3705253 [accessed 5 Sep. 2023].

Levy G. & Amitai P. 1983. Revision of the widow-spider genus *Latrodectus* (Araneae: Theridiidae) in Israel. *Zoological Journal of the Linnean Society* 71: 39–63. https://doi.org/10.1111/j.1096-3642.1983.tb01720.x

Lotz L.N. 1994. Revision of the genus *Latrodectus* (Araneae: Theridiidae) in Africa. *Navorsinge van die Nasionale Museum Bloemfontein* 10: 1–60. https://hdl.handle.net/10520/AJA00679208_1357

Luo A., Ling C., Ho Y.M. & Zhu C.D. 2018. Comparison of methods for molecular species delimitation across a range of speciation scenarios. *Systematic Biology* 67 (5): 830–846. https://doi.org/10.1093/sysbio/syy011

Marques R., Krüger R.F., Peterson A.T., de Melo L.F., Vicenzi N. & Jiménez-García D. 2020. Climate change implications for the distribution of the babesiosis and anaplasmosis tick vector, *Rhipicephalus* (*Boophilus*) *microplus*. *Veterinary Research* 51 (1): 1–10. https://doi.org/10.1186/s13567-020-00802-z

Melic A. 2000. El género *Latrodectus* Walckenaer, 1805 en la península Ibérica (Araneae: Theridiidae). *Revista Ibérica de Aracnología* 1 (12): 13–30.

Monaghan M.T., Wild R., Elliot M., Fujisawa T., Balke M., Inward D.J. & Vogler A.P. 2009. Accelerated species inventory on Madagascar using coalescent-based models of species delineation. *Systematic Biology* 58 (3): 298–311. https://doi.org/10.1093/sysbio/syp027

Morrone J. 2004. Panbiogeografía, componentes bióticos y zonas de transición. *Revista Brasileira de Entomologia* 48 (2): 149–162. https://doi.org/10.1590/S0085-56262004000200001

Morrone J. 2005. Hacia una síntesis biogeográfica de México. *Revista Mexicana de Biodiversidad* 76 (2): 207–252. https://doi.org/10.22201/ib.20078706e.2005.002.303

Morrone J. 2017. Mexican biogeographic provinces: map and shapefiles. *Zootaxa* 4277 (2): 277–279. https://doi.org/10.11646/zootaxa.4277.2.8

Navarro-Rodríguez C.I. 2019. *Delimitación de las Especies Mexicanas de Arañas del Género Loxosceles Heineken y Love (Araneae, Sicariidae) del Centro Occidente de México con Evidencia Molecular y Morfológica*. Masters thesis, Universidad Autónoma de Tlaxcala, México.

Navarro-Rodríguez C.I. & Valdez-Mondragón A. 2020. Description of a new species of *Loxosceles* Heineken & Lowe (Araneae, Sicariidae) recluse spiders from Hidalgo, Mexico, under integrative taxonomy: morphological and DNA barcoding data (CO1 + ITS2). *European Journal of Taxonomy* 704: 1–30. https://doi.org/10.5852/ejt.2020.704

Nolasco S. & Valdez-Mondragón A. 2022. To be or not to be… Integrative taxonomy and species delimitation in the daddy long-legs spiders of the genus *Physocyclus* (Araneae, Pholcidae) using DNA barcoding and morphology. *ZooKeys* 1135: 93–118. https://doi.org/10.3897/zookeys.1135.94628

Olson D.M., Dinerstein E., Wikramanayake E.D., Burgess N.D., Powell G.V.N., Underwood E.C., D'Amico J.A., Itoua I., Strand H.E., Morrison J.C., Loucks C.J., Allnutt T.F., Ricketts T.H., Kura Y., Lamoreux J.F., Wettengel W.W., Hedao P. & Kassem K.R. 2001. Terrestrial ecoregions of the world: a new map of life on Earth. *Bioscience* 51 (11): 933–938. https://doi.org/c635xt

Ortiz D. & Francke O.F. 2016. Two DNA barcodes and morphology for multi-method species delimitation in *Bonnetina* tarantulas (Araneae: Theraphosidae). *Molecular Phylogenetics and Evolution* 101: 176–193. https://doi.org/10.1016/j.ympev.2016.05.003

Padial J.M., Miralles A., de la Riva I. & Vences M. 2010. The integrative future of taxonomy. *Frontiers in Zoology* 7: 1–16. https://doi.org/10.1186/1742-9994-7-16

Pérez-Delgado A.J., Arribas P., Hernando C., López H., Arjona Y., Suárez-Ramos D., Emerson B.C. & Andújar C. 2021. Hidden island endemic species and their implications for cryptic speciation within soil arthropods. *Journal of Biogeography* 49: 1367–1380. https://doi.org/10.1111/jbi.14388

Phillips S.J., Anderson R.P. & Schapire R.E. 2006. Maximum entropy modeling of species geographic distributions. *Ecological Modelling* 190 (3–4): 231–259. https://doi.org/10.1145/1015330.1015412

Pickard-Cambridge F. 1902. On the spiders of the genus *Latrodectus*, Walckenaer. *Proceedings of the Zoological Society of London* 72 (1): 247–261.
Available from https://www.biodiversitylibrary.org/page/31575819 [accessed 5 Sep. 2023].

Planas E. & Ribera C. 2015. Description of six new species of *Loxosceles* (Araneae: Sicariidae) endemic to the Canary Islands and the utility of DNA barcoding for their fast and accurate identification. *Zoological Journal of the Linnean Society* 174 (1): 47–73. https://doi.org/10.1111/zoj.12226

Pons J., Barraclough T., Gomez-Zurita J., Cardoso A., Duran D., Hazell S., Kamoun S., Sumlim W.D. & Vogler A.P. 2006. Sequence-based species delimitation for the DNA taxonomy of undescribed insects. *Systematic Biology* 55: 595–609. https://doi.org/10.1080/10635150600852011

Puillandre N., Lambert A., Brouillet S. & Achaz G. 2012. ABGD, Automatic Barcode Gap Discovery for primary species delimitation. *Molecular Ecology* 21: 1864–1877.
https://doi.org/10.1111/j.1365-294X.2011.05239.x

Puillandre N., Brouillet S. & Achaz G. 2021. ASAP: assemble species by automatic partitioning. *Molecular Ecology Resources* 21: 609–620. https://doi.org/10.1111/1755-0998.13281

Rambaut A., Drummond A.J., Xie D., Baele G. & Suchard M.A. 2018. Posterior summarization in Bayesian phylogenetics using Tracer 1.7. *Systematic Biology* 67 (5): 901–904. https://doi.org/10.1093/sysbio/syy032

Rannala B. & Yang Z. 2020. Species delimitation. *In*: Scornavacca C., Delsuc F. & Galtier N. (eds) *Phylogenetics in the Genomic Era* 5.5:1–5.5:18.
Available from https://hal.archives-ouvertes.fr/hal-02536468 [accessed 5 Sep. 2023].

Rueda A., Lozano D., Muñoz-Charry V., Velásquez-Vélez M.I., Amézquita A., Parra D. & Realpe E. 2021. Phylogeny of the genus *Latrodectus* (Araneae: Theridiidae) and two new species from the dry forests in the Magdalena Valley-Colombia. *Species* 22 (70): 243–265.

Salceda-Sánchez B., Hernández-Hernández V., Conde-Sánchez E., Vargas-Olmos M., López-Cárdenas J. & Huerta H. 2017. Nuevos registros de distribución del género *Latrodectus* Walckenaer y *Loxosceles* Heineken y Lowe en México. *Southwestern Entomologist* 42 (2): 575–582. https://doi.org/10.3958/059.042.0226

Taucare-Ríos A., Bizama G. & Bustamante R.O. 2016. Using global and regional Species Distribution Models (SDM) to infer the invasive stage of *Latrodectus geometricus* (Araneae: Theridiidae) in the Americas. *Environmental Entomology* 45 (6): 1379–1385. https://doi.org/10.1093/ee/nvw118

Ubick D.P., Cushing P. & Roth V. (eds) 2005. *Spiders of North America: An Identification Manual*. American Arachnological Society.

Valdez-Mondragón A. 2020. COI mtDNA barcoding an morphology for species delimitation in the spider genus *Ixchela* Huber (Araneae: Pholcidae), with the description of two new species from Mexico. *Zootaxa* 4747 (1): 54–76. https://doi.org/10.11646/zootaxa.4747.1.2

Valdez-Mondragón A. & Francke O.F. 2015. Phylogeny of the spider genus *Ixchela* Huber, 2000 (Araneae: Pholcidae) based on morphological and molecular evidence (CO1 and 16S), with a hypothesized diversification in the Pleistocene. *Zoological Journal of the Linnean Society* 175 (1): 20–58. https://doi.org/10.1111/zoj.12265

Valdez-Mondragón A., Cortez-Roldán M.R., Juárez-Sánchez A.R. & Solís-Catalán K.P. 2018. A new species of *Loxosceles* Heineken & Lowe (Araneae, Sicariidae), with updated distribution records and biogeographical comments for the species from Mexico, including a new record of *Loxosceles rufescens* (Dufour). *ZooKeys* 802: 39–66. https://doi.org/10.3897/zookeys.802.28445

Valdez-Mondragón A., Navarro-Rodríguez C.I., Solís-Catalán K.P., Cortez-Roldán M.R. & Juárez-Sánchez A.R. 2019. Under an integrative taxonomic approach: the description of a new species of the genus *Loxosceles* (Araneae, Sicariidae) from Mexico City. *ZooKeys* 892: 93–133. https://doi.org/10.3897/zookeys.892.39558

Vink C.J., Derraik J.G., Phillips C.B. & Sirvid P.J. 2011. The invasive Australian redback spider, *Latrodectus hasseltii* Thorell 1870 (Araneae: Theridiidae): current and potential distributions, and likely impacts. *Biological Invasions* 13 (4): 1003–1019. https://doi.org/10.1007/s10530-010-9885-6

Waldock J.M. 2013. A review of the peacock spiders of the *Maratus mungaich* species-group (Araneae: Salticidae), with descriptions of four new species. *Records of the Western Australian Museum* 28 (1): 66–81. https://doi.org/10.18195/issn.0312-3162.28(1).2013.066-081

Waldock J.M. 2014. Two new species of peacock spider of the *Maratus mungaich* species-group (Araneae: Salticidae) from south-western Australia. *Records of the Western Australian Museum* 29 (2): 149–158. https://doi.org/10.18195/issn.0312-3162.29(2).2014.149-158

World Spider Catalog. 2023. *WSC. Version 24*. Natural History Museum Bern.
Available from http://wsc.nmbe.ch [accessed 13 May 2023]. https://doi.org/10.24436/2

Wright B.M.O.G., Wright C.D., Sole C.L., Lyle R., Tippett R., Sholto-Douglas C., Verburgt L. & Engelbrecht I. 2019. A new forest dwelling button spider from South Africa (Araneae, Theridiidae, *Latrodectus*). *Zootaxa* 4700 (4): 584–600. https://doi.org/10.11646/zootaxa.4s700.4.12

Zhang J., Kapli P., Pavlidis P. & Stamatakis A. 2013. A general species delimitation method with applications to phylogenetic placements. *Bioinformatics* 29: 2869–2876. https://doi.org/10.1093/bioinformatics/btt499

Manuscript received: 30 January 2023
Manuscript accepted: 25 May 2023
Published on: 4 October 2023
Topic editor: Magalie Castelin
Section editor: Rudy Jocqué
Desk editor: Pepe Fernández

Supplementary material

Supp. file 1. Measurements used for linear analyses in specimens of the genus *Latrodectus* Walckenaer, 1805 from Mexico. **A**. Angle between the spermathecae. **B**. Genital opening: length (blue line), width (red line). **C**. Carapace: length (red line), width (blue line). **D**. Sternum: length (red line), width (blue line). **E**. Measurements of the femur, patella + tibia: length (red line), width (blue line).
https://doi.org/10.5852/ejt.2023.897.2293.9919

Supp. file 2. Haplotypes recorded with the *CO1* gene of the five putative species of the genus *Latrodectus* Walckenaer, 1805 from Mexico. Abbreviation: NA = Not Applicable.
https://doi.org/10.5852/ejt.2023.897.2293.9921

Appendix 1 (continued on next two pages). Interspecific average *p* genetic distances of *CO1* between the species of *Latrodectus* Walckenaer, 1805 used in this work.

	L. umbukwane	***L. geometricus***	***L. curacaviensis***	***L. corallinus***	***L. thoracicus*** Chile	***L. antheratus***	***L. rhodesiensis***
L. geometricus	0.130						
L. curacaviensis	0.171	0.185					
L. corallinus	0.154	0.185	0.037				
L. thoracicus Chile	0.172	0.174	0.055	0.055			
L. antheratus	0.164	0.162	0.057	0.065	0.073		
L. rhodesiensis	0.129	0.104	0.175	0.162	0.160	0.189	
L. renivulvatus	0.125	0.144	0.127	0.121	0.113	0.120	0.163
L. hasseltii	0.164	0.168	0.143	0.135	0.137	0.139	0.193
L. katipo	0.164	0.168	0.139	0.131	0.133	0.128	0.172
L. tredecimguttatus	0.130	0.143	0.116	0.092	0.118	0.120	0.155
L. pallidus	0.163	0.177	0.093	0.106	0.089	0.126	0.143
L. pallidus / thoracicus Iraq	0.168	0.165	0.082	0.090	0.101	0.107	0.155
L. variolus	0.179	0.181	0.121	0.119	0.116	0.139	0.192
L. hesperus Mex-EU	0.169	0.187	0.115	0.121	0.111	0.129	0.176
Latrodectus sp. 1	0.179	0.195	0.100	0.106	0.116	0.121	0.179
L. hesperus Canada	0.174	0.183	0.106	0.103	0.107	0.120	0.192
L. mactans	0.165	0.167	0.103	0.100	0.118	0.121	0.175
Latrodectus sp. 2	0.183	0.187	0.105	0.116	0.117	0.110	0.194
L. occidentalis sp. nov.	0.175	0.177	0.094	0.099	0.103	0.112	0.167

Appendix 1 (continued). Interspecific average *p* genetic distances of *CO1* between the species of *Latrodectus* Walckenaer, 1805 used in this work.

	L. renivulvatus	***L. hasseltii***	***L. katipo***	***L. tredecimguttatus***	***L. pallidus***	***L. pallidus/ thoracicus*** Iraq	***L. variolus***
L. hasseltii	0.116						
L. katipo	0.126	0.035					
L. tredecimguttatus	0.079	0.113	0.123				
L. pallidus	0.116	0.145	0.144	0.113			
L. pallidus/ thoracicus Iraq	0.134	0.153	0.153	0.132	0.095		
L. variolus	0.109	0.126	0.140	0.130	0.113	0.130	
L. hesperus Mex-EU	0.106	0.168	0.164	0.131	0.107	0.111	0.081
Latrodectus sp. 1	0.113	0.140	0.150	0.131	0.100	0.123	0.093
L. hesperus Canada	0.111	0.156	0.159	0.104	0.099	0.116	0.079
L. mactans	0.091	0.157	0.157	0.123	0.107	0.109	0.082
Latrodectus sp. 2	0.113	0.147	0.155	0.128	0.102	0.128	0.098
L. occidentalis sp. nov.	0.111	0.149	0.154	0.129	0.089	0.102	0.089

Appendix 1 (continued). Interspecific average *p* genetic distances of *CO1* between the species of *Latrodectus* Walckenaer, 1805 used in this work.

	L. hesperus Mex-USA	***Latrodectus*** sp. 1	***L. hesperus*** Canada	***L. mactans***	***Latrodectus*** sp. 2
Latrodectus sp. 1	0.064				
L. hesperus Canada	0.062	0.067			
L. mactans	0.083	0.082	0.071		
Latrodectus sp. 2	0.068	0.029	0.067	0.082	
L. occidentalis sp. nov.	0.083	0.087	0.080	0.072	0.093